

**AUTOLYTIC CHARACTERIZATION OF
SELECTED *ENTEROCOCCAL* STRAINS,
(PREVIOUSLY *STREPTOCOCCAL*)**

By

MELISHA SUKKHU

Submitted in fulfilment of the academic requirements
for the degree of

MASTER OF SCIENCE

In the School of Biochemistry, Genetics,
Microbiology and Plant Pathology,
University of KwaZulu-Natal
Pietermaritzburg

2007

PREFACE

The experimental work described in this thesis was carried out in the Department of Genetics, School of Biochemistry, Genetics, Microbiology and Plant Pathology, University of KwaZulu-Natal, Pietermaritzburg from January 2006 to December 2007, under the supervision of Doctor Mervyn Beukes. The N-Terminal Amino acid analysis was conducted at the Molecular Biology Unit, at the University of KwaZulu- Natal, Pietermaritzburg.

These studies represent the original work by the author and have not otherwise been submitted in any form for any degree or diploma to any University. Where use has been made of the work of others, it is dually acknowledged in the text.

Melisha Sukkhu (Miss)

ACKNOWLEDGMENTS

This thesis is dedicated in memory of my late grandfather, Mr. Ramchandar Sukkhu (Chan), fondly known as “Dhadha”. Despite you not being here to witness this major milestone in my life, I know you are still guiding me and hope I have made your name extremely proud! I miss you dearly everyday!

I would like to express my sincere gratitude to the following individuals whom have contributed to the completion of this document:

Firstly, I thank God for blessing me and being my solace, protection and guidance throughout this MSc.

A warm thanks to my supervisor, Dr. Mervyn Beukes, for your guidance and supervision with this document. It is greatly appreciated!

To my dear grandmother (Mrs. S. Sukkhu, Snr), thank you for being there for me and providing me with the support I needed whenever I considered giving up. It is with your inspiration, strength and understanding that has got me this far, and I thank God for still being blessed with you as an elder in my life!

My parents, Mr. V. R. Sukkhu and Mrs S. Sukkhu (Jnr), no words can express the gratitude and appreciation I have for being blessed with a wonderful set of parents! Thank you both for being my pillars of strength and keeping me grounded and focused in my life. I am honoured to share this achievement with you both. Dad, thank you for all the sacrifices you have made throughout the years, and for single-handedly educating me. I hope I have made you proud and lived up to all your expectations. Mum, thank you for enduring my crazy behaviour. But most importantly, for just being there, and ensuring I had ample lunch for my late hours in the lab!

My darling brother, Kaveer, for religiously chaufferring me to and from the lab. Love you Bro! My sister, Anisha, despite the geographical locations, the distance was never an issue in giving me encouragement and strength when I needed it most. Thank you for all you have done and for keeping me inline and intouch with reality. Thank you both for all the fun and quirky remarks and for humouring me when I went throughout my emotional roller-coasters during this MSc. I love you guys, and could never have asked for better siblings. Thank you!

My best friend Terushka. You are the very essence of what a best friend should be. I thank you for also listening to my complaints and humouring me in all my situations. Thank you for being my escape!

My immediate and extentented families (numerous to name but know whom your'll are), I am blessed for having all your encouragement and support. Thank you.

Nirodh, thank you for walking into my life and being so understanding and supportive. You are my angel in disguise whom picks me up when my wings have trouble remembering how to fly! You are too precious for words and I love you to bits hun!

To the lab technician, Megan Brunkhorst, thank you for all your advice and promptness in aquiring unusual reagents at my request. Your assistance and guidance is greatly appreciated. Mr. Goodman Zondi, thank you for all the early morning laughs and jokes, attempts to teach me Zulu, and for the availability of clean glassware at my request. May God bless you both for all your efforts!

The gang of Lab B23, a special thank you to each one of you for entertaining my nonscence, sugar-rushes and giggles. My buddy in crime Abhita (AJ), we tolerated a lot, but never lost focused. Thank you for the wonderful company, hourly lunches, advice, drinks (the tree and pond area) laughter and tears! It made this MSc more bearable!

Jiren, thank you for all the wonderful memories, the giggles and for being my backup in calculations and reagents. Your friendship and generosity is truly appreciated. Prisca,

thank you for all your help, hour long conversations, laughs and for getting me hooked on Prison Break! We made it out of the “Titanic”! Those were great times, and I cherish those memories.

To Rizwana Mia and Rizwana Desai, thank you for always believing in me and for the encouragement through everything. And you were right, “goodness does prevail”! Your optimistic outlook is a huge inspiration to me.

To uncle Tad and Yegan, thank you both for all your encouragement and for just being there to listen to my complaints.

To Dr. York and the staff at Molecular Diagnostic Services (MDS), I am humbled to be associated with such a novel institution. Your patience and support is commendable and truly appreciated.

Finally, to the National Research Foundation and the University of KwaZulu-Natal, thank you for the financial support throughout this study.

Abstract

Autolysins are enzymes that cleave specific structural components within the bacterial cell wall. They contribute to numerous cellular activities such as cell growth, cell division, peptidoglycan recycling and turnover. In this study, twelve *Enterococcal* isolates (previously from the genus *Streptococcus*) were examined for susceptibility to the antibiotics Penicillin G and Vancomycin, using a Disk Diffusion and a Microtitre plate assay. In both methods, all twelve strains were resistant to Vancomycin. Six of these strains were susceptible to Penicillin G. The minimum inhibitory concentration (MIC) values were twice that of the disk diffusion assay values. In the presence of antibiotic, the growth rates for the six strains were halved.

Autolysins were extracted from the respective cell cultures using a 4% SDS precipitation method. The protein concentrations were calculated and estimated to be within the range of 5.47- to 6.35 $\mu\text{g}/\mu\text{l}$. Profiles of the SDS precipitate were analyzed on SDS-PAGE. Autolytic proteins were identified and partially analyzed by renaturing SDS-PAGE (zymograms) using gels containing cell wall substrate. Seven lytic bands of molecular weights 25, 30, 50, 63, 75, 95 and 145 kDa (designated Autolysin A to G, respectively) were selected for further analysis. The temporal distribution of the enzymes ranged from the mid exponential phase to the early death phase. The seven proteins were blotted onto polyvinylidene difluoride (PVDF) membranes and excised for N-terminal sequencing. Blast analysis of the respective N-terminal sequences showed autolysins A, C, D, E and F to have 100% similarity to the muramidase, amidase and peptidase from *S. cremoris*, *S. suis*, *S. pneumoniae*, *S. pyogenes* and *E. faecium*, respectively.

Biochemical characterization confirmed autolysins A, B, E and F to exhibit muramidase activity, and autolysin C and G to exhibit peptidase activity. Autolysin D displayed 100% similarity to the protein LytA, a peptidoglycan hydrolase that is known to exhibit amidase activity. Blast analysis could not determine any significant similarities for autolysins B and G to previously identified autolysins, thus indicating they may perhaps be novel autolysins.

TABLE OF CONTENTS

	PAGE
TITLE	i
PREFACE	ii
ACKNOWLEDGMENTS	iii
ABSTRACT	vi
TABLE OF CONTENTS	vii
LIST OF FIGURES	xi
LIST OF TABLES	xix
LIST OF ABBREVIATIONS	xxi
CHAPTER ONE: LITERATURE REVIEW	1
1.1 General Introduction	2
1.2 Introduction to <i>Streptococcus milleri</i>	4
1.2.1 Bacteriology and Grouping	4
1.2.2 Mode of Infection	5
1.3 Introduction of Autolysins	6
1.3.1 Types of Endogenous Bacteriocidal Enzymes and Specificities	6
1.3.2 Biological Function of Peptidoglycan Hydrolases	7
1.3.3 Control and Regulation of Peptidoglycan Hydrolases	9

	PAGE
1.4 The Peptidoglycan Hydrolase System	11
1.4.1 The Murein Hydrolases of <i>Escherichia coli</i>	11
1.4.1.1 Glycosidases	12
1.4.1.2 Peptidases, Endopeptidases, Exopeptidases and Amidases	14
1.4.2 Peptidoglycan Hydrolases from <i>Streptococcus pneumoniae</i>	18
1.4.3 Peptidoglycan Hydrolases from <i>Staphylococcus aureus</i>	18
1.4.4 Peptidoglycan Hydrolases of <i>Enterococcus hirae</i> ATCC 9790	20
1.4.5 Peptidoglycan Hydrolases of <i>Bacillus licheniformis</i>	20
1.4.6 Peptidoglycan Hydrolases of <i>Bacillus subtilis</i>	21
1.4.6.1 The Genetic Organisation of <i>Bacillus</i> hydrolases	21
1.4.7 Peptidoglycan Hydrolases in Other Bacterial species	22
1.5 Introduction to Bacterial Programmed Cell Death	23
1.5.1 PCD and Altruism	23
1.5.2 PCD in Bacteria	24
1.5.2.1 Morphological Evidence	24
1.5.2.2 Genetic Evidence	25
1.5.2.3 Antibiotic-Induced Killing	27
1.6 Conclusion	28

	PAGE
CHAPTER TWO: MATERIALS AND METHODS	29
2.1 Bacterial Culture and Growth Conditions	30
2.2 Disk Diffusion Assay	31
2.3 Minimum Inhibition Concentrations (MIC)	31
2.4 Relative Fitness Assay	32
2.5 Extraction of Autolytic Proteins	32
2.6 Preparation of Crude Cell Wall Extracts	32
2.7 Total Protein Concentrations	33
2.8 SDS-PAGE Gel Electrophoresis	34
2.9 Coomassie Blue Staining	35
2.10 Renaturing SDS-PAGE Gel Electrophoresis (Zymogram)	35
2.11 Elution of Lytic Proteins from Zymograms	36
2.12 Electro. Blot Transfer	36
2.13 N-Terminal Sequencing	38
2.14 Morgan-Elson Assay	41
2.15 N-dinitrophenyl (DNP) Assay	42
2.16 Protein Sequence Analysis	42
CHAPTER THREE: RESULTS AND DISCUSSION	43
3.1 Disk Diffusion Assay and Minimum Inhibitory Concentrations (MIC)	44
3.2 Relative Fitness Assay	49
3.3 Total Protein Concentration	55

	PAGE
3.4 SDS-PAGE profiles and Zymograms showing autolytic activity of proteins extracted	58
3.5 N-Terminal Sequencing	69
3.6 Morgan-Elson Assay	73
3.7 DPN Assay	75
CHAPTER FOUR: CONCLUSION AND FUTURE RESEARCH	77
CHAPTER FIVE: REFERENCES	81

List of Figures

Figure 1.1 Cell wall growth of *B. subtilis*. Side walls grow via inside-to-outside mechanism (Koch, 2002).

Page 9

Figure 1.2 Illustration of the chemical cell wall structure of *Escherichia coli*. Arrows indicate the bonds cleaved by specific peptidoglycan hydrolases.

Page 11

Figure 1.3 Illustration of glycosyltransferase interaction between the NAM and NAG residues (Smith, 2003).

Page 12

Figure 1.4 Illustration of the 3-D structure of *slt70* (Anon, 2006).

Page 13

Figure 1.5 Illustration of the peptidoglycan structure and sites of attack by cell wall hydrolases. The sites where cell wall hydrolases may attack peptidoglycan are indicated by arrows, but staphylococci contain only three of these wall hydrolases (amidase, glucosaminidase, and endopeptidase) (Giesbrecht *et al.*, 1998).

Page 19

Figure 1.6 Illustration of the ‘suicide module’ *mazEF* and how it can be activated. ppGpp and antibiotics that inhibit transcription and/or translation triggers *mazEF* dependant death. *mazEF* expression is induced in each case. Due to MazE being a labile protein, its cellular concentration is reduced below the level required to antagonize the toxic MazF (Engelberg-Kulka *et al.*, 2004).

Page 26

Figure 2.1 Illustration of the Mini Trans-Blot[®] electrophoretic transfer cell (BioRad, 2002).

Page 37

Figure 2.2 The coupling reaction in Edman degradation (Lottspeich, Houthaeve and Kellner, 1994).

Page 39

Figure 2.3 The formation of the DPTU by-product in Edman degradation (Lottspeich, Houthaeve and Kellner, 1994).

Page 39

Figure 2.4 The cleavage reaction in Edman degradation (Lottspeich, Houthaeve and Kellner, 1994).

Page 40

Figure 2.5 The conversion reaction in Edman degradation (Lottspeich, Houthaeve and Kellner, 1994).

Page 41

Figure 3.1 Disk diffusion assay for Enterococcal strain 382 tested against Penicillin and Vancomycin concentrations ranging from 5 to 60 μ g/ml. **(a)** Penicillin assay, with the MIC value established to be greater than 60 μ g/ml. **(b)** Vancomycin assay, where the culture was determined to be completely resistant.

Page 44

Figure 3.2 Plot of the diameter (mm) of the inhibition zones versus concentration of Penicillin G (μ g/ml), tested for strain E 21. The MIC was established on Tryptone soy agar plates, with 200 μ l of the starter culture inoculated into overlay agar and overlaid on the plate. The plots represent the following: Fit Curve (— —) and Raw Data (—).

Page 47

Figure 3.3 Minimal inhibitory concentration (MIC) of Enterococcal strains treated with the antibiotics, Penicillin G and Vancomycin. The results were determined after 24 hours of incubation at 37°C.

Page 48

Figure 3.4 Illustration of a typical sigmoidal bacterial growth curve, with each growth phase being represented (Torura, Funke and Case, 2004).

Page 49

Figure 3.5 Relative fitness profiles (raw data) for each Enterococcal strain, in the absence of antibiotic stress. The bacterial growth cycle was monitored as changes in the optical density at 600_{nm} over Time. The plots are represented as follows: **(a)** Strain E 21; **(b)** Strain E 175; **(c)** Strain E 406; **(d)** Strain E 859; **(e)** Strain E 904 and **(f)** Strain E 1393.

Page 52

Figure 3.6 Relative fitness profiles (raw data) for each Enterococcal strain, in the absence of antibiotic stress. The bacterial growth cycle was monitored as changes in the optical density at 600_{nm} over Time. The plots are represented as follows: **(g)** Strain E 908; **(h)** Strain E 468; **(i)** Strain E 943; **(j)** Strain E 382; **(k)** Strain E 301 and **(l)** Strain E 430.

Page 53

Figure 3.7 Relative fitness profiles (raw data) for each Enterococcal strain, in the presence of antibiotic stress (..°..). The bacterial growth cycle was monitored as changes in the optical density at 600_{nm} over Time. The plots are represented as follows: **(a)** Strain E 430; **(b)** Strain E 859; **(c)** Strain E 21; **(d)** Strain E 1393; **(e)** Strain E 406 and **(f)** Strain E 859.

Page 54

Figure 3.8 Standard curve of Bovine Serum Albumin (BSA) standards (0.5 - 200µg/ml). The plots represent the following: Fit Curve (—) and Raw Data (—).

Page 55

Figure 3.9 Protein profiles of Enterococcal strains analysed on 10% polyacrylamide gels, extracted with 4% SDS. The gels are represented as follows: **(a)** Strain E 21; **(b)** Strain E 175; **(c)** Strain E 406; **(d)** Strain E 1393; **(e)** Strain E 904 and **(f)** Strain E 859. Lanes 1-3: Represents extractions from different stages within the growth cycle. Lanes: 1, Mid exponential phase; 2, Early stationary phase; and 3, Early death phase. MwM: BioRad Precision Plus Unstained Standards Molecular Weight Marker.

Page 59

Figure 3.10 Protein profiles of Enterococcal strains on 10% polyacrylamide gels extracted with 4% SDS. The gels are represented as follows: **(g)** Strain E 382; **(h)** Strain E 943; **(i)** Strain E 908; **(j)** Strain E 468; **(k)** Strain E 430 and **(l)** Strain E 301. Lanes 1-3: Represents extractions from stages within the growth cycle. Lanes: 1, Mid exponential phase; 2, Early stationary phase; and 3, Early death phase. MwM: BioRad Precision Plus Unstained Standards Molecular Weight Marker.

Page 60

Figure 3.11 Gel slice of a 10% zymogram containing proteins extracted with 4% SDS from the different stages within the growth cycle of Enterococcus. The gels are represented as follows: **(a)** Strain E 859; **(b)** Strain E 175; and **(c)** Strain E 406. Each gel contains 0.1% (w/v) of the respective Enterococcal cell walls stained with 0.1% (w/v) Methylene Blue in 0.01% (w/v) KOH. Lanes 1-4: Represents autolytic activity from different stages within the growth cycle. Lanes: 1, Lag phase; 2, Mid exponential phase; 3, Early stationary phase; and 4, Early death phase. The arrows indicate putative autolysins which were selected for further characterization.

Page 62

Figure 3.12 Gel slice of 10% zymogram containing of proteins extracted with 4% SDS from different stages within the growth cycle of Enterococcus. The gels are represented as follows: **(d)** Strain E 21; **(e)** Strain E 301; and **(f)** Strain E 908. Each gel contains 0.1% of the respective Enterococcal cell walls stained with 0.1% Methylene Blue in 0.01% KOH. Lanes 1-4: Represents autolytic activity from stages within the growth cycle. Lanes: 1, Lag phase; 2, Mid exponential phase; 3, Early stationary phase; and 4, Early death phase. The arrows indicate putative autolysin selected for further characterization.

Page 64

Figure 3.13 Gel slice of 10% zymogram containing of proteins extracted with 4% SDS from different stages within the growth cycle of Enterococcus. The gels are represented as follows: **(g)** Strain E 382; **(h)** Strain E 943; and **(i)** Strain E 904. Each gel contains 0.1% of the respective Enterococcal cell walls stained with 0.1% Methylene Blue in 0.01% KOH. Lanes 1-4: Represents autolytic activity from stages within the growth cycle. Lanes: 1, Lag phase; 2, Mid exponential phase; 3, Early stationary phase; and 4, Early death phase. The arrows indicate putative autolysin selected for further characterization.

Page 66

Figure 3.14 Gel slice of 10% zymogram containing of proteins extracted with 4% SDS from different stages within the growth cycle of Enterococcus. The gels are represented as follows: **(j)** Strain E 430; **(k)** Strain E 1393; and **(l)** Strain E 468. Each gel contains 0.1% of the respective Enterococcal cell walls stained with 0.1% Methylene Blue in 0.01% KOH. Lanes 1-4: Represents autolytic activity from stages within the growth cycle. Lanes: 1, Lag phase; 2, Mid exponential phase; 3, Early stationary phase; and 4, Early death phase. The arrow indicates putative autolysin selected for further characterization.

Page 68

Figure 3.15 Sample PVDF blot of protein extracts from Strain E 175. The putative autolysin B was selected for further characterization. The blot was stained with Coomassie Blue. Lanes: 1, Lag phase; 2, Mid exponential phase; 3, Early stationary phase; and 4, Early death phase. MWM: BioRad Precision Plus unstained protein standards.

Page 69

Figure 3.16 BLAST alignment result for Autolysin A. Graphical overview of the alignments (a) and actual alignments (b).

Page 72

Figure 3.17 Graphical representation of the liberation of free reducing sugars from autolytic digests of Strain E 859 cell walls using the Morgan-Elson Assay. The liberation of free reducing sugars was monitored as changes in the optical density at 585_{nm} over Time after digestion with the selected autolysins (A, B, C, D, E, F and G).

Page 74

Figure 3.18 Graphical representation of the liberation of free amino groups from autolytic digests of Strain E 859 cell walls using 2,3-dinitrophenol (DNP) derivatization. The liberation of free reducing sugars was monitored as changes in the optical density at 585_{nm} over Time after digestion with the selected autolysins (A, B, C, D, E, F and G).

Page 76

List of Tables

Table 1.1 Characteristics in laboratory identification of *Streptococcus milleri* (*Streptococcus anginosus*) group (Gray, 2005).

Page 5

Table 1.2 The murein hydrolases of *Escherichia coli*, indicating enzymes whose genes have been mapped [Holtje, 1995].

Page 17

Table 2.1 Bacterial strains used in this study.

Page 30

Table 2.2 Experimental layout of the microtitre plates used during the Penicillin G and Vancomycin titrations respectively.

Page 31

Table 2.3 Preparation of diluted BSA standards for the protein concentration determination, using the BCA protein assay kit.

Page 33

Table 2.4 Composition of gels for the use in SDS-PAGE analysis.

Page 34

Table 2.5 Composition of gels prepared for Renaturation SDS-PAGE analysis.

Page 36

Table 3.1 Summary of the Disk diffusion and Micro titre plate assay's tested with the antibiotic Penicillin G, plates were incubated overnight at 37°C.

Page 45

Table 3.2a Protein Concentrations of 4% SDS autolytic extracts as determined from a standard curve constructed using the BCA assay.

Page 56

Table 3.2b Protein Concentrations of 4% SDS autolytic extracts as determined from a standard curve constructed using the BCA assay.

Page 57

Table 3.3 Summary of selected putative autolysins for further analysis.

Page 67

Table 3.4 N-Terminal Sequence results of the selected putative autolysins from the Enterococcal strains as determined via Edmund chemistry.

Page 71

List of Abbreviations

B. licheniformis

B. subtilis

E. coli

E. hirae

S. anginosus

S. aureus

S. constellatus

S. faecalis

S. intermedius

S. milleri

S. pneumoniae

Bacillus licheniformis

Bacillus subtilis

Escherichia coli

Enterococcus hirae

Streptococcus anginosus

Streptococcus aureus

Streptococcus constellatus

Streptococcus faecalis

Streptococcus intermedius

Streptococcus milleri

Streptococcus pneumoniae

AM

ATP

ATZ

BCA

BLAST

BSA

CAPS

CO₂

Da

DNA

DNP

DPTU

DTT

FDNB

N-acetylmuramoyl-L- alanine amidase

Adenosine triphosphate

Anilinothiazolinone

Bicinchoninic Acid

Basic Local Alignment and Search Tool

Bovine Serum Albumin

3-cyclohexylamino 1-propanesulfonic acid

Carbon dioxide

Dalton

Deoxyribose Nucleic Acid

N-dinitrophenyl

Diphenylthiourea

Dithiothreitol

Fluorodinitrobenzene

CHAPTER ONE

LITERATURE REVIEW

1.1 General Introduction

Autolysins (bacterial murein hydrolases) comprise of a diverse and broad spectrum of enzymes that cleave specific structural components within the bacterial cell wall. They participate in numerous cell activities during cell growth and division and peptidoglycan recycling and turnover.

The cell wall is a common component in bacteria. It comprises of a semi-rigid molecular complex, identified as the peptidoglycan or murein layer. This layer consists of two amino sugars, *N*-acetylglucosamine (NAG) and *N*-acetylmuramic acid (NAM), with a pentapeptide extension of the NAM structure. The cell shape is maintained by this cross-linked structure, which surrounds the cell (Rogers, Perkins and Ward, 1980).

The bacterial cell wall is under constant modification through hydrolysis, insertion of new material and the release of old material throughout the growth process. Therefore it is believed that hydrolase activity is crucial in the removal of peptidoglycan to ensure correct cell wall assembly. Autolysins are ubiquitous peptidoglycan hydrolases that are deemed responsible for the digestion of the cell wall in bacteria. The cell wall is the primary substrate for autolysins. Thus, this has lead to propositions that they are involved in cellular processes such as cell growth, cell wall turnover maturation of the peptidoglycan, cell division, motility, chemotaxis, genetic competence, protein secretion and pathogenicity (Foster, 1994).

Based on the substrate specificities, the autolysins are classified as *N*-acetylmuramidases, *N*-acetylglucosaminidases, *N*-acetylmuramyl-L-alanine amidases, or endopeptidases.

Programmed cell death (PCD) is a ubiquitous phenomenon that occurs in bacteria. It is instrumental in many cellular developmental processes, such as the lysis of the cell wall during sporulation. Autolysins have been associated with cell suicide. It is believed that this is advantageous for the long term survival of the bacteria.

Enterococcus is a member of the lactic acid bacteria genus. Initially, this genus was classified as *Group D Streptococcus*, but in 1984, through genomic DNA analysis, a separate genus classification was given (Schleifer and Kilpper-Balz, 1984). This group of bacteria has been taxonomical revised based on cultural, biochemical, serological and genetic characteristics. Consequently, due to these studies, a transfer of species occurred from the *Streptococcus* genus to a new separate genus, *Enterococcus* (Devriese *et al.*, 1993; Hardie and Whiley 1994; Devriese *et al.*, 1996; Leclerc *et al.*, 1996; Baele *et al.*, 2000; Bourne *et al.*, 2001).

Hence, throughout literature, the *Streptococcus* and *Enterococcus* genus has been used interchangeably. Therefore, for this study, the *Enterococcus* genus will be used. *Enterococcus* strains are separated into four distinct species, namely, *Enterococcus avium*, *Enterococcus durans*, *Enterococcus faecalis* and *Enterococcus faecium*.

The aim of this study was to isolate and characterise extracted autolysins from selected *Enterococcal* strains (previously from the genus *Streptococcus*). The objectives were to:

- (i) determine the relative fitness of selected enterococcal strains in the presence and absence of vancomycin and penicillin G.
- (ii) isolate autolysin from various growth stages of these strains as determined by the relative fitness assay.
- (iii) quantify the autolysins from the various growth stages.
- (iv) identify and partially analyse the autolysins by electrophoresis, Western blotting and Zymogram techniques.
- (v) biochemically characterise the autolysins .
- (vi) purify and sequence the isolates.

This thesis is divided into five chapters. The first chapter comprises of the general introduction and literature review. Chapter two presents details of the materials, methods and techniques used in this study. Included in chapter three are the results and discussion of the experiments utilized in chapter two. Chapter four presents the conclusions and thoughts on future research.

1.2 Introduction to *Streptococcus milleri*

Three closely related bacterial species have been addressed by the group name *Streptococcus milleri*. The three species are *Streptococcus anginosus*, *Streptococcus constellatus* and *Streptococcus intermedius* (Wanahita *et al.*, 2002). All three organisms collectively form part of the normal microbial flora in humans. However, once their normal growth conditions are disturbed, they result in human oral infections and abscess formation, of which isolates have been obtained from the mouth, female urogenital tracts and gastrointestinal tracts (Wiley *et al.*, 1992; Ruolff, 1995; Shinzato and Saito, 1995; Jerng *et al.*, 1997, Yamamoto *et al.*, 1999, Tomohisa, Kimura and Mori, 2005). In a recent study, it has been established that this group is a contributing pathogen in empyema and lung abscess, thus resulting in increased levels of morbidity and mortality (Jerng *et al.*, 1997). Further studies have revealed that the *S. milleri* group is susceptible to a range of antibiotics.

1.2.1 Bacteriology and Grouping

Based on DNA homology and 16S rRNA gene sequence analysis and phenotypic characteristics (Table 1.1), the *Streptococcus anginosus* or *Streptococcus milleri* group is now composed of 3 distinct species: *S. anginosus*, *Streptococcus constellatus*, and *Streptococcus intermedius* (Whiley *et al.*; 1990, 1992; Whiley and Beighton, 1991; Clarridge *et al.*, 1999). This group is part of the viridans group of streptococci. The members within the viridans group are considered to be susceptible to penicillin, however, resistant strains do exist (Jacobs and Stobberingh, 1996). A biochemical method of specie identification had been proposed by Whiley and Beighton (1991). This method allows for the phenotypic identification by testing for the production of α -galactosidase, β -galactosidase, α -glucosidase, β -glucosidase, β -*N*-acetylglucosaminidase, β -_D-fucosidase and sialidase with the aid of a 4-methylumbelliferyl-linked fluorogenic substrate.

Table 1.1 Characteristics in laboratory identification of *Streptococcus milleri* (*Streptococcus anginosus*) group (Gray, 2005).

Trait	Result
Colony Characteristics	Small, grey, pin point colonies on agar
Hemolysis	Alpha hemolysis*
Biochemical Reaction :	
Catalase	Negative
Voges-Proskauer	Positive*
Mannitol	Negative*
Sorbitol	Negative*
Arginine	Positive
Esculin	Positive
Urease	Negative
Lancefield Group Reaction	Group F*
Other	Butterscotch odor of colony on blood agar

* Indicates that other results are possible

1.2.2 Mode of Infection

The mode and mechanism of infection of this group remains a mystery. Thus, it is believed that these organisms produce extracellular enzymes, which degrades connective tissue thus preventing it from phagocytosis and therefore aiding in its pathogenicity. The enzymes include ribonucleases, deoxyribnucleases, hyaluronidases, gelatinases and collagenases (Piscitelli *et al.*, 1992; Lunn, Rahman and Macey, 2001).

A report by Wanahaita *et al.*, (2002) indicated that the three streptococcal species were present in clinical abscesses obtained from patients. As a result, *S. intermedius* was deduced to cause pleuropulmonary infections, central nervous abscesses as well as abscesses of deep soft tissue. The second species, *S. constellatus*, results in soft tissue, pleuropulmonary and intra-abdominal abscesses. The third specie, *S. anginosus*, as isolated from soft tissue, the pleural space and peritoneal cavity. Further studies revealed that these species are still present within the human polymorphonuclear leukocytes (PMNL), however, resisting digestion completely. As a result, an immune suppressive

substance is believed to aid in its pathogenicity, therefore allowing it to survive within an abscess (Yoshinori *et al.*, 1999).

1.3 Introduction of Autolysins

The bacterial cell wall contains a variety of endogenous peptidoglycan hydrolases. These hydrolases also occur in other organisms. Hen egg white lysozyme is a widely occurring example. It is located in animal tissue, milk, tears, cervical mucus, urine and plant tissue. Specialized enzymes allow for the cleavage of the existing covalent bonds within the bacterial cell wall, facilitating expansion during the growth stages and the splitting of the septum prior to cell separation. It is well understood that once microbes are placed in unfavorable growth conditions or experiences antibiotic stress, they die. This phenomenon is due to the autolysis of the cell wall, where bonds are hydrolyzed by enzymes, resulting in the disintegration of cells (Rogers, Perkins and Ward, 1980). Thus, by definition, an autolysin is a “self-digesting” enzyme, located within a cell, which specifically cleaves the structural components of the cell wall. In addition, these enzymes are also deemed responsible for the pathogenicity of bacteria and possible involvement in antibiotic susceptibility (Holtje and Tuomanen, 1991).

1.3.1 Types of Endogenous Bacteriocidal Enzymes and Specificities

There are four types of autolytic enzymes present within a microbe. The enzymes are muramidase, amidase, peptidase and glucosamidase (Shibata, *et al.*, 2005). Muramidase is a lysozyme-like enzyme that hydrolyses the NAM and NAG (1,4- β -*N*-acetylglucosamine) bonds, releasing free-reducing groups of *N*-acetylmuramic acid. In *Escherichia coli* (*E. coli*) and phage lambda, muramidase-like enzymes were isolated. They also displayed similar lysozyme activity, by cleaving the bond between the NAM and NAG residues. However, the difference occurred in the transfer of the muramyl bond onto the carbon-6-hydroxyl group of the same muramic acid, resulting in the formation of a 1-6-anhydromuramic acid (Holtje and Tomasz, 1975, Holtje and Tuomanen, 1991).

Amidasases are responsible for hydrolyzing the bond between the peptidoglycan chains and the peptide. They occur in numerous bacteria and are essential in maintaining the separation of the peptide components from the amino chains of the cell wall (Harz, Burgdorf and Holtje, 1990).

Peptidases are responsible for the hydrolysis of the main peptides when they occur between the D-alanyl terminus of the peptide chain. Thus, they display exo- and endopeptidase activities. The DD-carboxypeptidases convert the pentapeptide into a tetrapeptide, through the cleavage of the terminal D-alanyl-D-alanine bond of the stem peptides (Gmeiner and Kroll, 1981).

Finally, glycosamidases are responsible for the liberation of free-reducing groups of *N*-acetylglucosamine (Rogers, Perkins and Ward, 1980).

1.3.2 Biological Functions of Peptidoglycan Hydrolases

The proposed roles of autolysins are numerous. They are vital in the growth processes of the bacterial cell such as providing new acceptor sites, enlargement of the peptidoglycan, restructuring, cell division and separation and peptidoglycan turnover (Koch, 2000).

Biosynthesis of the peptidoglycan involves countless processes. Growth of the sacculus involves the generation of new bonds and the hydrolysis of the old bonds. Peptidoglycan hydrolases are instrumental in the growth of a Gram positive rod. They are necessary for cylindrical elongation in *Bacillus subtilis* (*B. subtilis*) (Koch, 2000). To achieve this function, the autolysins cleave the outermost layer of the cell wall, thus facilitating the addition of new layers of peptidoglycan. The addition of these layers results in the cell stretching as it grows longer, as illustrated with the thinning of the lines indicating the stretching of the murein (Figure 1.1), as they move towards the surface. Eventually, the autolysins dissolve the outermost murein (Koch, 2000).

Murein turnover, is the direct result of the growth process in bacteria. It is usually defined as the systematic loss of insoluble cell wall material. This usually occurs during the

vegetative growth in bacteria, thus implying that the peptidoglycan hydrolases must be actively involved in this process. In *E. coli*, murein turnover is associated with an efficient recycling pathway, resulting in the formation of murein precursors. The products are transported into the cytoplasm, where they are digested by recycling-specific murein hydrolases, including the amidases, glucosamidases and carboxypeptidases (Vollmer and Höltje, 2001). In *B. subtilis*, analysis of peptidoglycan fragments from the supernatant, revealed that an amidase was the sole enzyme involved in cell wall turnover. Due to the absence of amidase in the growth medium, the investigators presumed that the enzyme bound to the cell surface was instrumental in the removal of cell wall (Fiedler and Glaser, 1973).

In addition, peptidoglycan hydrolases are essential in the liberation of a mature spore during spore germination. This is achieved by dis-integrating the glycosidic bonds between the peptidoglycan monomers, and the peptide cross-bridges linking the rows of sugars together. This therefore facilitates cell wall expansion during cell growth (Rogers, Perkins and Ward, 1980). However, the most fundamental, if not the most important, role is the initiation of cell suicide (Lewis, 2000).

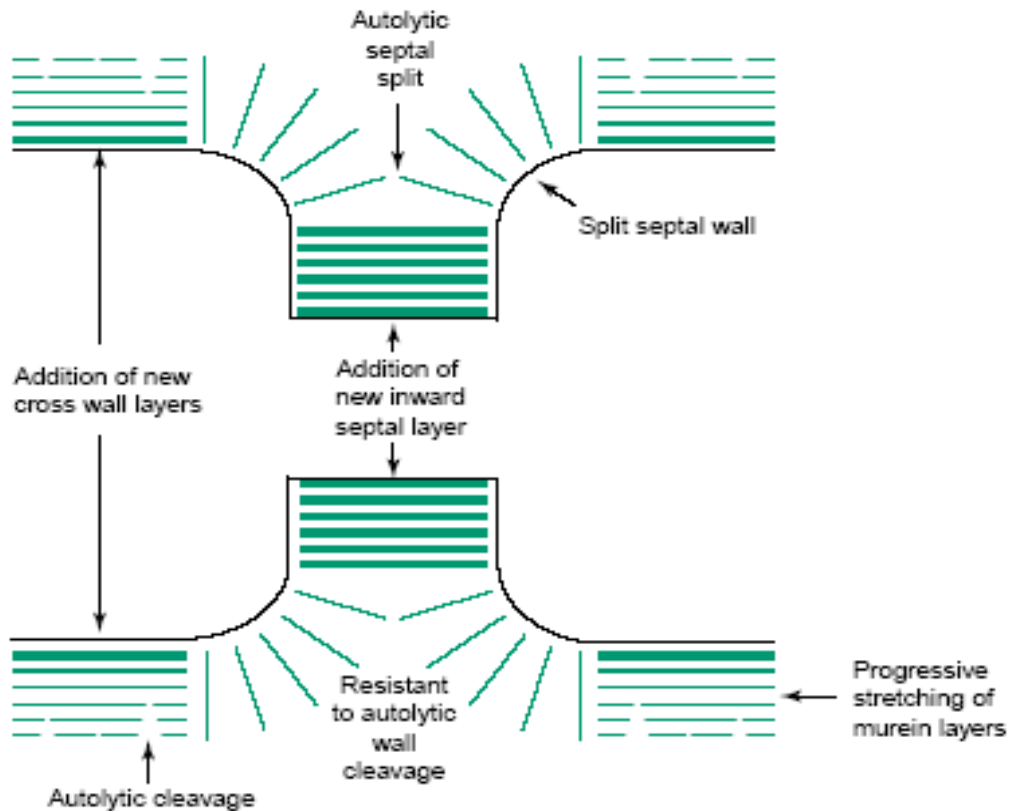


Figure 1.1 Cell wall growth of *Bacillus subtilis*. Side walls grow via inside-to-outside mechanism (Koch, 2002).

1.3.3 Control and Regulation of Peptidoglycan Hydrolases

Due to the high capacity of cell wall degradation, these hydrolases must be tightly regulated within the organism. This was evident at the posttranscriptional level, where murein hydrolase activity is regulated by cellular activities such as substrate modification, selective transport, interactions with lipoteichoic acids, peptides, and cleavage by proteolytic enzymes (Holtje and Tuomanen, 1991; Shockman and Holtje, 1994).

Within *E. coli*, it has been suggested that a “barrier” prevents the interaction of the peptidoglycan hydrolases with the peptidoglycan (Hartmann, Bock-Hennig and Schwartz, 1974). Betzner and Keck (1989) observed this phenomenon when the lytic

transglycosylase, *Slt70*, was over expressed in *E. coli*, and did not result in cell lysis. The conclusion was that this “barrier” could be limiting access to precise areas on the cell’s surface. In the case of *Enterococcus hirae* (*E. hirae*), such an area could be at or near nascent cross walls, whereas in *E. coli*, it could be attributed to the periplasmic ring structure (Higgins, Pooley and Shockman, 1970; Joseph and Shockman, 1974; Foley *et al.*, 1989). Even in *E. hirae*, the muramidase has no lytic effect on the growing cell. Thus Kariyama and Shockman (1992) have proposed that an exterior molecule could be protecting the cell wall from autolysis. In addition, the folding and orientation of the protein could also be instrumental in the autolytic activity of the muramidase.

The binding specificities of the autolysins are also instrumental in the control and regulation of autolysis. This has been observed in *E. hirae* and *S. faecalis*, where their peptidoglycan hydrolases bind with a high affinity to their substrates, thus limiting the number of binding sites (Beliveau *et al.*, 1991). The substrate specificity could also be limited with the availability of polysaccharides and teichoic acids for autolysin bondage. Clark and Dunpont (1992) reported that autolytic activity could also be limited by the alterations of the chemical nature of the peptidoglycan. Thus, *O*- and *N*-acetylation of the peptidoglycan decreased its susceptibility to hydrolysis upon addition of a hen egg white lysozyme.

Metabolic process can also be attributed to the regulation of peptidoglycan synthesis. As observed in *B. subtilis*, its energized state is crucial in the regulation of its amidase activity (Jolliffe, Doyle, and Streips, 1981). Furthermore, bacterial cultures of *E. hirae* ATCC 9790 have exhibited a low capacity to autolyze in the stationary phase, thus further emphasizing the role of metabolic processes and its relationship to the growth rate, cell division and death of the cell (Pooley and Shockman, 1970).

1.4 The Peptidoglycan Hydrolase System

1.4.1 The Murein Hydrolases of *Escherichia coli*

This organism harbors many cell wall degrading activities, and enzymes for virtually each type of covalent bond within the peptidoglycan. It contains glycosidases and peptidases, responsible for interacting with the polysaccharide chains and cleavage of peptidyl structure, respectively (Figure 1.2). In research conducted by Kitano, Tuomanen and Tomasz (1986), the authors isolated and characterized two major cell wall hydrolyzing enzymes in *E. coli*. The two autolytic products were a transglycosylase and an endopeptidase that were responsible for splitting the transpeptidase bonds between neighboring stem peptides in the murein, upon inhibition of cell wall synthesis.

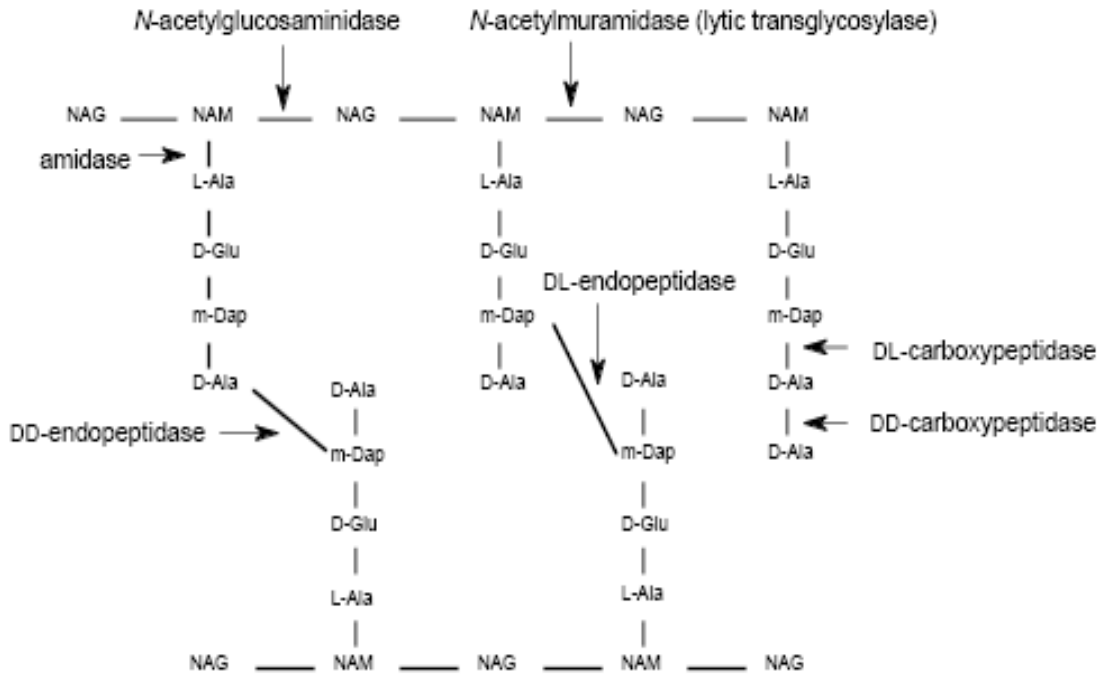


Figure 1.2 Illustration of the chemical cell wall structure of *Escherichia coli*. Arrows indicate the bonds cleaved by specific peptidoglycan hydrolases.

1.4.1.1 Glycosidases

There are three muramidase-like enzymes that are responsible for catalyzing specific reactions (Romeis, Vollmer and Holtje, 1993). These enzymes cleave the same bond as lysozyme, but the difference lies in the resultant muropeptide which does not contain a reducing end group. This enzyme was purified by Holjie *et al.*, (1975) and identified as a peptidoglycan hydrolase. It cleaved the β -1,4-glycosidic bond between the NAM and NAG residues, but also catalyzed an intramolecular glycosyltransferase reaction, producing a bond between the carbon 6 and carbon 1 of the muramic acid residue. Due to this intramolecular transglycosylation, the enzyme was termed a “lytic transglycosylase” (Holtje, Mirelman and Schwarz, 1975) (Figure 1.3).

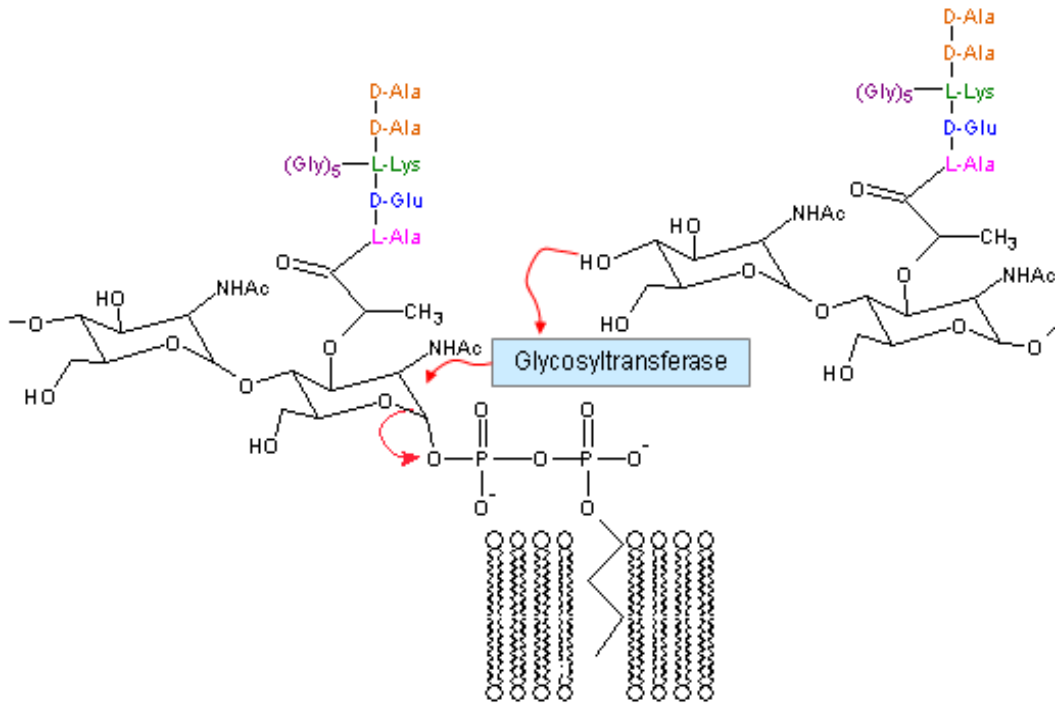


Figure 1.3 Illustration of glycosyltransferase interaction between the NAM and NAG residues (Smith, 2003).

The soluble form of the lytic transglycosylase (*Slr70*) was isolated from the periplasm. It had a molecular weight of 70 kDa, from which the *sltY* gene was mapped on the chromosome (Betzner and Keck, 1989). Due to the over production of the protein, this enabled for purification of the protein for crystallographic studies. Through X-ray crystallography, the three dimensional structure was elucidated (Figure 1.4). The protein comprises of three domains, an N-terminal domain, a linker domain and the C-terminal domain. The linker domain together with the N-terminal domain form a closed ring, referred to as “the doughnut”. The domains comprise of 27 α -helices which are spherically arranged. The C-terminal domain occurs on top of the ring domain. It is almost completely comprises of α -helices, except that it only contains three short stretches of β -sheets (Thunnissen, *et al*, 1994).

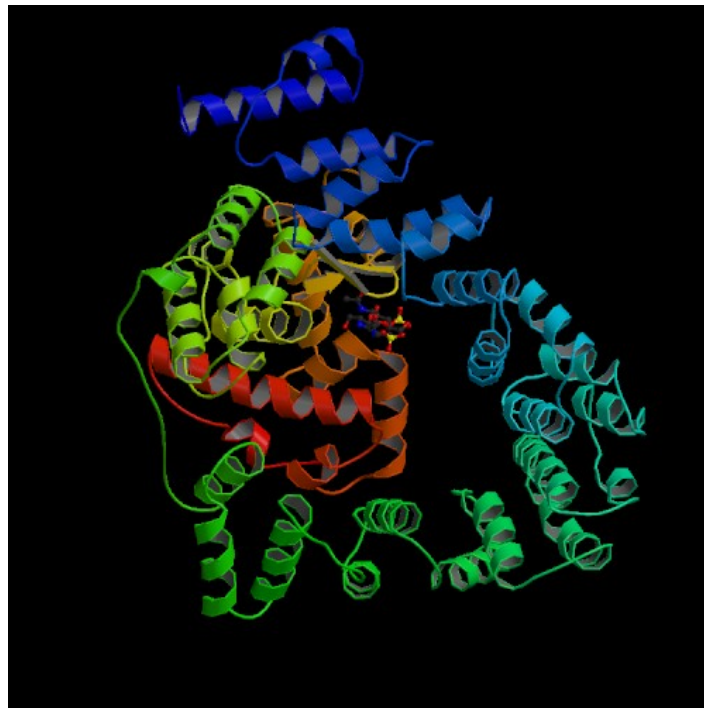


Figure 1.4 Illustration of the 3-D structure of *slt70* (Anon, 2006).

However, two other lytic transglycosylases were identified and mapped. They were the *MltA* and *MltB* respectively, which were both membrane bound. They both proved to be lipoproteins occurring in the outer membrane. Both enzymes were purified and *MltA* had a molecular mass of 38 kDa, while *MltB* had a molecular mass of 36 kDa (Ursinus and Holtje, 1994). Yet, when *MltB* was cleaved into its active soluble form, it had a molecular mass of 35 kDa (Ehlert, Holtje and Templin, 1995). Previously, this degraded product of *MltB* was known as “soluble lytic transglycosylase 35” (*Slr35*) (Engel, van Wijngaarden and Keck, 1992).

In *E. coli*, a β -*N*-acetylglucosaminidase was initially shown to be present by Yem and Wu (1976). The authors confirmed the presence of the enzyme within the cytoplasm, as well as its activity on murein degradative products. It was also responsible for releasing *N*-acetylglucosamine from the isolated murein lipoprotein complex. The relative size of this enzyme was 36 kDa, and confirmed by SDS-PAGE.

1.4.1.2 Peptidases, Endopeptidases, Exopeptidases and Amidases

A peptidase is an enzyme that catalyzes the cleavage of peptide bonds, resulting in the reduction of peptides in to amino acids.

An endopeptidase essentially cleaves the peptide cross bridges, thus dissolving the murein network (Figure 1.2). There are three different murein endopeptidases in *E. coli*, which have been characterized. These DD-endopeptidases hydrolyze the DD-peptide bonds between the D-alanine and meso-diaminopimelic acid. Two of these endopeptidases are the penicillin binding proteins, PBP4 and PBP7 (Table 1.2).

The analysis of PBP4 has revealed it is encoded by the *dacB* gene. The estimated molecular mass, as determined by SDS-PAGE, was 44 kDa. Yet, over production of the *dacB* gene results in a decrease in cross linking (Korat, Mottl and Keck, 1991). This further suggests that it acts as a DD-endopeptidase and as a DD-carboxypeptidase *in vivo*. In addition, this further implies that the specific activity of PBP4 is increased just before

cell-separation, therefore signifying a possible role of this protein in cell division (Hakenbeck and Messer, 1977).

The recent cloning and characterization of PBP7 has revealed it to also display DD-endopeptidase activity (Henderson, Templin and Young, 1995). It is loosely bound to the cell membrane, and cleaves the D-alanyl-D-diaminopimelyl bond, in the presence of high molecular weight murein. However, this activity is not observed in soluble dimeric peptides, which is cleaved by PBP4. The degradation product of PBP7 is PBP8, an OMPT protease (Henderson, Dombrosky and Young, 1994). Tuomanen and Schwartz (1987), have also described the PBP7 to have a high affinity for the penem antibiotics. These antibiotics are capable of inducing lysis in non-growing bacteria which are normally resistant to the effects of other β -lactams.

The third DD-endopeptidase is a penicillin insensitive enzyme, which is encoded by the *mepA* gene (Keck *et al.*, 1990). This gene codes for a 30 kDa protein, which cleaves the main dap-D-Ala cross links and the dap-dap cross links, thus playing a role in the autolysis of the peptidoglycan (Keck *et al.*, 1990).

Within *E. coli*, two groups of carboxypeptidases have been recognized. They are the DD-carboxypeptidases and the LD-carboxypeptidases. The DD-carboxypeptidases have been identified as PBP5 and PBP6 respectively. PBP5 and PBP6 are the gene products of *dacA* and *dacC*, respectively (Broome-Smith *et al.*, 1988). However, overproduction of PBP5 instigates the spherical growth of *E. coli* (Markiewicz *et al.*, 1982). These enzymes have been proposed to regulate the degree of cross linking, by removing the terminal alanine from the stem peptide (van der Linden *et al.*, 1992). The function for PBP6 is yet to be established.

Recently, an LD-carboxypeptidase (32 kDa) had been purified with the aid of nocardidin A-sepharose affinity chromatography. This enzyme is the primary target of nocardicin A, a D-amino-acid-substituted β -lactam antibiotic. Its role is to remove the second D-ala, resulting in the formation of a tripeptide. Two other LD-carboxypeptidases have also been isolated from *E. coli*, with molecular masses of 12 and 86 kDa respectively (Metz, Henning and Hammes, 1986; Ursinus and Holtje, 1992).

The amidases are responsible for the cleavage of the amide bond between the lactyl group of muramic acid and L-alanine of the peptidyl moiety. In *E. coli*, two *N*-acetylmuramyl-L-alanine amidases have been identified. The periplasmic amidase, *amiA* (39 kDa), has been reported to only accept low molecular weight muropeptides as a substrate. Thus it has been assumed that it is required in the recycling of the peptidoglycan (van Heijenoort *et al.*, 1975; Parquet *et al.*, 1983).

Table 1.2 The murein hydrolases of *Escherichia coli*, indicating enzymes whose genes have been mapped [Holtje, 1995].

Enzyme	Gene	Molecular mass (kDa)	Localization	Comments
[I]				
Lytic transglycosylases				
(It)				
Soluble It 70 (Slit70)	<i>sltY</i>	70.5	Periplasm	
Membrane-bound ItA (MltA)	<i>mltA</i>	38.9	Outer membrane	Lipoprotein
Membrane-bound ItB (MltB)	<i>mltB</i>	39.0	Outer membrane	Lipoprotein
(Soluble It35 (Slit35))		35	Periplasm	Proteolytic product of MltB
[II]				
<i>N</i> -acetylmuramyl-L-alanine-amidases				
AmiA	<i>amiA</i>	39	Periplasm	Does not accept whole sacculi
AmiD	<i>amiD</i>	20.3	Cytoplasm	Negative regulator of β -lactumase expression
[III]				
DD-Endopeptidases				
PBP4	<i>dacB</i>	49.6	Membrane associated	Additional DD-carboxypeptidases activity
PBP7	<i>pbhG</i>	32	Membrane associated	Inhibition by certain pneum antibiotics
MepA	<i>mepA</i>	30	Periplasm	Penicillin-insensitive
[IV]				
DD-Carboxypeptidases				
PBP4	<i>dacB</i>	49.6	Membrane associated	Additional DD-endopeptidases activity
PBP5	<i>dacA</i>	41.3	Inner membrane	
PBP6	<i>dacC</i>	40.8	Inner membrane	

1.4.2 Peptidoglycan Hydrolases from *Streptococcus pneumoniae*

With *Streptococcus pneumoniae* (*S. pneumoniae*), its autolytic enzymes have been extensively researched and characterized. It harbors the *LytA*, *LytB* and *LytC* autolysins. The *LytA*, is an *N*-acetylmuramoyl-*L*-alanine amidase, which is essential for the majority of autolysis within this organism. In a *LytA* mutant, *LytC* is responsible for autolysis (Garcia *et al.*, 1999). The *lytA*, is an amidase that cleaves the bond between the glycan chain and the stem peptide (Figure 1.5). Therefore, it is responsible for cell wall solubilization and cell lysis in the stationary growth phase and during β -lactam treatment (Ronda *et al.*, 1987; Majcherczyk *et al.*, 1999). This enzyme interacts with the choline containing teichoic acid in the cell wall, by specifically binding to them. The synthesis of this enzyme occurs in the cytoplasm, in the “E” form, which has minor peptidoglycan activity. However, in the absence of the choline rich residues within the cell wall, it is not converted into the active “C” form, nor is it transported through the membrane. An allosteric change in the enzyme and the formation of a choline-amidase complex, results in the “C” configuration of the enzyme (Höltje and Tomasz, 1975). Yet, a deletion in *lytA* results in a tolerance to β -lactam antibiotics. This was reported by Berry *et al.* (1989), that upon inactivation of the *lytA* gene in a capsulated virulent strain, the export of the major virulence factor, pneumolysin, was disturbed. Consequently, this suggested that an autolysin is instrumental in protein export.

1.4.3 Peptidoglycan Hydrolases from *Staphylococcus aureus*

S. aureus possess three kinds of catalytic peptidoglycan hydrolases. The three hydrolases are: an *N*-acetylmuramoyl-*L*-alanine amidase (AM), an endo- β -*N*-acetylglucosaminidase (GL) and an endopeptidase, which hydrolyses the peptidoglycan at specific sites (Figure 1.5). In a study conducted by Groicher *et al.* (2000), a mutant strain was generated, and the resultant stationary phase zymographs indicated that the *lrgAB* mutant exhibited higher extracellular murein hydrolase activity as compared to the wild-type strain, due to the presence of more intense band patterns in the gel. They concluded that the gene products of the *lrgAB* Operon in *Staphylococcus aureus* (*S. aureus*), inhibits murein hydrolase activity, therefore elevating the penicillin tolerance in the organism.

In another study, zymographic analyses revealed numerous bands on the gel, thus implying that a greater number of enzymes are responsible for the autolytic activities. However, extracts from the stationary phase of growth exhibited a lower presence of autolytic enzymes (Komatsuzawa *et al.*, 1995). In addition, this activity appeared to be genetically regulated by the *lytS-lytR* regulatory locus within *S. aureus* (Brunskill and Bayles, 1996; Giesbrecht *et al.*, 1998).

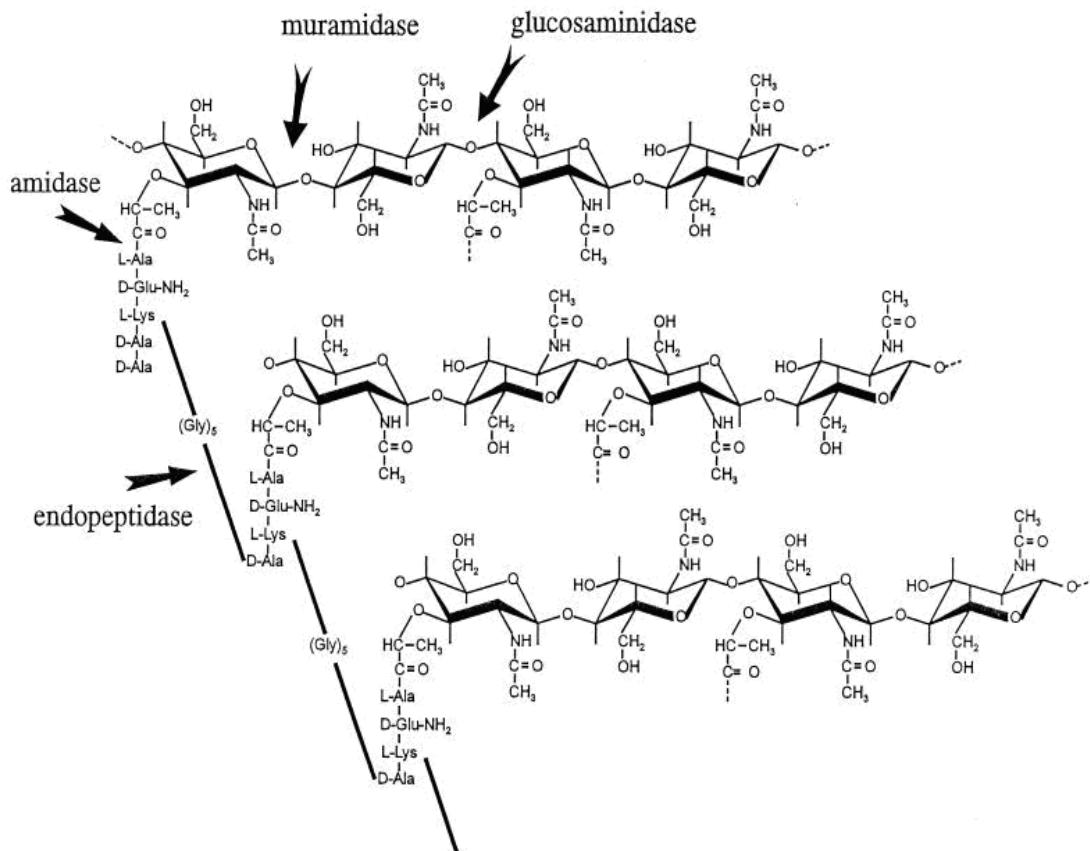


Figure 1.5 Illustration of the peptidoglycan structure and sites of attack by cell wall hydrolases. The sites where cell wall hydrolases may attack peptidoglycan are indicated by arrows, but staphylococci contain only three of these wall hydrolases (amidase, glucosaminidase, and endopeptidase) (Giesbrecht *et al.*, 1998).

1.4.4 Peptidoglycan Hydrolases of *Enterococcus hirae* ATCC 9790

This well studied bacterium has two muramidases responsible for cleaving the β -1,4 bond between MurNac and GlcNAc (Kawamura and Shockman, 1983; Shockman and Holtje, 1994). The muramidases are known as muramidase-1 and muramidase-2. Kawamura and Shockman (1983) established muramidase-1 to be a glycoprotein due to its ability to hydrolyze the re-acetylated peptidoglycan and the sodium dodecyl sulphate treated cell walls of *E. hirae* 9790. The 130 kDa muramidase-1 can be converted to the active 87 kDa form by the addition of proteinases. The muramidase-2 differs from muramidase-1 in its substrate and its ability to hydrolyze the non acetylated peptidoglycan fraction of *E. hirae* walls of *Micrococcus luteus*. Thus muramidase-2 is an unusual enzyme. However, when muramidase-2 is extracted from bacteria, the purified preparations contain two polypeptides of approximately 125 and 74 kDa. Both the polypeptides exhibit peptidoglycan hydrolase activity (Dolinger *et al.*, 1989).

1.4.5 Peptidoglycan Hydrolases of *Bacillus licheniformis*

A gene coding for the cell wall hydrolase of *B. subtilis*, was cloned into *E. coli*. The gene was termed *cwlM*, of which the sequencing results indicated the presence of an open reading frame encoding a polypeptide of 253 amino acids. It had a molecular mass of 27513 Da. This gene played a role in cell lysis. Further amino acid analysis confirmed a repeat sequence of 33 amino acids in the C-terminal region. However, cell wall activity was not affected upon deletion of the C-terminal. Further characterization of *cwlM*, with regards to specific bond cleavage, revealed that the enzyme was an *N*-acetylmuramoyl-L-alanine amidase. In addition, its hydrolytic activity was more effective in the presence of a *Micrococcus luteus* cell wall than in comparison to *B. licheniformis* and *B. subtilis*. In contrast, this efficiency was lost due to the absence of the C-terminal (Kuroda, Rashid and Sekiguchi, 1992).

1.4.6 Peptidoglycan Hydrolases of *Bacillus subtilis*

Two major autolysins have been clone and characterized to participate in the vegetative growth process. They are an *N*-acetylmuramoyl-L-alanine amidase (*lytC*) and an endo- β -*N*-acetylglucosaminidase (*lytD*), which are 50 kDa and 90 kDa respectively (Kuroda and Sekiguchi, 1991; Margot, Mauel and Karamata, 1994; Rashid, Mori, Sekiguchi, 1995). The *lytC* is an amidase which hydrolyzes the *N*-acetylmuramoyl-L-alanine link in the peptidoglycan (Yamamoto, Kurosawa and Sekiguchi, 2003).

1.4.6.1 The Genetic Organization of *Bacillus* hydrolases

Within *B. subtilis* 168 exists a three-gene regulatory operon, *lytABC*. The *lytC* is part of this operon, which also divergently transcribes for *lytR*. The *lytR* gene encodes for a putative DNA-binding protein (35 kDa), which represses the expression of the *lytABC* and *lytR* operons (Lazarevic *et al.*, 1992). Two sigma promoters are responsible for the transcription of the *lytABC* operon: σ^D and σ^A . The σ^D promoter controls the expression of the genes involved in chemotaxis and motility, whereas the σ^A promoter controls majority of the transcription during growth (Smith and Foster, 1995).

The *lytA* product is believed to be an acidic protein which is considered to be associated with the cell membrane, is 9.4 kDa (Kuroda, Asami and Sekiguchi, 1993). In contrast, the *lytB* product is a cell-wall associated modifier protein, that upon its bondage with *lytC*, its activity is further enhanced (Lazarevic *et al.*, 1992). Upon cleavage of the signal peptide, both their molecular masses are 74.1 and 49.9 kDa respectively. The N-terminal moieties, for *lytB* and *lytC*, are considerably homologous to each other. In addition they have three GSNRY consensus motifs, a characteristic of virtually all amidases (Kuroda, Asami and Sekiguchi, 1993).

Further investigation of the glucosamidase region showed a monocistronic operon which encodes for a 95.6 kDa protein. This was achieved through nucleotide sequencing. This protein consisted of 880 amino acid residues with a typical signal peptide. Through amino acid sequencing, two types of direct repeats were evident. Each repeat was present twice in the N-terminal to central region of the glucosamidase. It is presumed that these

repeats denote the cell wall binding domain. The glucosamidase was subjected to zymographic analysis, which showed that it was partly processed to numerous smaller proteins, thus preserving its lytic activity. On the contrary, serial deletions from the N-terminus uncovered the loss of more than one repeat unit, therefore radically reducing its autolytic activity to cell walls (Rashid, Mori and Sekiguchi, 1995).

Inclusively, two minor autolysins have been found to be present in the surface extract of the vegetative cell. They are *lytE* and *lytF* respectively (Ohnisi, Ishikawa and Sekiguchi, 1999). The product of *lytE* is a 33 kDa cell wall-bound protein CWBP33, which is expressed during the exponential phase of growth. Sequence analyses uncovered two domains, where the N-terminal domain had a threefold-repeated motif, while the C-terminal domain shared homology to a few exoproteins (Margot *et al.*, 1998). In addition, the C-terminal of *lytE* possesses DL-endopeptidase activity. Transcription of the *lytE* gene is controlled by the $E\sigma^A$ and $E\sigma^H$ RNA polymerases (Ohnisi, Ishikawa and Sekiguchi, 1999; Yamamoto, Kurosawa and Sekiguchi, 2003).

The C-terminal domain of *lytF* (50 kDa) possesses DL-endopeptidase activity resulting in linkage disruption of D- γ -glutamyl-*meso*-diaminopimelic acid in the murein peptide. The transcription of *lytF* is controlled by the $E\sigma^D$ RNA polymerase. Both *lytE* and *lytF* have been implicated in cell separation.

1.4.7 Peptidoglycan Hydrolases in Other Bacterial species

The presences of peptidoglycan hydrolases are common to most bacteria. However, constant investigations are revealing additional bacterial species that display evidence of peptidoglycan hydrolases. Currently, the primary issue is to establish whether all bacterial species do produce these autolytic enzymes, and if so, what are their roles in terms of cell activities and cell wall production. With the availability of various isolation and cloning methods, these questions can be answered, thus enabling for the further characterization of the autolytic genes and proteins present within the bacterial cell.

1.5 Introduction to Bacterial Programmed Cell Death

Programmed cell death (PCD), commonly known as apoptosis, is a fundamental process that occurs in bacterial cell development. This mechanism results from a variety of stimuli within the cell. However, the survival or demise of the cell is purely dictated by its ability of resistance or susceptibility to death. Over the years, research has resulted in the characterization of numerous molecular components of the apoptotic machinery (Aravind, Dixit and Koonin, 1999). Programmed cell death is thought to be vital during the development of fruiting bodies in *Myxococcous xanthus* and *B. subtilis* spore elimination (Wireman and Dworkin, 1977; Smith and Foster, 1995). This phenomenon is also instrumental in the release of damaged cells, induced by antibiotic stress (Lewis, 2000). Cell apoptosis can occur through two pathways, either the intrinsic (mitochondrial) pathway or the extrinsic (death receptor) pathway. Both pathways results in the activation of the caspase cascade eventually leading to cell death (Hengartner, 2000).

1.5.1 PCD and Altruism

These bacterial activities have raised the question that as a consequence of evolution, bacteria have selected PCD as a survival strategy. In addition, within multicellular organisms, altruism has been observed, thus researchers are curious to identify whether altruism also occurs in bacterial populations. Altruism, by definition, is behavior that reduces the reproductive success of the altruist, thus increasing the reproductive success of other. This behavior has been well documented in honeybees and could be applicable to bacteria. Hamilton (1964), had proposed a model suggesting that the genetic material within an individual is equivalent to related individuals containing the same number of shared alleles. Therefore, if the fitness of the gene is favored, an increase in frequency of the genes occurs, regardless whether the genes occur within the individual or in closely related kin. This model can be applied to bacteria, since within a bacterial colony there is 100% genetic relatedness. Therefore, the possibility of an individual organism exhibiting this behavior is quite possible, thus aiding in the hypothesis that this selection could have given rise to PCD.

1.5.2 PCD in Bacteria

1.5.2.1 Morphological Evidence

As mentioned, PCD has been proposed to occur in bacterial development. An example of this was found in the life-cycle of *Streptomyces*. This Gram positive soil bacterium, produces multinucleoid hyphae and within its life-cycle, the hyphae die. Thus, research has revealed that the reason for this is due to the hyphae undergoes a systematic process of internal cellular disassembly. The steps involved include the formation of an open network of DNA, genome digestion, degradation of cytoplasmic components, retraction of the membrane and the formation of vesicles. These re-organizational and degradative steps share similarity to eukaryotic processes, thus suggesting that the hyphal death within this organism is a genetically programmed process (Miguelé et al., 1999).

PCD has also been observed in *Xanthomonas campestris*, which is the causative agent of bacterial pustule disease of soy bean. Gautam and Sharma (2002) reported that *in vitro* studies of this organism revealed that in the post-exponential phase of growth, it underwent rapid cell death. Further analysis of the supernatant revealed the presence of nicked DNA as well as the presence of a 55 kDa endogenous enzyme, which displayed caspase-3-like activity. The presence of this enzyme and the nicked DNA was then associated to features similar in eukaryotic apoptosis, suggesting PCD activity.

The organism, *Helicobacter pylori*, also exhibits apoptotic activity, in response to changes in its environmental conditions. Its morphology is affected, as it changes from a helical appearance to a coccoid form, particularly when the culture has aged or exposed to unfavorable conditions such as nutrient depletion, aerobiosis, antibiotics and high temperatures (Berry et al., 1995; Benaissa et al., 1996; Kusters et al., 1997). Kusters et al. (1997) have also reported that the bacterium displays a loss of membrane components and a decrease in the DNA and RNA content, suggesting that in the coccoid form, it is undergoing cell death. This morphological manifestation is further evidence of PCD.

PCD has been proposed to occur in the photosynthetic cyanobacterium species *Anabaena* (Hochman, 1997). Ning *et al.* (2002), has recently reported that when several strains of this *Anabaena* are exposed to salt stress, they exhibit similar features of eukaryotic PCD. This includes DNA fragmentation, increased protease activities and disorganization, fragmentation and the autolysis of the bacterial cell.

1.5.2.2 Genetic Evidence

Increasing research has suggested that PCD could be mediated through a genetic system. This is evident in *E. coli*, due to the presence of the *mazEF* system. In this system (Figure 1.6) the *mazF* gene encodes for the toxin, while *mazE* codes for the labile antitoxin that interferes with the action of the toxin (Pederson *et al.*, 2002). The *mazEF* genes form an operon upstream with the *relA* gene. The *relA* gene product is an ATP:GTP 3'pyrophosphotransferase (ppGpp). Upon amino acid starvation, ppGpp synthesis is activated, and the accumulation of ppGpp inhibits the expression of *mazEF* (Aizenman *et al.*, 1996). Therefore, under stressful conditions, the labile antitoxin (*mazE*) would be degraded, thus allowing for the expression of the toxin (*mazF*), which promotes cell lysis. the suggestion that *mazEF* plays a role in PCD was further strengthened with studies in thymine starvation. In this study, Sat *et al.* (2003) showed that the mutant *mazEF* strain was 100% viable when subjected to thymine starvation, whereas the wild-type strain lost its viability. In addition, the activity of the P₂ promoter, responsible for transcription and regulation of *mazEF*, was greatly reduced upon thymine starvation (Engelberg-Kulka *et al.*, 2004). Thymine starvation has prompted research of similar activation of PCD in other bacterial species.

Within *S. aureus*, exists a locus involved in the regulation of murein hydrolase activity. This locus contains the *lytSR* operon encoding for the sensor and response regulatory proteins, *lytS* and *lytR*, respectively (Brunskill and Bayles, 1996; Koch, 2001). Characterization of the mutant *lytSR*, revealed evidence that the *lytSR* operon was involved in the regulation of murein hydrolase activity. The strain used was KB300. It was noted that the cell growth in liquid media formed large aggregates, which suggested that the cell were undergoing spontaneous lysis. This was also observed upon the addition

of Triton-X100 and penicillin, where the murein hydrolase activity was altered. Electron microscopic analyses further verified this occurrence in the mutant strain (Brunskill and Bayles, 1996).

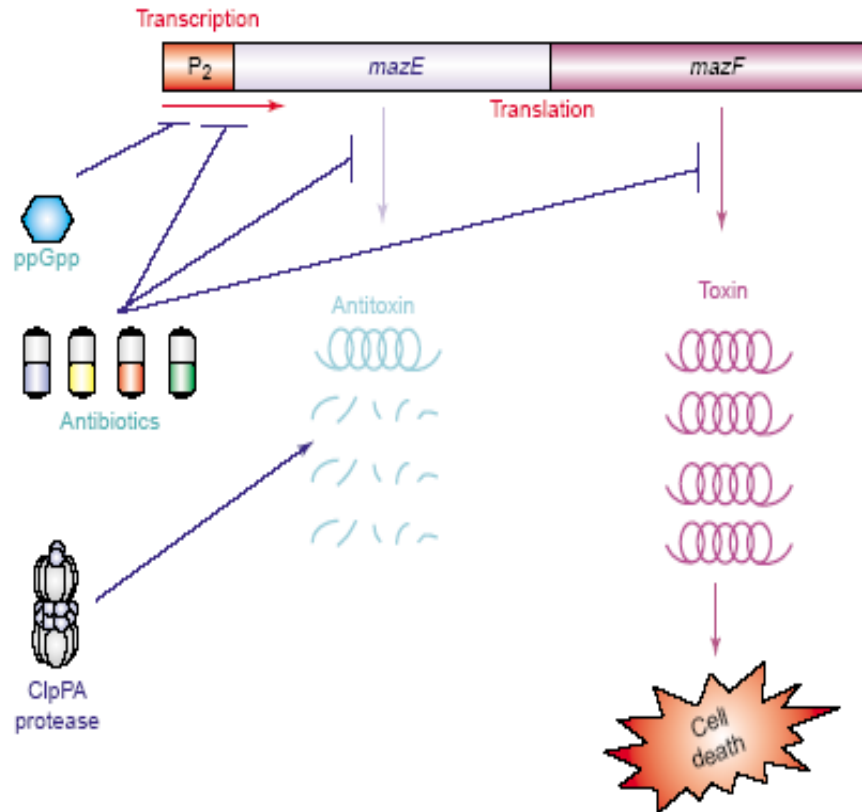


Figure 1.6 Illustration of the ‘suicide module’ *mazEF* and how it can be activated. ppGpp and antibiotics that inhibit transcription and/or translation triggers *mazEF* dependant death. *mazEF* expression is induced in each case. Due to MazE being a labile protein, its cellular concentration is reduced below the level required to antagonize the toxic MazF (Engelberg-Kulka *et al.*, 2004).

1.5.2.3 Antibiotic-Induced Killing

Deregulation of murein hydrolase activity can lead to autolysis of the bacterial cell. This has been observed during the stationary phase of cell growth as well as upon addition of an antibiotic (Heidrich *et al.*, 2001). However, the exact trigger for PCD with the addition of an antibiotic, is still unknown. A theory has been suggested that the deregulation of autolytic activity, upon antibiotic exposure, is a manifestation of bacterial PCD (Lewis, 2000; Normark and Normark, 2002). This theory has sparked numerous investigations using *S. pneumoniae*, which implies murein hydrolysis is a requirement for antibiotic-induced lysis. On the contrary, in a study conducted by Moreillon *et al.* (1990), they found that penicillin-induced killing and penicillin-induced lysis are two separate events. This was demonstrated with a mutant *S. pneumoniae* strain, containing an inactivated *lytA* gene, which was still destroyed in the presence of penicillin. Thus, it was concluded that this mechanism if antibiotic-induced killing could be a step in the PCD pathway which is induced upon antibiotic exposure (Moreillon *et al.*, 1990).

In *S. pneumoniae*, exists a two component signal transduction system, *VncR/S*. It is believed to be responsible for triggering PCD in response to antibiotics (Novak *et al.*, 1999; Novak *et al.*, 2000). This system was identified by screening a *S. pneumoniae* library of mutants for penicillin tolerance. Studies on this system revealed that it was part of a signal transduction pathway, which leads to antibiotic-induced cell death. Characterization of this system revealed a small open reading frame (ORF) upstream from *vncRS*, encoding for an amino acid peptide (Pep²⁷). A Pep²⁷ mutant showed tolerance to several antibiotics, but upon addition of the synthetic version, it induced the loss of cell viability (Novak *et al.*, 2000). In addition, over-expression of *VncS*, induced autolysis, thus suggesting that it is a negative regulator. Therefore, it was concluded that Pep²⁷ is a “death signal peptide” that, in some way, interacts with *VncS* upon antibiotic exposure (Novak *et al.*, 2000, Koch, 2001).

1.6 Conclusion

Autolysins are enzymes that seem to be present in all bacteria, and are instrumental in the regulation of autolytic activity. However, there is no other evidence of other enzymes that are capable of such activity.

In literature, there is a large amount of evidence that points towards the existence of PCD in bacteria. These stresses occur during the course of the bacterial development, and are indicated as either molecular or morphological changes. Despite being historically studied in eukaryotes, further investigations in bacterial systems will shed light as to the control and regulation of the autolytic events in all bacteria. In addition, further research needs to be done to provide a solid link between the molecular elements involved in apoptosis in eukaryotic organisms and bacterial PCD.

A recent increase in global infections caused by bacteria, has re-initiated research into drug and vaccines development. In addition, mechanisms of bacterial growth and resistance have been explored as to gain insight to this phenomenon. Therefore, the identification of novel targets, within a bacterial cell, has become a crucial step in the development of therapeutics. As a result, research is being directed into establishing the exact sequence of cellular events that lead to cell lysis, and the effects of antibiotic induced lysis. As a consequence, cell wall physiology and the regulation of murein hydrolase activity is currently being explored.

Further characterization of bacteria will contribute to our knowledge of autolysins, thus allowing for the design of effective vaccines and drugs that would specifically interact with these components and assist in curbing emerging and potential pathogens.

CHAPTER TWO

MATERIALS AND METHODS

2.1 Bacterial Culture and Growth Conditions

In this study, 12 Enterococcal strains (Table 2.1) were kindly provided by Dr. Mervyn Beukes (University of Kwa-Zulu Natal, Pietermaritzburg, South Africa). The cultures were grown over-night in Tryptone Soy Broth (TSB) (Merck) medium at 37°C, with vigorous shaking (Sambrook, Fritsch, and Maniatis, 1989). Glycerol stocks of the cultures were maintained at -70°C in 30% (v/v) glycerol. Working cultures were grown on Tryptone Soy Agar (TSA) (Merck) plates. The plates were sub-cultured weekly and stored at 4°C.

Table 2.1 Bacterial strains used in this study.

Strain	Strain designation in this study
<i>Enterococcus</i> 382	E 382
<i>Enterococcus</i> 1393	E 1393
<i>Enterococcus</i> 904	E 904
<i>Enterococcus</i> 430	E 430
<i>Enterococcus</i> 943	E 943
<i>Enterococcus</i> 301	E 301
<i>Enterococcus</i> 21	E 21
<i>Enterococcus</i> 908	E 908
<i>Enterococcus</i> 406	E 406
<i>Enterococcus</i> 859	E 859
<i>Enterococcus</i> 468	E 468
<i>Enterococcus</i> 175	E 175

2.2 Disk Diffusion Assay

Over-night cultures (150µl), of the test strains, were inoculated into 5ml toplayer agar (half strength agar, 7% w/v), and spread onto the surface of TSA (Merck) plates using a hockey stick spreader. The relative antibiotic susceptibilities were tested using sterile paper disks containing penicillin and vancomycin, ranging from 0.1µg/ml to 60µg/ml. After over-night incubation at 37°C, plates were checked for inhibition zones. The relative size of the inhibition zones were measured and tabulated.

2.3 Minimum Inhibition Concentrations (MIC)

The MIC was established for each strain using the Micro Broth dilution method. A 1% inoculation (2µl) of the respective over-night cultures was added to microtitre plate wells containing Muller Hinton Broth (Becton, Dickson and Company), to a final volume of 200µl per well. *E. coli* was used as a control organism. A 10mg/ml stock solution of the antibiotics Penicillin G (Roche) and Vancomycin (SIGMA) was prepared respectively. The antibiotic concentrations tested ranged from 0 to 70µg/ml for each antibiotic. In Table 2.2, well number 11 was denoted as the positive control, as no antibiotic was added to this well. However, well number 12 were denoted as the negative control as no inoculation was performed, and no antibiotic was added. The microtitre plates were incubated for 36 hours at 37°C in a 5% CO₂ atmosphere.

Table 2.2 Experimental layout of the microtitre plates used during the Penicillin G and Vancomycin titrations respectively.

Well position	1	2	3	4	5	6	7	8	9	10	11	12
Antibiotic conc.[µg/ml]	70	60	50	40	30	20	10	5	1	0.5	+ve	-ve
Antibiotic (µl)	14	12	10	8	6	4	2	1	0.2	0.1	-	-
dH₂O (µl)	6	8	10	12	14	16	18	19	19.8	19.9	20	20
Broth	Add 180µl of Muller Hinton Broth into wells											
Total Volume	200µl across each well											

2.4 Relative Fitness Assay

Overnight-cultures of each strain were inoculated into sterile 10ml TSB (Merck) respectively. A 1% inoculation, of the pre-cultures, was done in 100ml of TSB (Merck) medium in 250ml Erlenmeyer flasks. The flasks were placed in a 37°C shaking water-bath to allow for aeration. The growth monitored at hourly intervals by determining the optical density (OD) of 600nm using a spectrophotometer. Growth curves were constructed using SIGMA PLOT 2000 by plotting the OD vs time.

2.5 Extraction of Autolytic Proteins

A pre-culture of each strain was prepared by inoculating a single colony in 10ml of TSB (Merck). The cultures were grown over-night at 37°C with vigorous shaking. For the extraction of autolysins 200µl of this overnight culture was inoculated into 200ml of TSB (Merck). The cultures were incubated at 37°C, with agitation. Autolytic enzymes were extracted at different stages of the growth cycle based on the results from the relative fitness assays. At the correct growth stage the cultures were dispensed into 250ml sterile centrifuge tubes, and centrifuged at 7700 x g, for 10 min, at 4°C. The resulting pellet, was resuspended in 4% SDS (w/v), and incubated overnight with gentle agitation at room temperature. The SDS extracts were stored at -20°C until further use.

2.6 Preparation of Crude Cell Wall Extracts

Crude cell walls (peptidoglycan) were prepared from overnight cultures grown in TSB (Merck) at 37°C. This culture was prepared with a 1% inoculation, of the overnight culture, in 200ml TSB (Merck) and incubated at 37°C to an OD_{600nm} of approximately 0.9. Cells were pelleted by centrifugation at 8000 x g, for 10 min, at 4°C. The pellet was resuspended in 3ml of sterile distilled water. The suspension was placed in a boiling water bath for 30 minutes and centrifuged at 12100 x g, for 15 min, at 4°C. The pellet was washed twice with 50mM phosphate buffer (pH 7.5), centrifuged and resuspended in a minimal volume of 50mM phosphate buffer (pH 7.5). This served as the crude cell wall substrate to be used in the renaturation SDS-PAGE (Zymogram) assay.

2.7 Total Protein Concentrations

Total protein concentrations were determined using the Micro BCA Kit (Pierce Biotechnology, Rockford, USA), according to the manufacture's instructions. Briefly, a fresh set of Bovine Serum Albumin (BSA) Protein Standards were prepared from the content of one BSA ampule. This was diluted into several clean 15ml vials according to Table 2.3. The working reagent was prepared in a ratio of 25:24:1 of MA:MB:MC reagents, respectively. In addition, a 1:1 ratio of the sample to working reagent was prepared. The samples, and standards, were incubated in a waterbath at 60°C for 1 hour. The optical densities were measured at an OD_{562nm} , and a standard curve was plotted using, SIGMA PLOT 2000. The standard curve was used to calculate the concentration of the extracted autolysins.

Table 2.3 Preparation of diluted BSA standards for the protein concentration determination, using the BCA protein assay kit.

Vial	Volume of Dilute (ml)	Volume of BSA (ml)	Final BSA Concentration ($\mu\text{g/ml}$)
A	4.5	0.5 of BSA Stock	200
B	8.0	2.0 of vial A dilution	40
C	4.0	4.0 of vial B dilution	20
D	4.0	4.0 of vial C dilution	10
E	4.0	4.0 of vial D dilution	5
F	4.0	4.0 of vial E dilution	2.5
G	4.8	3.2 of vial F dilution	1
H	4.0	4.0 of vial G dilution	0.5
I	8.0	0	0 = Blank

2.8 SDS-PAGE Gel Electrophoresis

Gels were prepared, using a modified Laemmli system (Laemmli, 1970), and a Hoefer SE 250 Mighty Small II vertical slab system (Amersham). Briefly, two gels were prepared, a 10% separating gel and 4% stacking gel (Table 2.4). The gel was left to polymerize for an hour at room temperature, then assembled according to the manufacturer's instructions. The unit and chambers were filled with pre-cooled tank buffer [0.025M Tris, 0.192M glycine, 0.1% (w/v) SDS, pH 8.3]. The samples contained an equal volume of sample buffer [125mM Tris-HCl, 4% (w/v) SDS, 20% (v/v) glycerol, 0.2M dithiothreitol (DTT) (Roche, South Africa), 0.02% (w/v) bromophenol blue, pH 6.8]. Prior to loading onto the gel, samples were boiled for 5 minutes, to completely denature the proteins. Electrophoresis was carried out at a current of 18mA per gel, until the bromophenol blue marker migrated to the bottom to the gel (approximately 2 hours). Gels were stained with Coomassie blue and protein bands analysed.

Table 2.4 Composition of gels for the use in SDS-PAGE analysis.

Reagents	Running Gel	Stacking Gel
Acrylamide (BDH)	3.15ml	650µl
Distilled water	5.4ml water	3.0ml
0.5 M Tris HCl (pH 6.8)	-	1.25ml
3 M Tris HCl (pH 8.8)	1.25ml	-
50% (v/v) Glycerol	200µl	-
20% (v/v) SDS	50µl	25µl
TEMED	15µl	5µl
10% APS	36µl	25µl

2.9 Coomassie Blue Staining

The gel was placed in staining solution [0.025% (w/v) Coomassie Brilliant Blue R 250, 40% (v/v) methanol, 7% (v/v) acetic acid], and agitated over-night on a Hoefer PR 50 rotary shaker. The staining solution was replaced with destaining solution II [7% (v/v) acetic acid, 5% (v/v) methanol] and further agitated until proteins bands were visual and the background sufficiently low.

2.10 Renaturing SDS-PAGE Gel Electrophoresis (Zymogram)

Renaturing gels were prepared as a slight modification of the Sugai *et al.*, (1997) paper. The 10% separating gel component contained 0.1% (w/v) of the isolated crude cell wall substrate. This substrate used was from the same strain as the lytic extract being analysed for lytic activity. Gels were allowed to polymerized (Table 2.5) overnight at 4°C prior to use. The samples were mixed with sample buffer (as previously described) in a 1:1 (v/v) ratio, and boiled for 5 minutes. The boiled samples were loaded onto the gel which was subsequently run at 32mA constant current for 90 minutes. Upon completion of the electrophoresis, the gels were soaked for 2 hours in 250ml distilled water at room temperature, with agitation. The distilled water was changed every half hour. In the final half hour, the gels were soaked in fresh distilled water, and incubated at 37°C. The gels were subsequently placed in 150ml of renaturation buffer [50mM Phosphate buffer, pH 7.5 containing 1% (v/v) Triton-X100] and incubated at 37°C for 18 hours. Lytic activity was observed as clear bands in the opaque gel. To enhance the visibility of the lytic activity, the gels were stained for 5 minutes in zymogram stain [0.1% (w/v) methylene blue, 0.01% (w/v) potassium hydroxide], and destained extensively with distilled water.

Table 2.5 Composition of gels prepared for Renaturation SDS-PAGE analysis.

Reagents	Running Gel	Stacking Gel
Acrylamide	3.15ml	650µl
Distilled water	1ml crude extract + 4.4ml water	3.0ml
0.5 M Tris HCl (pH 6.8)	-	1.25ml
3 M Tris HCl (pH 8.8)	1.25ml	-
50% (v/v) Glycerol	200µl	-
20% (v/v) SDS	50µl	25µl
TEMED	15µl	5µl
10% APS	36µl	25µl

2.11 Elution of Lytic Proteins from Zymograms

Protein bands linked to lytic activity were excised from the zymogram. The gel slices were placed in a Model 422 Electro-Eluter (BIO-RAD, California), and extractions were performed according to the manufacture's instructions. The eluted proteins were stored in renaturation buffer [50mM Phosphate buffer, pH 7.5], at -20 °C for further usage.

2.12 Electro. Blot Transfer

Duplicate gels, 10% and 4% SDS PAGE, were prepared to resolve the proteins. A gel blotting sandwich was prepared as illustrated in Figure 2.1. The proteins were transferred onto a Sequi-Blot[®] polyvinylidene (PVDF) membrane (BIO-RAD) in CAPS buffer [10mM 3-cyclohexylaminol 1-propanesulfonic acid, 10% (v/v) methanol, pH 11], using the Mini Trans-Blot[®] electrophoretic transfer cell (BIO-RAD) according to the manufacturer's instructions (Figure 2.1). The transfer was performed at 90 volts, maximum current for 120 minutes. The blots were stained for 5 minutes in PVDF staining solution [0.025% (w/v) Coomassie Brilliant Blue R 250, 40% (v/v) methanol], and destained for 15 minutes in PVDF destain solution [50% (v/v) methanol]. The blots were dried between filter paper, and stored at 4°C for further analysis.

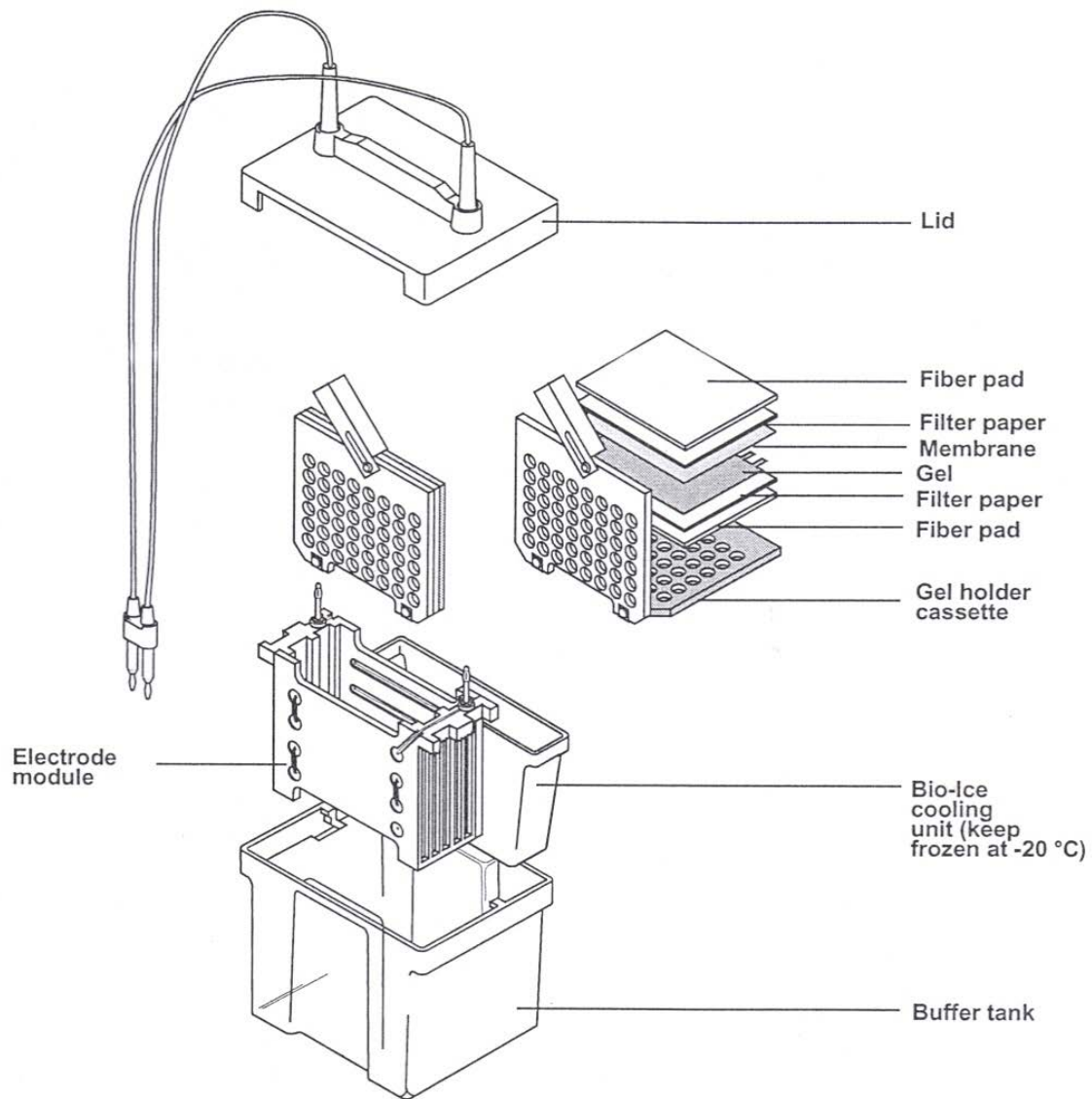


Figure 2.1 Illustration of the Mini Trans-Blot[®] electrophoretic transfer cell (BioRad, 2002).

2.13 N-Terminal Sequencing

From the blots, individual bands corresponding to the lytic activity on the respective zymograms were excised for N-terminal sequencing. The amino acid sequences were obtained by automated Edman Chemistry on a Procise, Applied Biosystems 491 Protein sequencer (PE, Applied Biosystems). These experiments were performed at the Molecular Biology Unit (MBU) of the University of Kwa-Zulu Natal (Pietermaritzburg, South Africa).

Edman degradation reaction involves the sequential cleavage and derivitization of the N-terminal amino acid from a peptide, thus allowing for the derivatized residue to be identified. The procedure is a three step process comprising of a coupling, cleavage and conversion step respectively. This results in the formation of a PTH amino acid (derivatized residue) which can be identified via HPLC and UV detection (Lottspeich, Houthaeve and Kellner, 1994).

The Coupling Step

In this step, the Edman reagent phenylisothiocyanate (PITC) is coupled to the free N-terminal amino group of the target peptide. The reaction occurs within 15-30 minutes at a pH of 9.0 and temperature ranging between 40-55°C. An unprotonated amine group is essential for the coupling reaction to occur which results in a phenylthiocarbamyl (PTC) peptide (Figure 2.2). Additional increases in pH increases the hydrolysis of the PITC side chain, producing aniline. The free amino group of aniline reacts with the PITC, resulting in a diphenylthiourea (DPTU) by-product (Figure 2.3) (Lottspeich, Houthaeve and Kellner, 1994).

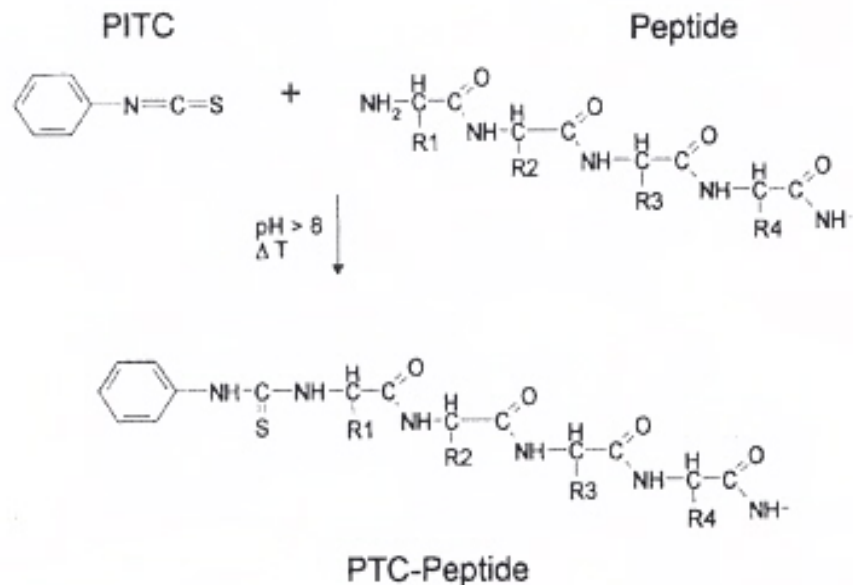


Figure 2.2 The coupling reaction in Edman degradation (Lottspeich, Houthaeve and Kellner, 1994).

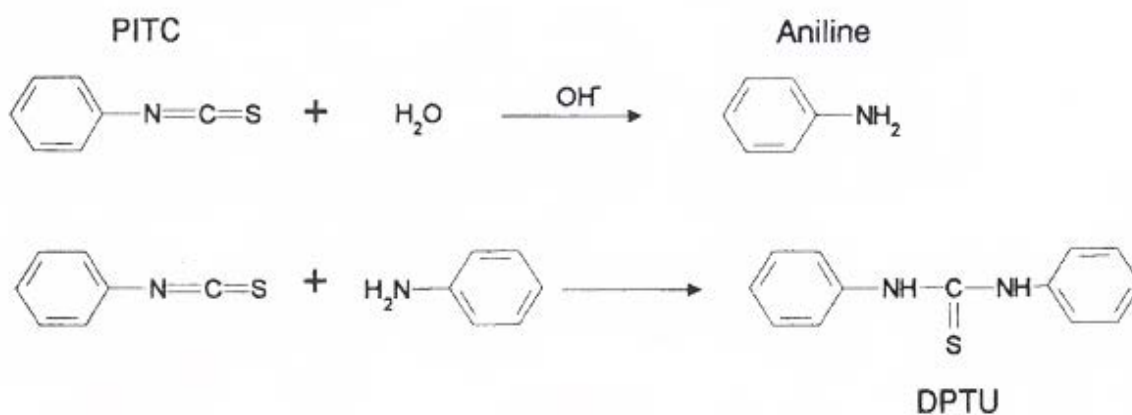


Figure 2.3 The formation of the DPTU by-product in Edman degradation (Lottspeich, Houthaeve and Kellner, 1994).

The Cleavage Step

The first amino acid of the PTC peptide is cleaved as a heterocyclic derivative, and identified as an anilinothiazolinone (ATZ) amino acid (Lottspeich, Houthaeve and Kellner, 1994). The ATZ amino acid is highly unstable after cleavage (Figure 2.4).

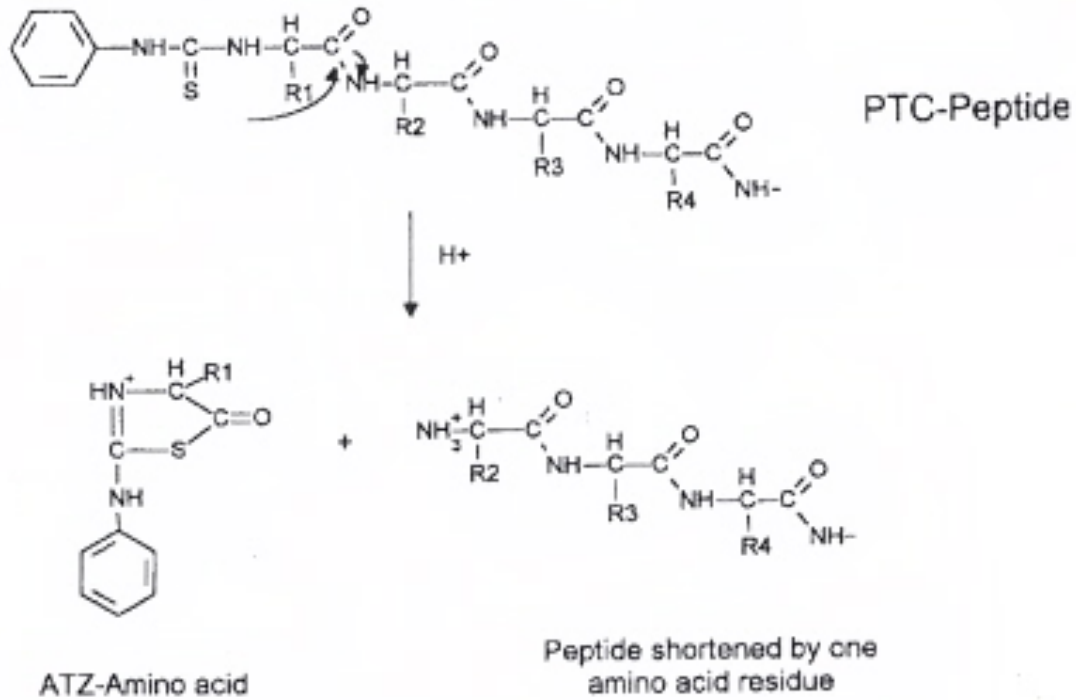


Figure 2.4 The cleavage reaction in Edman degradation (Lottspeich, Houthaeve and Kellner, 1994).

The Conversion Step

In this step, the ATZ amino acid is re-arranged to form the stable PTH derivative (Figure 2.5). The N-terminus of the newly shortened peptide is subjected into another cycle to undergo the three steps of Edman degradation.

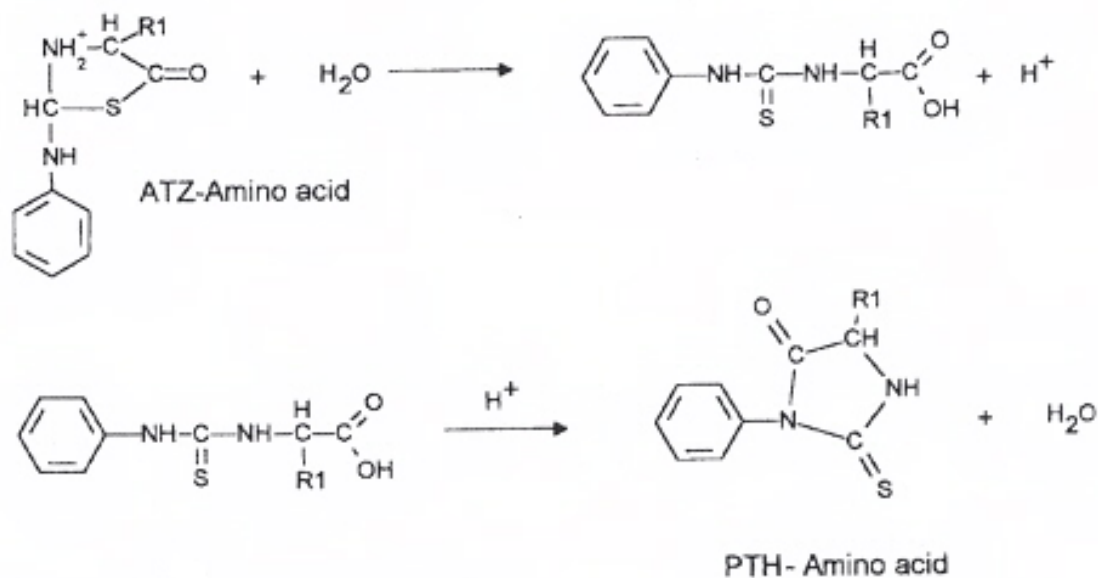


Figure 2.5 The conversion reaction in Edman degradation (Lottspeich, Houthaevé and Kellner, 1994).

2.14 Morgan-Elson Assay

The appearance of *N*-acetylamino sugars was assayed by the Morgan-Elson reaction (Ghuysen *et al.*, 1966; Beukes *et al.*, 2000). The *Enterococcal* cell walls (1mg) were digested at 37°C with the gel extracted autolytic enzyme (1µg/ml) in 50mM Phosphate buffer (pH 7.5). Mutanolysin (SIGMA, Germany) was used as the control, and was digested under the same conditions. These digests were centrifuged and the resultant supernatant was dried under a vacuum and redissolved in 1% (w/v) Potassium Tetraborate ($K_2B_7O_4$, Sigma). This mixture was then assayed for reduced sugars (Ghuysen *et al.*, 1966; Beukes *et al.*, 2000). The Morgan-Elson reagent was prepared by dissolving *p*-Dimethylaminobenzaldehyde (Sigma) (16g) in acetic acid (95ml), to which concentrated hydrochloric acid (HCl) was added (5ml). This stock reagent was diluted 1:8 with acetic acid to produce the colour reagent. The redissolved samples (20µl) were heated for 30 minutes at 100°C. Upon cooling, 90µl of fresh colour reagent was added and the mixtures incubated for 20 minutes at 37°C. The absorbance was read at an optical density of 585nm.

2.15 N-dinitrophenyl (DNP) Assay

The appearance of free amino groups was assayed using the N-dinitrophenyl assay. Fluorodinitrobenzene (FDNB) (Sigma) reagent was prepared by diluting 130 μ l in 10ml of 100% ethanol. The 1% (w/v) $K_2B_7O_4$ resuspension was mixed with 2 μ l of FDNB reagent and incubated at 60°C for 30 minutes. This mixture was acidified with 2N HCl (80 μ l) and absorbency readings were read at the wavelength of 420nm.

2.16 Protein Sequence Analysis

Sequences obtained from the N-terminal amino acid sequencing were analyzed for homology to other protein sequences, by performing a BLAST analysis. Analysis were performed via the EXPAZY web interface using the SwissProt database For this method, the query sequence was aligned with sequences present within the NCBI database, and significant alignment sequences were obtained.

CHAPTER THREE

RESULTS AND DISCUSSION

3.1 Disk Diffusion Assay and Minimum Inhibitory Concentrations (MIC)

The sensitivity of a bacterial strain when exposed to any antibiotic is expressed as the MIC. This is the minimum antibiotic dosage that prevents microbial growth (Atlas, 1995). Two methods were used to determine the MIC values for the 12 Enterococcal strains used in this study. For both methods, all the strains tested were resistant when exposed to Vancomycin (Figure 3.1). The antibiotic susceptibility data, including Disk Diffusion and Micro titre plate results, are summarized in Table 3.1. After 24 hours of incubation, 6 of the 12 strains tested displayed resistance to Penicillin G.

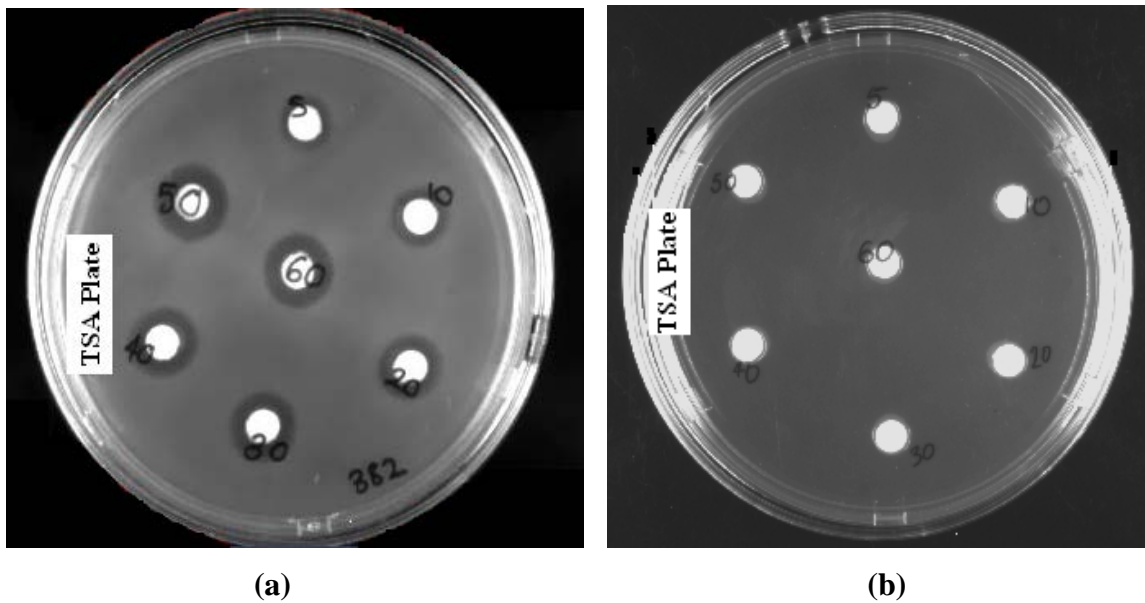


Figure 3.1 Disk diffusion assay for Enterococcal strain 382 tested against Penicillin and Vancomycin concentrations ranging from 5 to 60µg/ml. (a) Penicillin assay , with the MIC value established to be greater than 60µg/ml. (b) Vancomycin assay, where the culture was determined to be completely resistant.

Table 3.1 Summary of the Disk diffusion and Micro titre plate assay's tested with the antibiotic Penicillin G, plates were incubated overnight at 37°C.

Strain	Disk Diffusion Assay with Penicillin G (µg/ml)	Micro Titre Plate Assay with Penicillin G (µg/ml)
E 21	10	20
E 430	10	20
E 406	5	10
E 859	10	20
E 1393	10	20
E 943	10	30
E 904	> 60	> 80
E 468	> 60	> 80
E 908	> 60	> 80
E 382	> 60	> 80
E 301	> 60	> 80
E 175	> 60	> 80

As shown in Table 3.1, only 6 of the 12 strains tested were resistant to Penicillin G. In Figure 3.3, a similar trend was noticed for Penicillin G but not for Vancomycin, as all the strains showed resistance. Vancomycin is a glycopeptide antibiotic. Thus, resistance is mediated by two gene clusters, the *vanA* and *vanB* gene clusters. Vancomycin acts by binding to the D-alanyl-D-alanine terminus of the stem pentapeptides within the bacterial peptidoglycan. This allow for altering this site to D-alanine-D-lactate. As a consequence, it inhibits a late stage in extracellular bacterial cell wall synthesis (Waltho and Williams, 1991; Arthur, Reynolds and Courvalin, 1996). Previous findings have established that the MIC for Penicillin G to be greater than 64µg/ml, which is consistent with the MIC values in this study (Weinstein, 2001).

It has been reported that enterococci are acquiring resistance to vancomycin by producing peptidoglycan precursors ending in a depsipeptide D-alanyl-D-lactate, instead of the dipeptide D-Ala-D-Ala that occur in susceptible variants of enterococci. This substitution prevents the formation of complexes between glycopeptides and peptidoglycan

precursors at the cell surface, which in turn are responsible for inhibition of cell wall biosynthesis (Baptists *et al.*, 1996; Cetinkaya, Falk and Mayhall, 2000).

Mutations are considered as another factor facilitating bacterial resistance. According to literature, certain lactam tolerant bacteria are able to mutate, giving rise to resistant cells (Novak *et al.*, 2000). This type of mutation preferentially occurs at specific loci on the organisms' chromosome, under selective antibiotic pressure. According to Koch (2001), bacteria possess several genetic regions capable of rapid mutation. These regions are depicted by the presence of successive tandem repeats with varying lengths. These arrangements in particular, facilitate miss repairing or miss copying, resulting in the production of an altered protein, and possibly assisting in the organisms' resistant phenotype.

The disk diffusion technique was utilized to measure the radii of the resultant inhibition zones. Figure 3.2 graphically represents the relationship between the MIC and the corresponding values of antibiotic stress. When compared to the data in Figure 3.3, it can be established that for sample E 21, there is a direct correlation to the MIC value, where increasing levels of antibiotic produced an increase in the diameter of the zone of inhibition. A similar trend was noted for the remaining 5 samples (not shown). This trend characteristically represented a relationship between the antibiotic levels and the inhibition zones, which increased proportionally.

These results was in accordance with a study done by Kohner *et al.* (1997), where they established that the disk diffusion method produced high levels of errors. Their results also indicate that the microtitre plate assay is more sensitive and reliable than the disk diffusion assay. Therefore, in this study, further experiments were based on the MIC values established from the microtitre plates (Table 3.1). The MIC was interpreted as the lowest concentration of drug at which no growth was visible in the well of the microtitre plate.

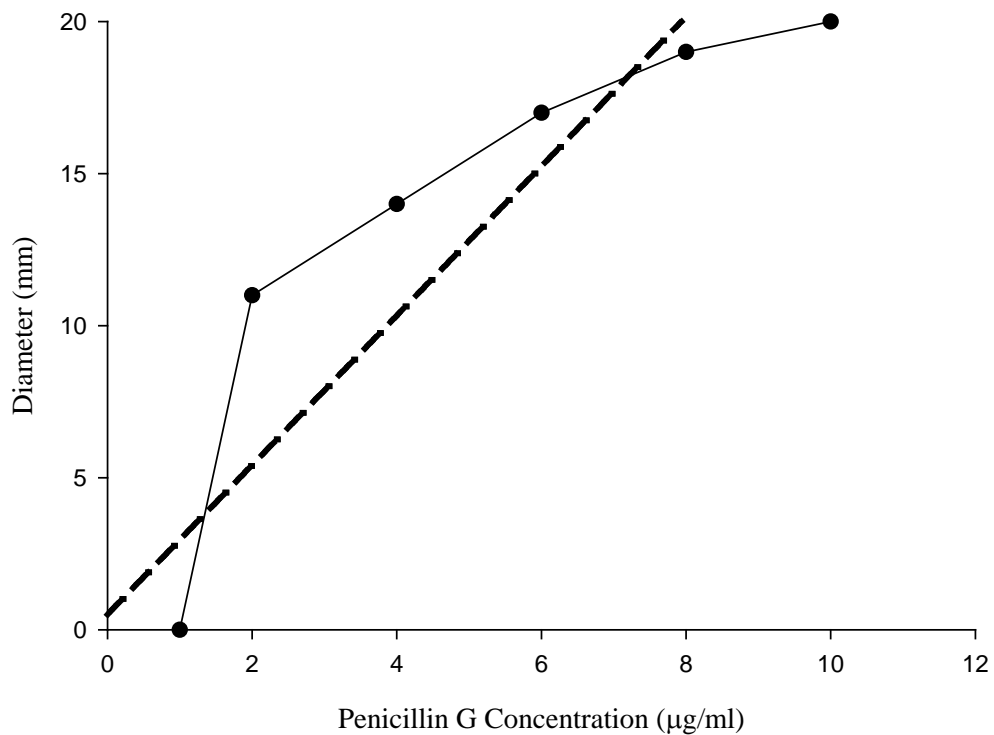


Figure 3.2 Plot of the diameter (mm) of the inhibition zones versus concentration of Penicillin G ($\mu\text{g/ml}$), tested for strain E 21. The MIC was established on Tryptone soy agar plates, with $200\mu\text{l}$ of the starter culture inoculated into overlay agar and overlaid on the plate. The plots represent the following: Fit Curve (— —) and Raw Data (—).

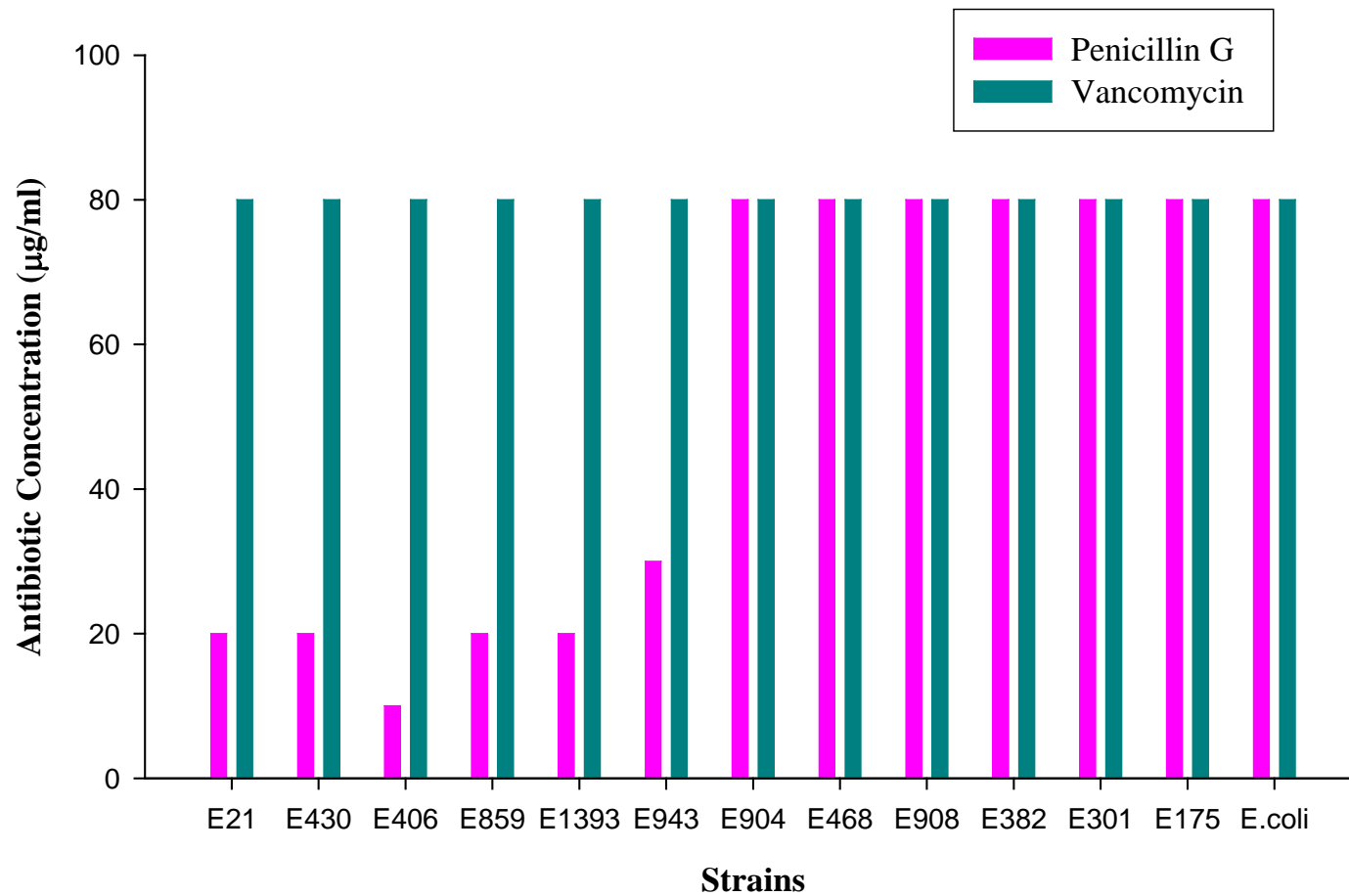


Figure 3.3 Minimal inhibitory concentration (MIC) of Enterococcal strains treated with the antibiotics, Penicillin G and Vancomycin. The results were determined after 24 hours of incubation at 37°C.

3.2 Relative Fitness Assay

The typical growth stages of a bacterial population are represented in Figure 3.4. The lag phase involves the adaptation of the organism to the medium. This is followed by the exponential phase, where the organism divides and the population increases exponentially. This continues until nutrients are depleted and toxic products accumulate. At this point the stationary phase commences, where the population is constant. Thereafter, the cells die and the population exponentially decreases resulting in the death phase (Prescott, Harley and Klein, 1999).

Thus, the relative fitness assays were performed to establish the growth curves for the 12 strains.

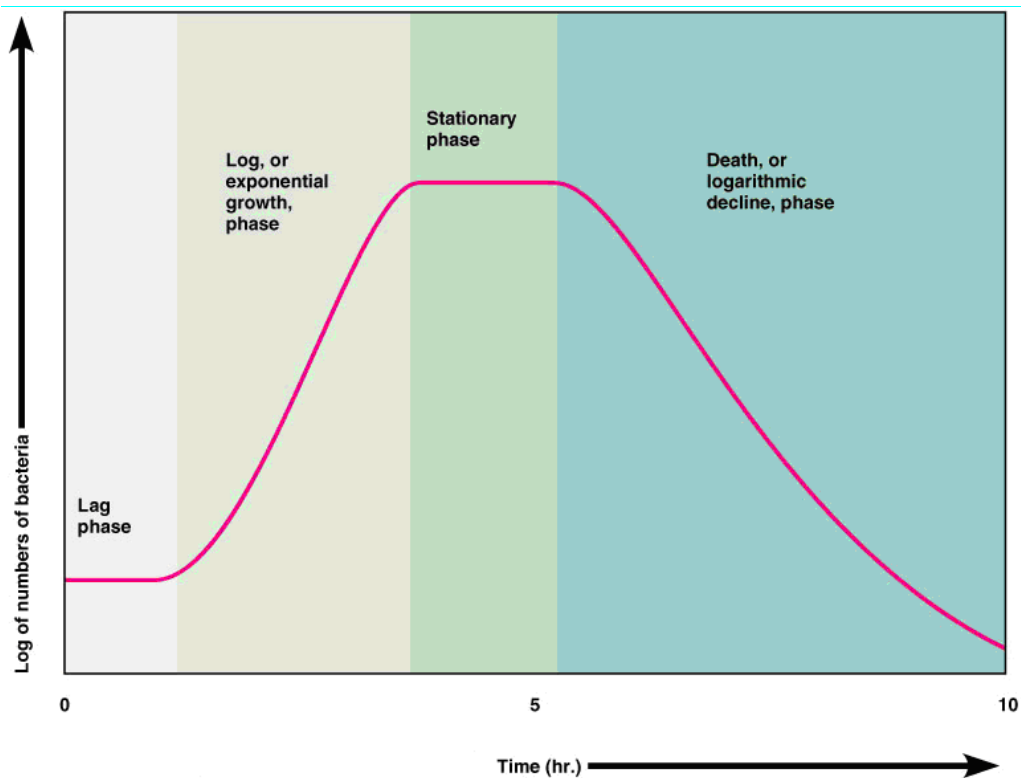


Figure 3.4 Illustration of a typical sigmoidal bacterial growth curve, with each growth phase being represented (Torura, Funke and Case, 2004).

The relative fitness assay was monitored in the absence of antibiotic stress, over a 24 hour time frame (Figures 3.5 and 3.6). As the Graphs illustrates, all 12 Enterococcal strains exhibited similar relative fitness profile characteristics which included a short lag phase, extended exponential phase and stationary phase.

Growth curves were established using sub-minimum concentrations of Pencillin G. The growth profiles in the presence of Vancomycin were the same as the profiles in the absence of antibiotic stress (results not shown). Thus, it was concluded that all the strains are vancomycin tolerant, as they probably failed to express the autolysins necessary for cell enlargement and division (Koch, 2001). Bacteria can become resistant via *de novo* mutation or by the acquisition of foreign genetic material. Typically, resistant bacteria suffer a loss of fitness seen as reduced growth rate and/or a loss of virulence. Thus, most antibiotic-resistant bacteria risk being out-competed by antibiotic- sensitive bacteria. However, if the resistant bacteria can acquire mutations restoring fitness, without losing antibiotic resistance, then they can be stabilised in the population (Naidoo, 2005).

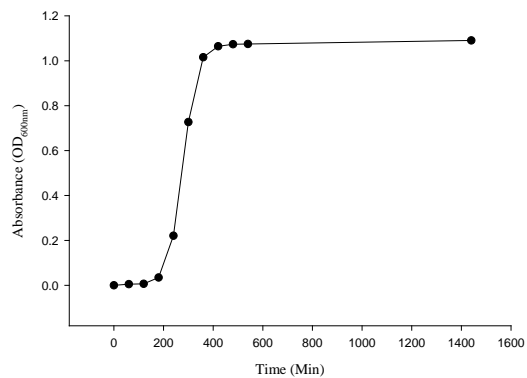
As illustrated in Figure 3.7, growth was affected upon the introduction of Penicillin G into the growth media, as culture viability was shortened. The results show a change in OD₆₀₀ of the antibiotic induced cultures. It is probable that the area of activity for Penicillin G is concentrated on the parts of the cell wall that are expanding (Giesbrecht *et al.*, 1998). Penicillin G specifically inhibits the final step in peptidoglycan synthesis. The bound antibiotic inhibits the formation of the peptidic link. This result in abnormal glycopeptide formation, thus weakening the cell walls (Hammond and Lambert, 1978).

The exponential growth phase of strain E 406 differed from the original growth profile. This can be seen as an increase in the slope due to the presence of the antibiotic in the growth media. This change can be assigned as a consequence of Penicillin G targeting susceptible bacteria during the division phase of cellular growth (Giesbrecht *et al.*, 1998). In addition, the exponential growth time was shorter for this strain. This was the expected result due to the MIC being established as 10µg/ml for strain E 406. As a consequence of the low antibiotic concentration, the growth adjustment was quicker (Figure 3.7(e)).

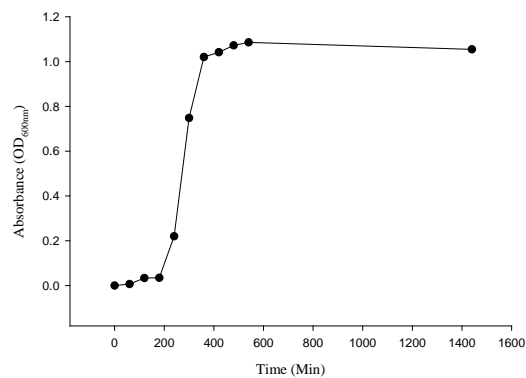
However, with strain E 943, growth was greatly reduced (Figure 3.7(b)). The exponential phase was noticeably shorter than the original growth profile, thus halving the initiation of the stationary phase. Due to antibiotic stress, the stationary phase began at the OD_{600nm} of 1.0, in comparison to the initial OD_{600nm} of 1.4, respectively. The growth time for this strain was halved, since E 943 exhibited the highest MIC value of 30µg/ml.

The remaining 4 strains (Figure 3.7(a), (c), (d) and (f)), displayed similar profiles. All the stationary phases commenced at the OD_{600nm} of 1.0, respectively. In addition, the exponential growth profiles were similar. This could be ascribed to the MIC being 20µg/ml, which is regarded as an intermediate concentration (Table 3.1). Thus the time frames for the exponential phases are similar; however, a gradual increase in growth was noted.

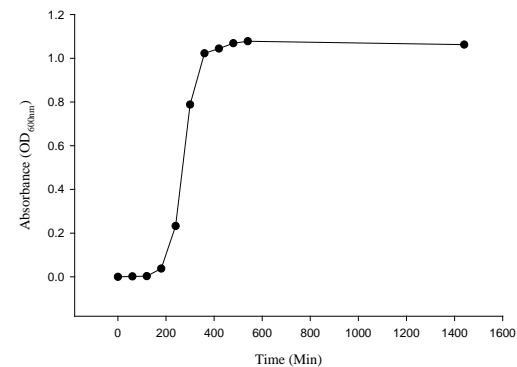
These results are consistent with the findings of Normark *et al.*, 2001. The authors reported that antibiotic tolerant strains survive longer in the presence of antibiotic under stress conditions. Tolerance to Penicillin was frequent in strains with reduced susceptibility to Penicillin G. In addition, of the 116 clinical isolates, 9 strains were tolerant to vancomycin and displayed reduced susceptibility to Penicillin G. Therefore, they concluded that tolerance was possibly responsible for bacteria gaining resistance to antibiotics.



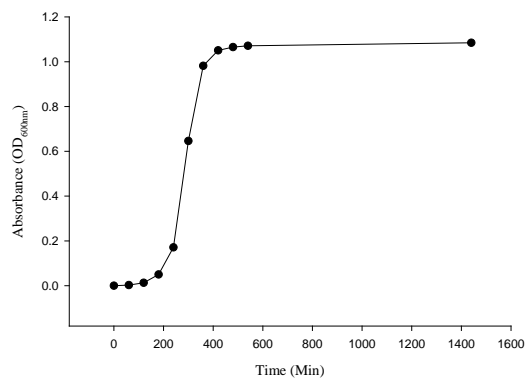
(a)



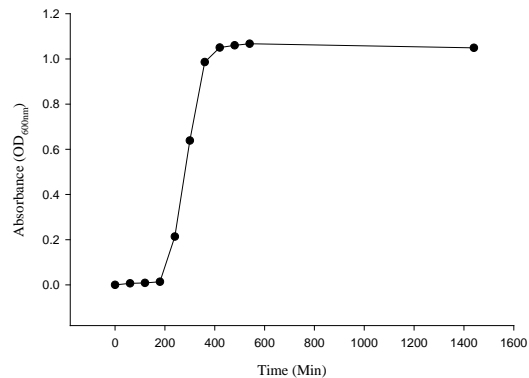
(b)



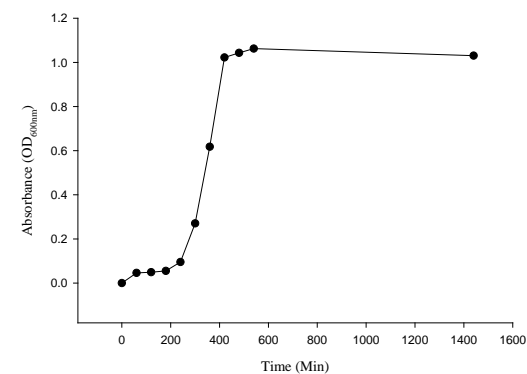
(c)



(d)

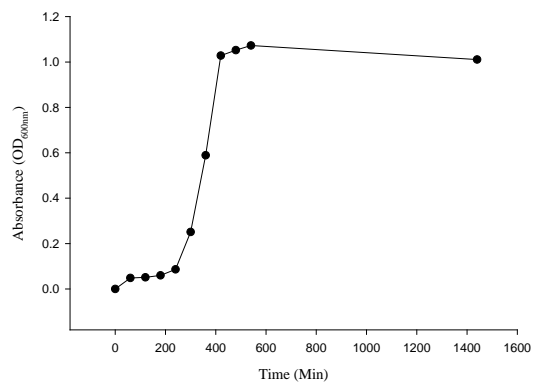


(e)

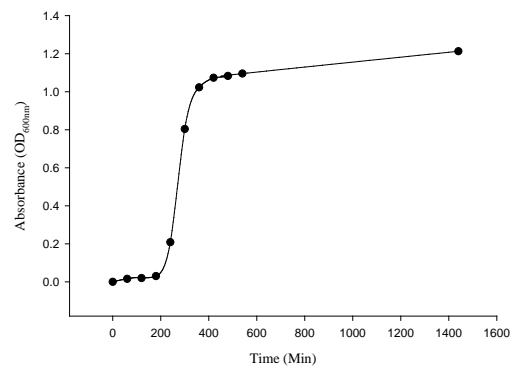


(f)

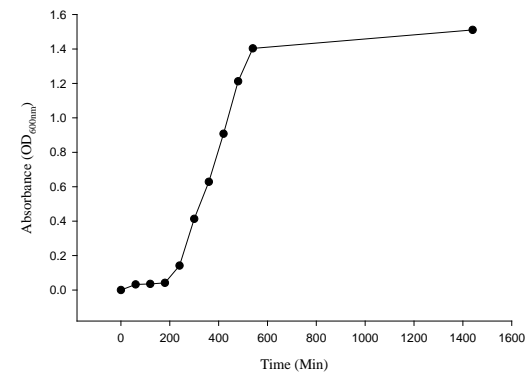
Figure 3.5 Relative fitness profiles (raw data) for each Enterococcal strain, in the absence of antibiotic stress. The bacterial growth cycle was monitored as changes in the optical density at 600_{nm} over Time. The plots are represented as follows: (a) Strain E 21; (b) Strain E 175; (c) Strain E 406; (d) Strain E 859; (e) Strain E 904 and (f) Strain E 1393.



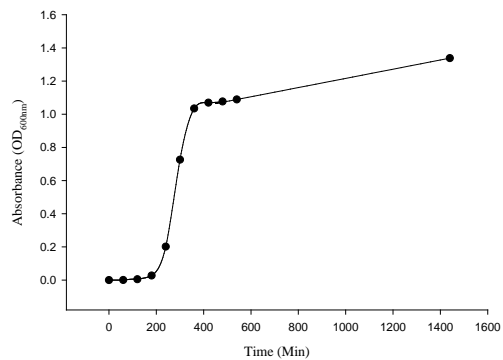
(g)



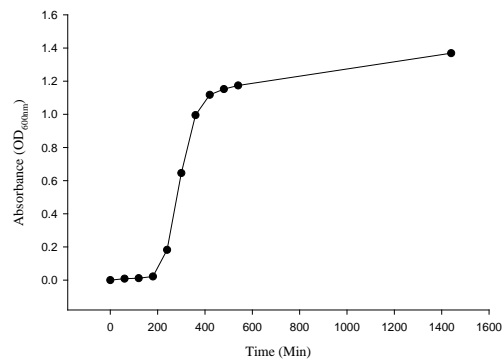
(h)



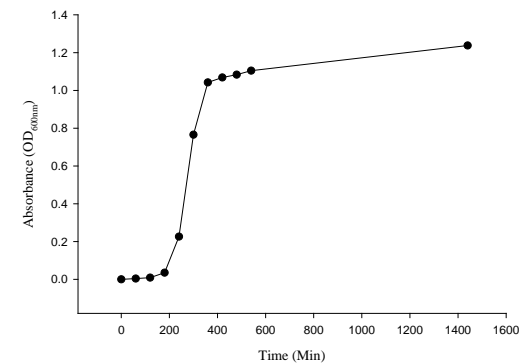
(i)



(j)

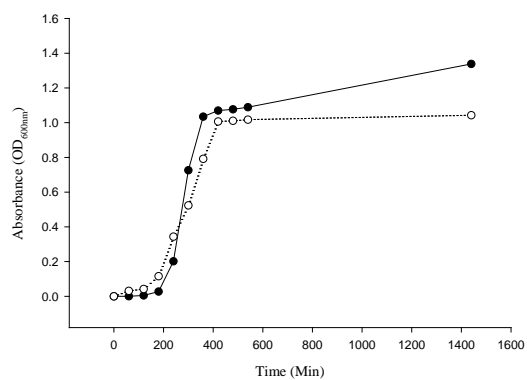


(k)

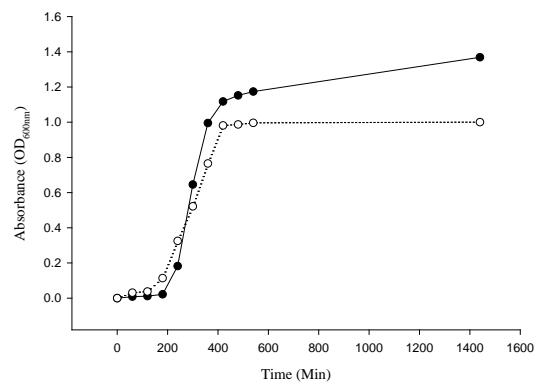


(l)

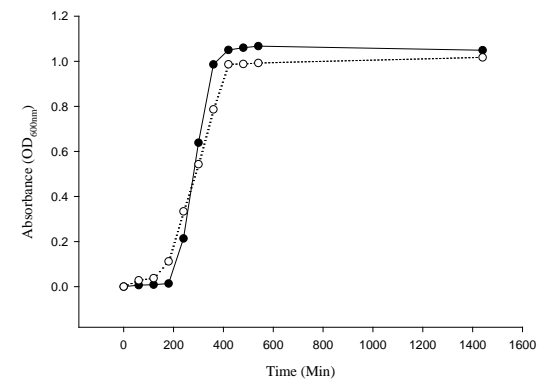
Figure 3.6 Relative fitness profiles (raw data) for each Enterococcal strain, in the absence of antibiotic stress. The bacterial growth cycle was monitored as changes in the optical density at 600_{nm} over Time. The plots are represented as follows: **(g)** Strain E 908; **(h)** Strain E 468; **(i)** Strain E 943; **(j)** Strain E 382; **(k)** Strain E 301 and **(l)** Strain E 430.



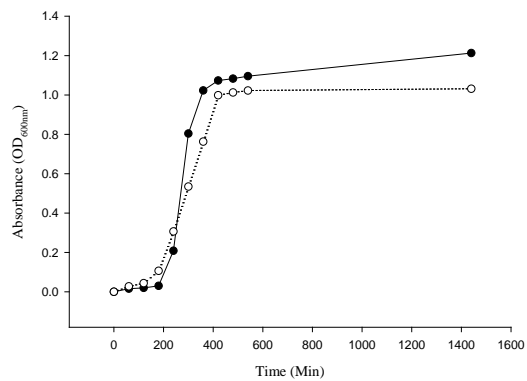
(a)



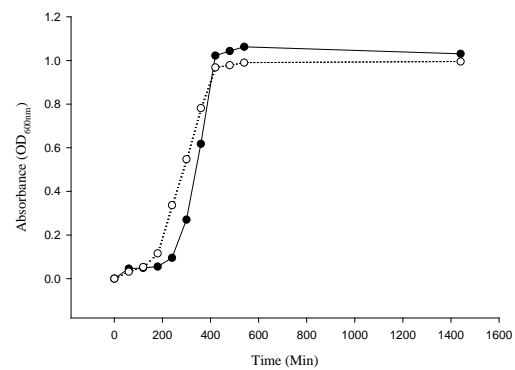
(b)



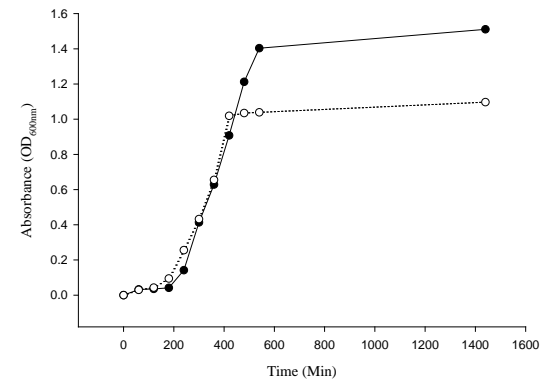
(c)



(d)



(e)



(f)

Figure 3.7 Relative fitness profiles (raw data) for each Enterococcal strain, in the presence of antibiotic stress (..°.). The bacterial growth cycle was monitored as changes in the optical density at 600_{nm} over Time. The plots are represented as follows: (a) Strain E 430; (b) Strain E 859; (c) Strain E 21; (d) Strain E 1393; (e) Strain E 406 and (f) Strain E 859.

3.3 Total Protein Concentration

The Bicinchoninic acid (BCA) protein assay method was used to quantify protein concentrations from the extracts of the autolytic protein preparations. In this assay the BCA is employed as the detection reagent for Cu^{+1} , upon reduction of Cu^{+2} by protein in an alkaline environment. The resultant purple color product is due to the chelation of two molecules of BCA with Cu^{+1} (Smith *et al.*, 1985). Thus, this complex exhibits a strong linear absorbance with increasing protein concentration, from which the standard curve was plotted from the average of three replicates (Figure 3.8). From the standard curve, the protein concentration for each strain was calculated and estimated to be in the range of between 5.47- to 6.35 $\mu\text{g}/\mu\text{l}$ (Table 3.2(a) and (b)). Therefore, this concentration was used for the zymogram analyses.

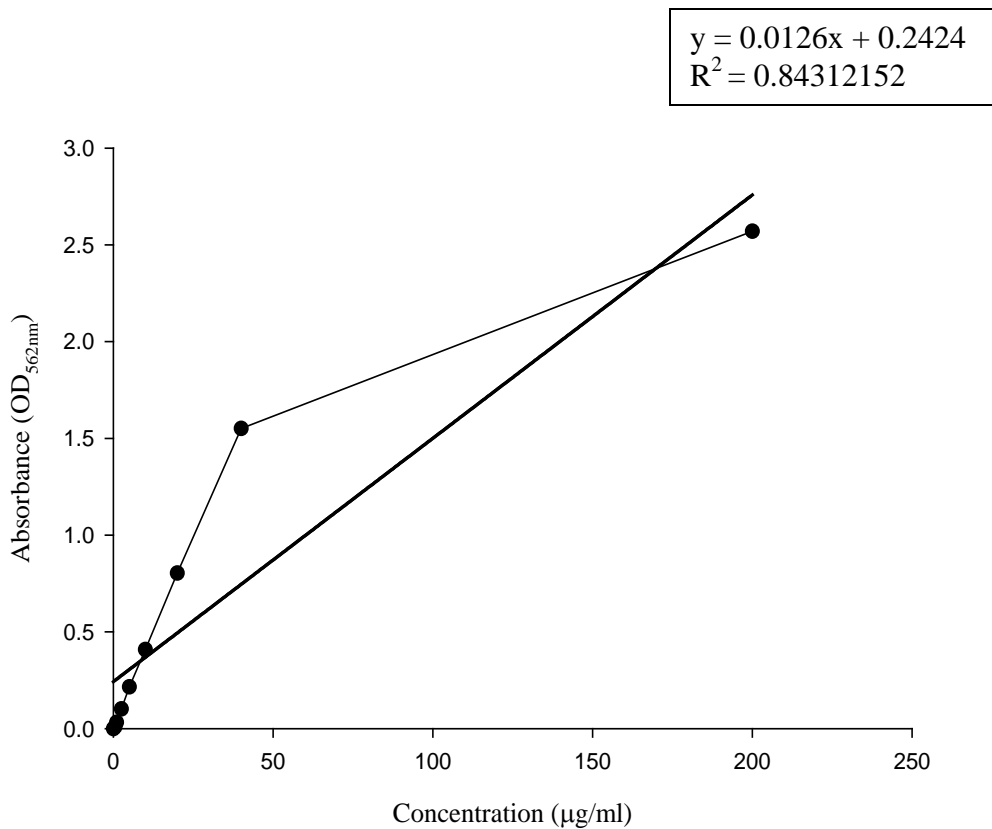


Figure 3.8 Standard curve of Bovine Serum Albumin (BSA) standards (0.5 - 200 $\mu\text{g}/\text{ml}$). The plots represent the following: Fit Curve (—) and Raw Data (—).

Table 3.2a Protein Concentrations of 4% SDS autolytic extracts as determined from a standard curve constructed using the BCA assay.

Sample	Growth Phase	OD_{562nm}	Concentration ($\mu\text{g}/\mu\text{l}$)
Strain E 21	Early Exponential	2.6143	5.90
	Mid Exponential	2.6630	6.03
	Early Stationary	2.6345	5.96
	Early Death	2.5148	5.64
Strain E 175	Early Exponential	2.5059	5.62
	Mid Exponential	2.5842	5.82
	Early Stationary	2.5012	5.60
	Early Death	2.5512	5.74
Strain E 406	Early Exponential	2.4496	5.47
	Mid Exponential	2.7345	6.23
	Early Stationary	2.6687	6.05
	Early Death	2.6298	5.95
Strain E 382	Early Exponential	2.6647	6.04
	Mid Exponential	2.7828	6.35
	Early Stationary	2.6932	6.12
	Early Death	2.6445	5.99
Strain E 301	Early Exponential	2.8077	6.42
	Mid Exponential	2.6192	5.92
	Early Stationary	2.5954	5.85
	Early Death	2.6192	5.92
Strain E 430	Early Exponential	2.5515	5.74
	Mid Exponential	2.6924	6.11
	Early Stationary	2.5841	5.82
	Early Death	2.5311	5.68

Table 3.2b Protein Concentrations of 4% SDS autolytic extracts as determined from a standard curve constructed using the BCA assay.

Sample	Growth Phase	OD_{562nm}	Concentration ($\mu\text{g}/\mu\text{l}$)
Strain E 859	Early Exponential	2.5779	5.81
	Mid Exponential	2.7853	6.36
	Early Stationary	2.7351	6.23
	Early Death	2.5410	5.71
Strain E 904	Early Exponential	2.6463	5.99
	Mid Exponential	2.6603	6.03
	Early Stationary	2.7644	6.31
	Early Death	2.6603	6.03
Strain E 1393	Early Exponential	2.4690	5.52
	Mid Exponential	2.7700	6.32
	Early Stationary	2.4964	5.59
	Early Death	2.7278	6.21
Strain E 943	Early Exponential	2.6133	5.90
	Mid Exponential	2.5437	5.72
	Early Stationary	2.6813	6.08
	Early Death	2.7361	6.23
Strain E 468	Early Exponential	2.6062	5.88
	Mid Exponential	2.5270	5.67
	Early Stationary	2.6124	5.90
	Early Death	2.5704	5.79
Strain E 908	Early Exponential	2.6725	6.06
	Mid Exponential	2.4894	5.57
	Early Stationary	2.6318	5.95
	Early Death	2.6755	6.07

3.4 SDS-PAGE profiles and Zymograms showing autolytic activity of proteins extracted.

Following the 4% SDS extraction of putative autolytic proteins, SDS protein profiles were established for the 12 strains. However, as indicated by Figure 3.9 and Figure 3.10, the strains exhibited similar protein profiles, correlating to the similar relative fitness assay profiles (Figure 3.5 and Figure 3.6). The early lag phase extractions displayed no autolytic protein profiles (results not shown). This is as a consequence of the organisms adjusting to the growth media, thus the cell wall synthesis is at a minimum (Prescott, Harley and Klein, 1999). In addition, range of volumes of the extracted protein was used to establish a uniform protein concentration. As a result, the bacterial cell numbers would vary based on the growth cycle. This factor would influence the protein profiles, thus contributing to the difference in intensity of the autolytic activity.

In Figure 3.9, the expression of autolytic proteins was at the highest in the mid exponential phase and decreases for the remaining stages of the growth cycle. A similar trend in profiles was noted for strains E 943 and E 430 respectively (Figure 3.10(h) and (k)). On the contrary, the remaining strains in Figure 3.10 confirmed increases in autolytic protein expressions from the early stationary phase to the early death phase. Therefore, this result is a direct correlation to previous findings where autolysin activity and expression levels were proven to increase from the exponential to the death phases in a bacterial growth cycle (Naidoo, 2005).

Overall, the majority of autolytic protein expression was evident in strain E 382 and strain E 468 (Figure 3.10(g) and (j)). The lowest level of autolytic protein expression was evident in strain E 908 as observed by the protein profile (Figure 3.10(i)), and from the low total protein concentration of 6 μ g/ μ l (Table 3.2(a) and (b)).

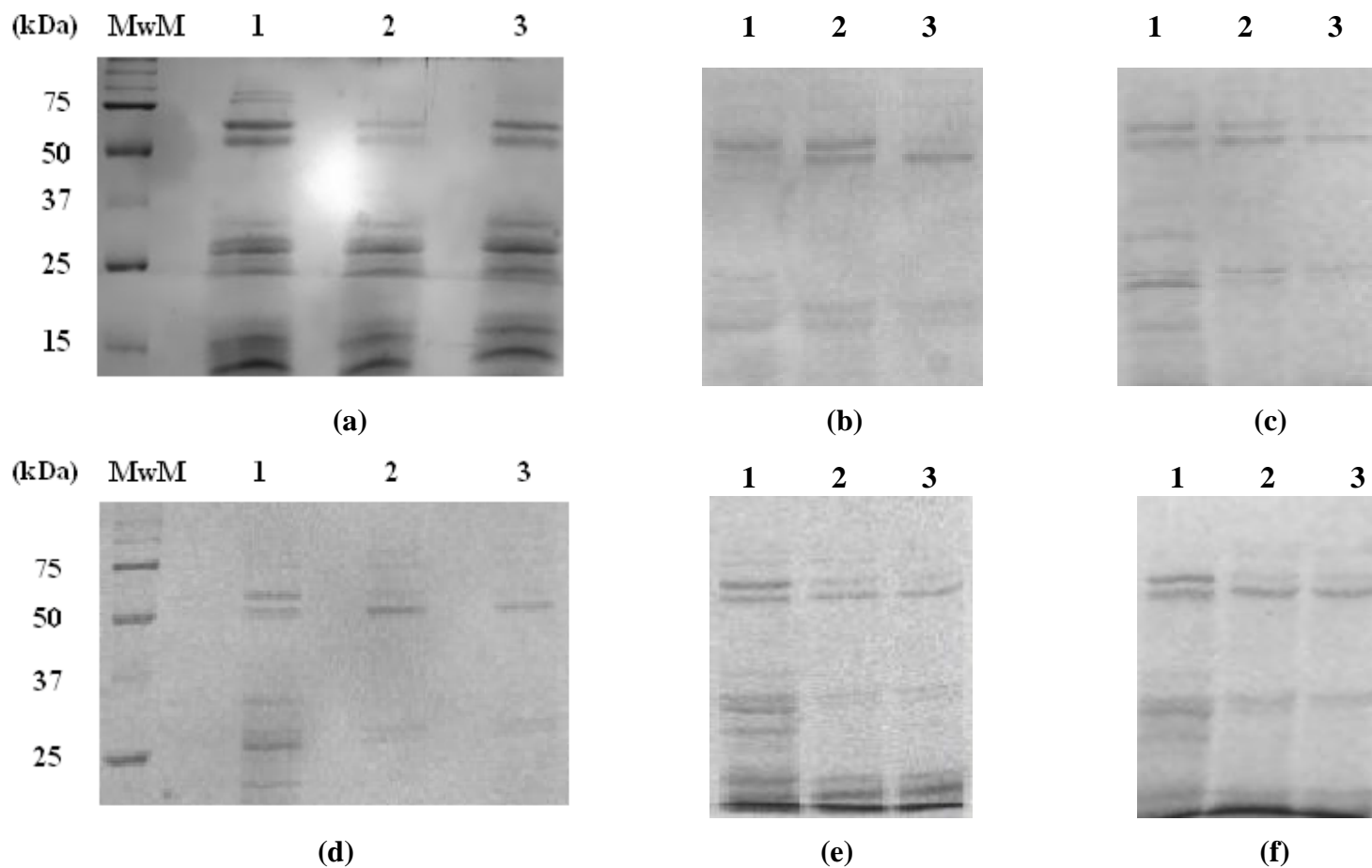


Figure 3.9 Protein profiles of Enterococcal strains analysed on 10% polyacrylamide gels, extracted with 4% SDS. The gels are represented as follows: **(a)** Strain E 21; **(b)** Strain E 175; **(c)** Strain E 406; **(d)** Strain E 1393; **(e)** Strain E 904 and **(f)** Strain E 859. Lanes 1-3: Represents extractions from different stages within the growth cycle. Lanes: 1, Mid exponential phase; 2, Early stationary phase; and 3, Early death phase. MwM: BioRad Precision Plus Unstained Standards Molecular Weight Marker.

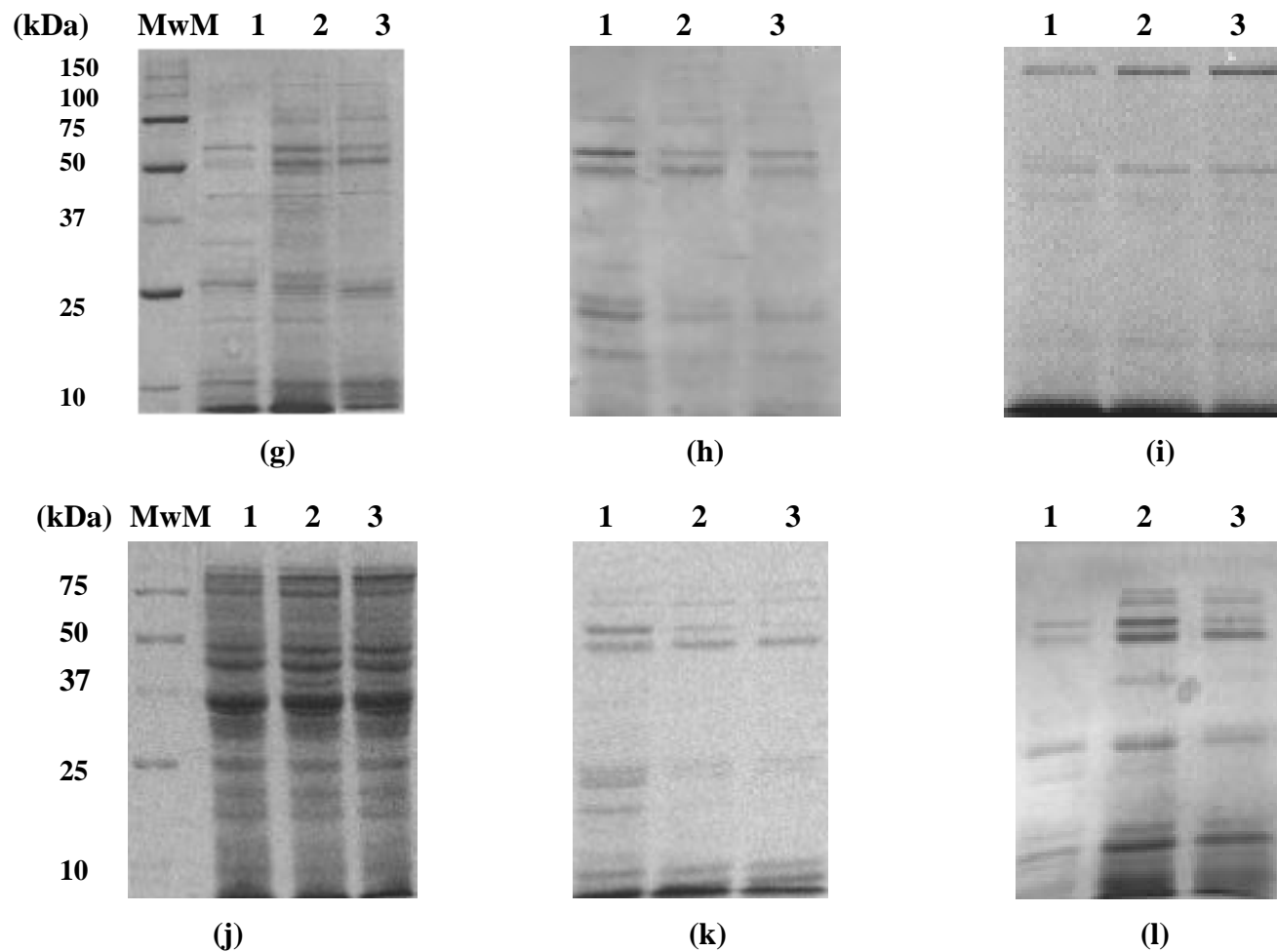


Figure 3.10 Protein profiles of Enterococcal strains on 10% polyacrylamide gels extracted with 4% SDS. The gels are represented as follows: **(g)** Strain E 382; **(h)** Strain E 943; **(i)** Strain E 908; **(j)** Strain E 468; **(k)** Strain E 430 and **(l)** Strain E 301. Lanes 1-3: Represents extractions from stages within the growth cycle. Lanes: 1, Mid exponential phase; 2, Early stationary phase; and 3, Early death phase. MwM: BioRad Precision Plus Unstained Standards Molecular Weight Marker.

To establish the presence of autolytic proteins, the isolated proteins, produced by the different strains, were examined by renaturation SDS-PAGE (zymography) (Figures 3.11 – 3.14). The autolytic activity was detected by incorporating the cell wall extracts into the gel matrix of the SDS-PAGE gel. The cell wall extracts served as the substrate for cell wall (peptidoglycan) digestion, as described in Chapter 2. Visualization of the autolytic activity is enhanced by methylene blue staining. Methylene blue is a water-soluble dye that interacts with the bacterial cell wall complex. Autolytic activity is characterized as clear bands where the cell wall complex has been hydrolyzed (Strating and Clarke, 2001).

All the strains contained proteins that exhibited lytic activity throughout the growth cycle, as evident by the opaque bands, within the 25-145 kDa range (Figures 3.11, 3.12, 3.13 and 3.14) of the zymograms.

In Figure 3.11, autolytic activity visually increased between the lag phase and the other remaining phases. However, there is no observable increase in autolytic activity between the mid exponential to the early death phase. This observation is based on the increase in intensity of the opaque bands, which may be attributed to differences between the initial cell numbers. Although strain E 859 and E 175 (Figure 3.11(a) and (b)), displayed similar autolytic profiles, their molecular weights differed. In addition two dominant lytic bands were observed in both these strains. Strain E 406 (Figure 3.11(c)) exhibited the highest lytic activity in its mid exponential and early stationary phases. In addition, a single minor band of approximately 60kDa was observed in the mid exponential phase, which was absent in the remainder of the growth cycle. The low intensity of the band indicated very low autolytic activity of the 60kDa autolysin.

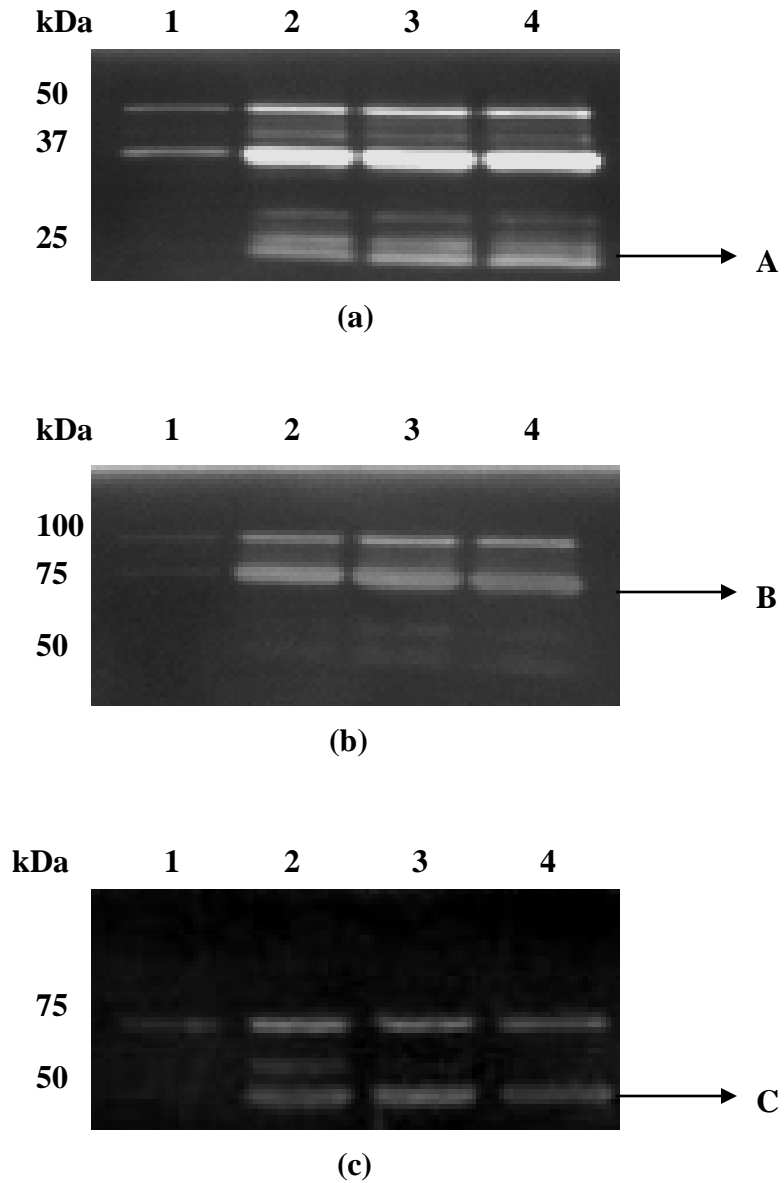
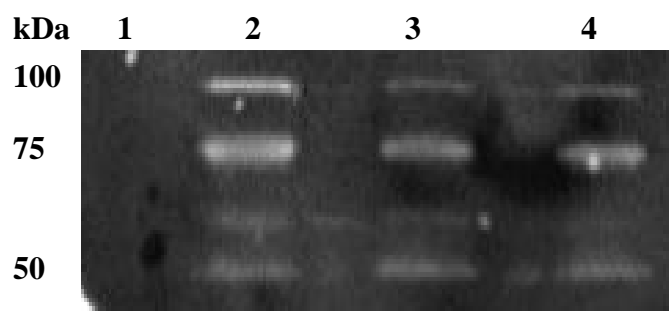


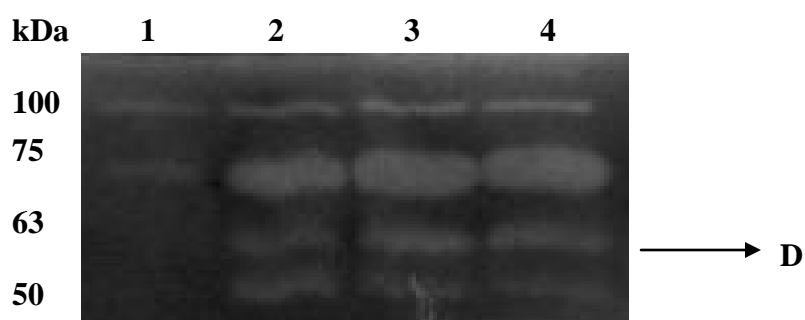
Figure 3.11 Gel slice of a 10% zymogram containing proteins extracted with 4% SDS from the different stages within the growth cycle of *Enterococcus*. The gels are represented as follows: **(a)** Strain E 859; **(b)** Strain E 175; and **(c)** Strain E 406. Each gel contains 0.1% (w/v) of the respective *Enterococcal* cell walls stained with 0.1% (w/v) Methylene Blue in 0.01% (w/v) KOH. Lanes 1-4: Represents autolytic activity from different stages within the growth cycle. Lanes: 1, Lag phase; 2, Mid exponential phase; 3, Early stationary phase; and 4, Early death phase. The arrows indicate putative autolysins which were selected for further characterization.

In Figure 3.12, autolytic proteins were expressed throughout the bacterial growth cycle. Despite the lack of autolytic proteins expressed within the lag phase of strain E 21 (Figure 3.12(d)), the remaining profiles were the same in comparison to E 301 (Figure 3.12(e)). In the lag phase of strain E 21 (Figure 3.12(d)), two dominant bands could be observed, the first band with a molecular weight of approximately 100kDa and the second band of approximately 75 kDa. The lytic band at 100 kDa shows some increase in lytic activity between the lag phase and the mid exponential phase. In addition the band intensity is reduced between the mid exponential to the early stationary and death phase. Furthermore, the 75 kDa lytic band exhibits an increase in expression between the lag and mid exponential phase. No further observable increase in intensity for the other phases were observed. However, the lytic band at 75kDa (Figure 3.12 (e)), displayed an increase in autolytic activity, being produced constitutively from the mid exponential phase till the death phase, thus appearing enlarged. Essentially, the profiles for the mid exponential phase till the early death phases were the same, showing the presence of the two autolytic bands at 63 and 50 kDa, respectively (Figure 3.12 (d), (e)).

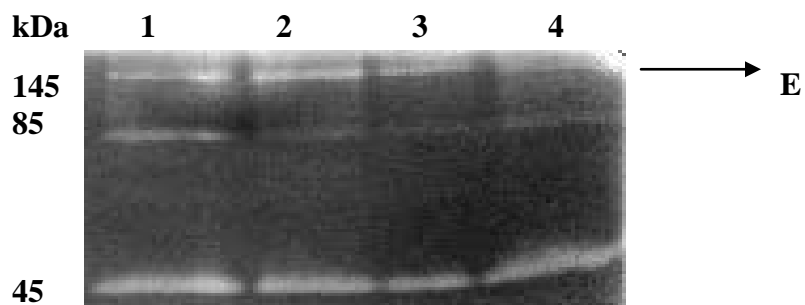
The zymogram for strain E 908 (Figure 3.12 (f)), showed consistent lytic activity throughout the growth cycle. Three lytic bands were present at 145-, 85- and 45 kDa. The lytic band at 145 kDa decreased in activity in the early stationary phase and early death phase. The 85 kDa lytic band was dominant in the lag phase. However, the 45 kDa was present throughout the growth cycle, but showed a substantial increase in activity in the early death phase. It is probable that the lytic activity increases in the death phase, giving rise to cell lysis.



(d)



(e)



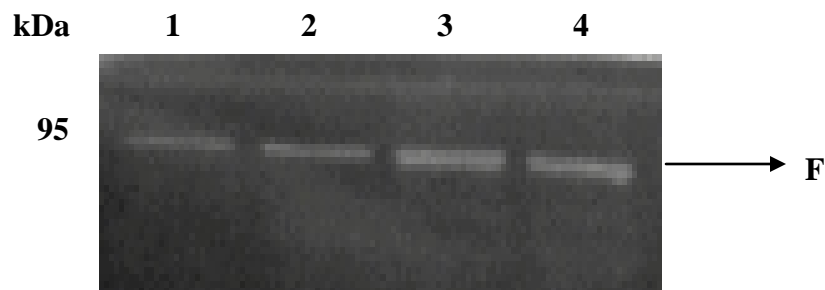
(f)

Figure 3.12 Gel slice of 10% zymogram containing of proteins extracted with 4% SDS from different stages within the growth cycle of *Enterococcus*. The gels are represented as follows: **(d)** Strain E 21; **(e)** Strain E 301; and **(f)** Strain E 908. Each gel contains 0.1% of the respective *Enterococcal* cell walls stained with 0.1% Methylene Blue in 0.01% KOH. Lanes 1-4: Represents autolytic activity from stages within the growth cycle. Lanes: 1, Lag phase; 2, Mid exponential phase; 3, Early stationary phase; and 4, Early death phase. The arrows indicate putative autolysin selected for further characterization.

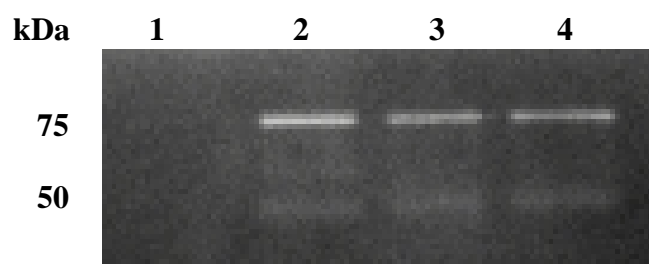
In Figure 3.13, lytic bands were visualized ranging from 50 kDa to 95 kDa. The profile of strain E 382 displayed the presence of one lytic band at 95 kDa, which occurred throughout the growth cycle (Figure 3.13 (g)).

Strain E 943 showed two lytic bands, a major band at 75 kDa and a minor band at 50 kDa, respectively (Figure 3.13 (h)). The two bands were present from the mid exponential phase till the early death phase. On the contrary, no lytic bands were present in the lag phase. This was expected due to growth and cellular activity being minimal at this particular growth phase.

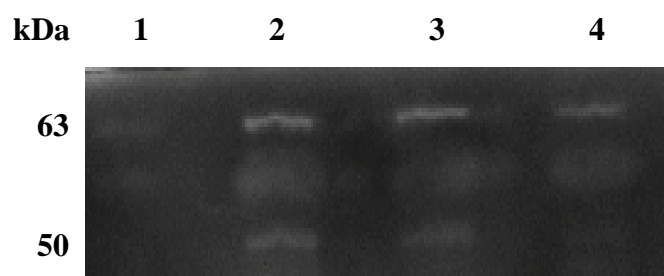
Three lytic bands were present for strain E 904, a major band at 63 kDa and two minor bands corresponding to the molecular weights of 55 kDa and 50 kDa (Figure 3.13 (i)). The major lytic band was present throughout the growth cycle, although it was dominant in the mid exponential and early stationary growth phases. In addition, the first minor band was present from the mid exponential till the early death phases, and exhibited enlarged lytic bands. The second minor band was present in the mid exponential and early death stationary phases, thus indicative of inferior autolytic activity for this autolysin within this strain.



(g)



(h)



(i)

Figure 3.13 Gel slice of 10% zymogram containing of proteins extracted with 4% SDS from different stages within the growth cycle of *Enterococcus*. The gels are represented as follows: (g) Strain E 382; (h) Strain E 943; and (i) Strain E 904. Each gel contains 0.1% of the respective *Enterococcal* cell walls stained with 0.1% Methylene Blue in 0.01% KOH. Lanes 1-4: Represents autolytic activity from stages within the growth cycle. Lanes: 1, Lag phase; 2, Mid exponential phase; 3, Early stationary phase; and 4, Early death phase. The arrows indicate putative autolysin selected for further characterization.

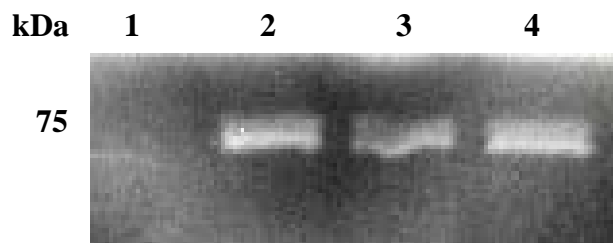
Invariable zymographic profiles were displayed by strains E 430 and E 1393 (Figure 3.14 (j), (k)). For both strains, a single lytic band occurred at 75 kDa, from the mid exponential till the early death phase of the growth cycle. However, E 430 exhibited dominant bands in comparison to E 1393, which displayed minor bands in appearance. This could be attributed to stronger regulatory mechanisms in strain E 430. In addition, strain E 468 exhibited lytic activity throughout the growth cycle. A single lytic band at 30 kDa was observed towards the bottom of the gel.

However, all the profiles may not be the precise reflection of every autolytic enzyme that potentially exists, as enzyme activity is regulated within different growth stages of the organism. Nevertheless, most of the autolytic activity was located from the mid exponential phase till the early death phase. This is supported by literature, as zymographic analysis reveals only the SDS-stable autolysins, thus giving rise to the possibility of them being isoenzymes of the same autolysin (Valence and Lortal, 1995). These results show that there was no increase in the amount of autolysins as the cell entered the early stationary phase. However, the results do reflect an increase in the total autolysin activity within the cultures as a consequence of an increase in total cell mass. In addition, the similarity in autolytic profiles suggests that the autolysins are well-conserved enzymes within the twelve strains. However, between strains, some variation in band intensity was noted.

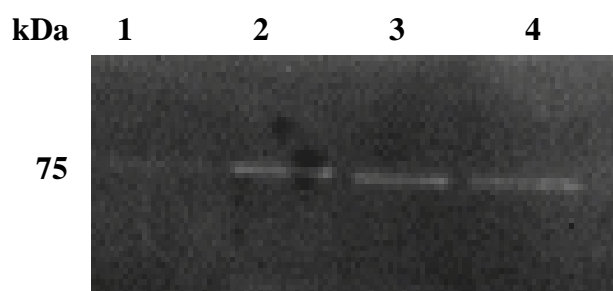
Upon comparison to the SDS-PAGE gel protein profiles, alphabetical letters were assigned to putative autolysins, which were selected for further characterization (Table 3.3).

Table 3.3 Summary of selected putative autolysins for further analysis.

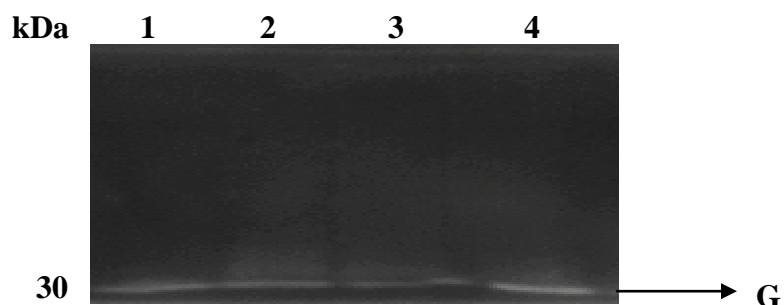
Strain	Selected Autolysin	Size (kDa)
E 859	A	25
E 175	B	75
E 406	C	50
E 301	D	63
E 908	E	145
E 382	F	95
E 468	G	30



(j)



(k)



(l)

Figure 3.14 Gel slice of 10% zymogram containing of proteins extracted with 4% SDS from different stages within the growth cycle of *Enterococcus*. The gels are represented as follows: **(j)** Strain E 430; **(k)** Strain E 1393; and **(l)** Strain E 468. Each gel contains 0.1% of the respective *Enterococcal* cell walls stained with 0.1% Methylene Blue in 0.01% KOH. Lanes 1-4: Represents autolytic activity from stages within the growth cycle. Lanes: 1, Lag phase; 2, Mid exponential phase; 3, Early stationary phase; and 4, Early death phase. The arrow indicates putative autolysin selected for further characterization.

3.4 N-Terminal Sequencing

The autolytic proteins were transferred onto PVDF membranes as described in Chapter 2. Upon comparison to the protein and zymographic profiles, the identified autolysins were excised and sequenced. As illustrated by Figure 3.15, the bands identified as Autolysin B were excised for N-terminal sequencing. The polyvinylidene difluoride (PVDF) membrane is suitable for N-terminal sequencing, due to its ability to retain proteins under extreme conditions. This membrane has a high binding efficiency and a greater retention during sequencing, since information is obtained from low abundance proteins (BioRad, 2002).

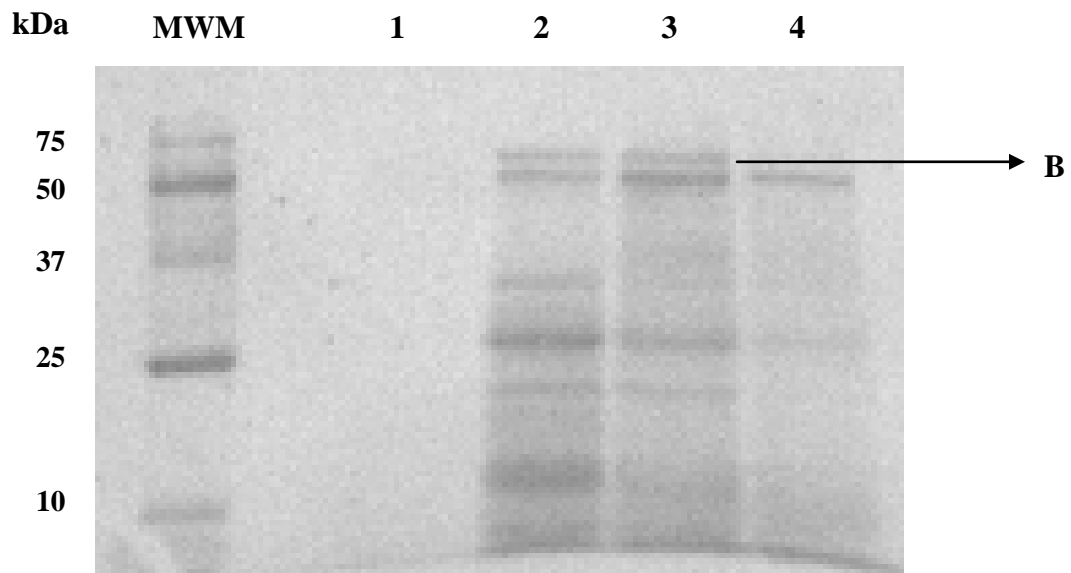
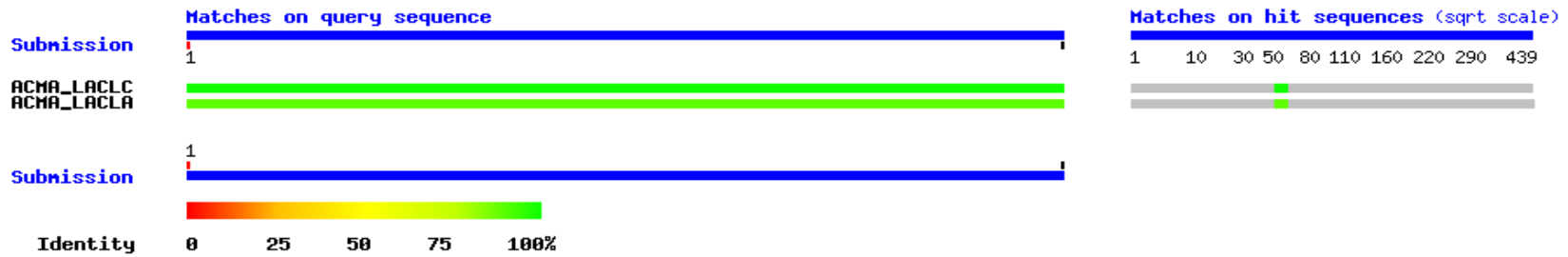


Figure 3.15 Sample PVDF blot of protein extracts from Strain E 175. The putative autolysin B was selected for further characterization. The blot was stained with Coomassie Blue. Lanes: 1, Lag phase; 2, Mid exponential phase; 3, Early stationary phase; and 4, Early death phase. MWM: BioRad Precision Plus unstained protein standards.

The first 10 amino acids were sequenced for each putative autolysin. Using the Swiss-Prot/TrEMBL protein database, the N-terminal sequences were searched for sequence similarities within the database. The N-termini of autolysins A, C, D, E and F revealed 100% sequence similarity to several previously identified putative autolysins. Autolysins B and G rendered inconclusive results, thus indicating that they may be novel putative proteins (Table 3.4).

Table 3.4 N-Terminal Sequence results of the selected putative autolysins from the Enterococcal strains as determined via Edmond chemistry.

Autolytic Protein	N-Terminal Sequence	Sequence Identity	Strain Identity	Percentage Sequence Similarity
Protein A	ATNSSEAFIE	N-acetylmuramidase (Lysozyme)	<i>Lactococcus lactis</i> subsp. <i>cremoris</i> (<i>Streptococcus cremoris</i>)	100
Protein B	SYTVYFDRGF	Undefined Sequence	-	-
Protein C	PSSQVSSSQV	Cell wall hydrolase (autolysin precursor)	<i>Streptococcus suis</i> 89/1591	100
Protein D	AWDVGGGWNM	N-acetylmuramoyl-L-alanine amidase (LytA)	<i>Streptococcus pneumoniae</i>	100
Protein E	KGNGIDSWNM	Putative choline binding protein [SPs0026]	<i>Streptococcus pyogenes</i> serotype M3	100
Protein F	VSSTNSTVTK	Cell wall hydrolase (autolysin)	<i>Enterococcus faecium</i> DO	100
Protein G	KGSNGISWMS	Undefined Sequence	-	-



(a)

Sp [POC2T5](#) Probable N-acetylmuramidase precursor (EC 3.2.1.17) 437 AA
 ACMA_LACL (Peptidoglycan hydrolase) (Autolysin) (Lysozyme) [acmA] [align](#)
 [Lactococcus lactis subsp. cremoris (Streptococcus cremoris)]

Score = 33.7 bits (72), Expect = 1.2
 Identities = 10/10 (100%), Positives = 10/10 (100%)

Query: 1 ATNSSEAFIE 10
 ATNSSEAFIE
 Sbjct: 58 ATNSSEAFIE 67

(b)

Figure 3.16 BLAST alignment result for Autolysin A. Graphical overview of the alignments (a) and actual alignments (b).

3.5 Morgan-Elson Assay

The Morgan-Elson assay was used to photometrically test for the hydrolysis of the glycan bond between the *N*-acetylmuramic acid and *N*-acetylglucosamine subunits of the peptidoglycan layer. This assay requires a free 1-aldo-2-amino sugar that is condensed with acetylacetone, upon heating in an alkaline solution. The resultant product is reacted with Ehrlich's *p*-dimethylaminobenzaldehyde reagent in acid, producing a red chromogen. Thus, a positive reaction denotes a cleavage that yields free disaccharide fragments (Ghysen *et al.*, 1966). Based on the zymographic profiles, strain E 859 was selected to conduct the assay with the chosen putative autolysins.

In Figure 3.17, an increase in the liberation of reduced sugars were noted for Mutanolysin, and Autolysins A, B, E and F. With the autolytic digests, a minimal increase in reduced sugars was noticed, but not as profound as compared to Mutanolysin. The absorbancy values were not as considerable as Mutanolysin, as this could be attributed to the low protein concentration of 6 μ g/ μ l (Table 3.2b). Autolysins C, D and E did not display any significant increases (Figure 3.17). From Figure 3.17, it can be established that Autolysins A, B, E and F displays muramidase activity, based on their ability to liberate reducing sugars from a cell wall substrate.

The characteristic red chromagen was not observed. This could be indirectly associated to the presence of crude hydrolyzates, as neutral sugars and amino acids contribute to the interference of the reaction. In addition, the alkaline buffer or the heating time could have affected the prochromagen formation before the reaction with the Ehrlich reagent (Ghysen *et al.*, 1966).

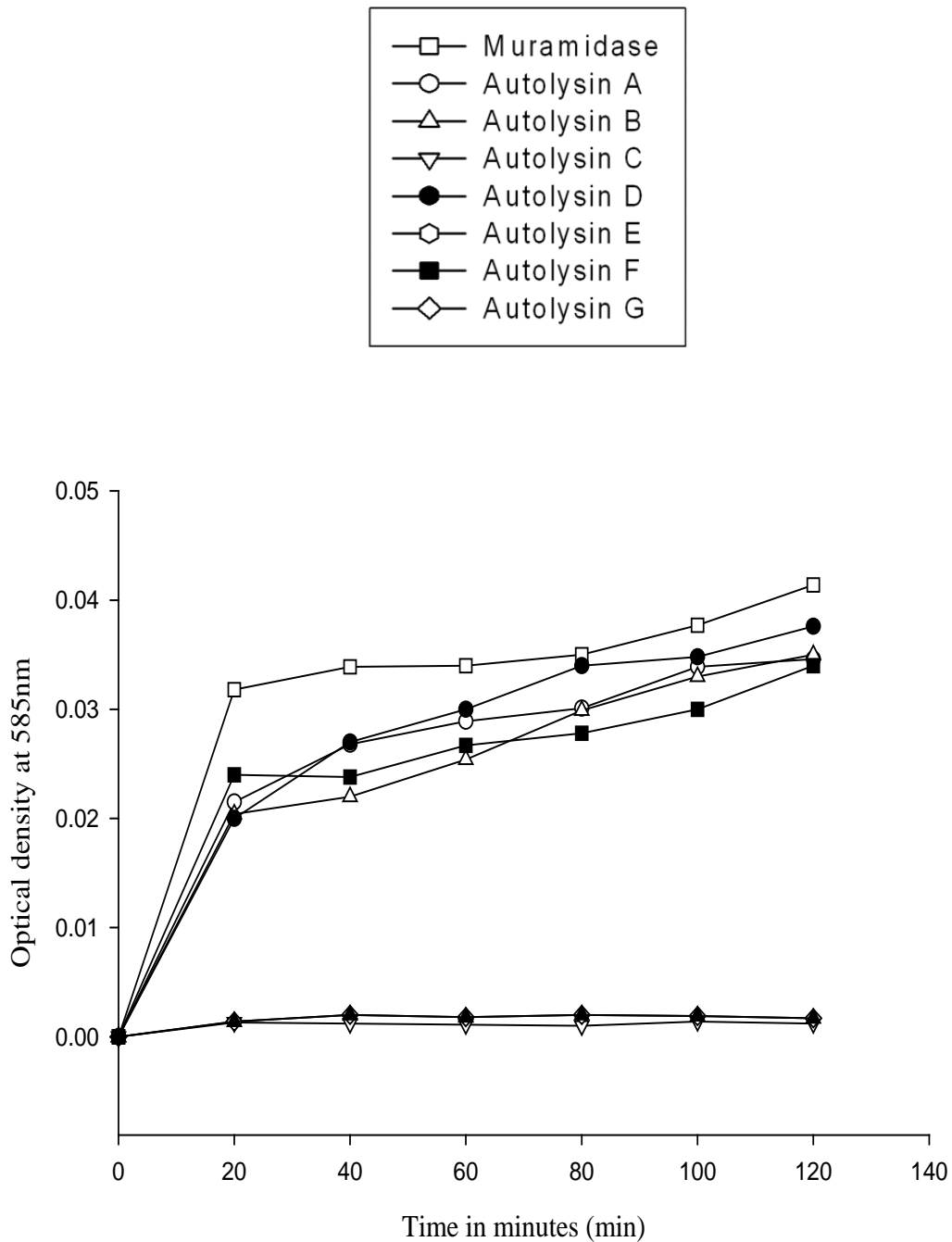


Figure 3.17 Graphical representation of the liberation of free reducing sugars from autolytic digests of Strain E 859 cell walls using the Morgan-Elson Assay. The liberation of free reducing sugars was monitored as changes in the optical density at 585_{nm} over Time after digestion with the selected autolysins (A, B, C, D, E, F and G).

3.6 DPN Assay

Endopeptidase activity was detected by a colorimetric assay using N-dinitrophenyl derivatization. In this assay, the fluorodinitrobenzene reagent (FDNB) is acidified with potassium tetraborate to produce a color change, indicative of free amino groups during cell wall lysis (Ghysen *et al.*, 1966). Based on the zymographic profiles, strain E 859 was selected to conduct the assay with the chosen putative autolysins.

From the graphical representation of the assay (Figure 3.18), an increase in the liberation of free amino groups were noted for Autolysins C, D, and G. For the remaining autolysins and Mutanolysin, there was no cleavage activity. From this result, it can be concluded that Autolysins C, D, and G harbor peptidase activity. However, Autolysin D displayed amidase activity (Table 3.4). Amidase activity involves the cleavage of the bond between the glycan chain and the stem peptide. On the contrary, the exact bond cleaved by Autolysins C, D and G could not be elucidated with this experiment, which could be attributed to the low protein concentration of $6\mu\text{g}/\mu\text{l}$ (Table 3.2b).

The remaining autolysins (A, B, E and F) displayed no significant increase in the liberation of free amino groups, as noted by the similar assay profiles (Figure 3.18). This could be as a consequence of the cell walls containing a content of N-terminal groups which may have masked the liberation of the new amino groups during autolytic digestion (Ghysen *et al.*, 1966).

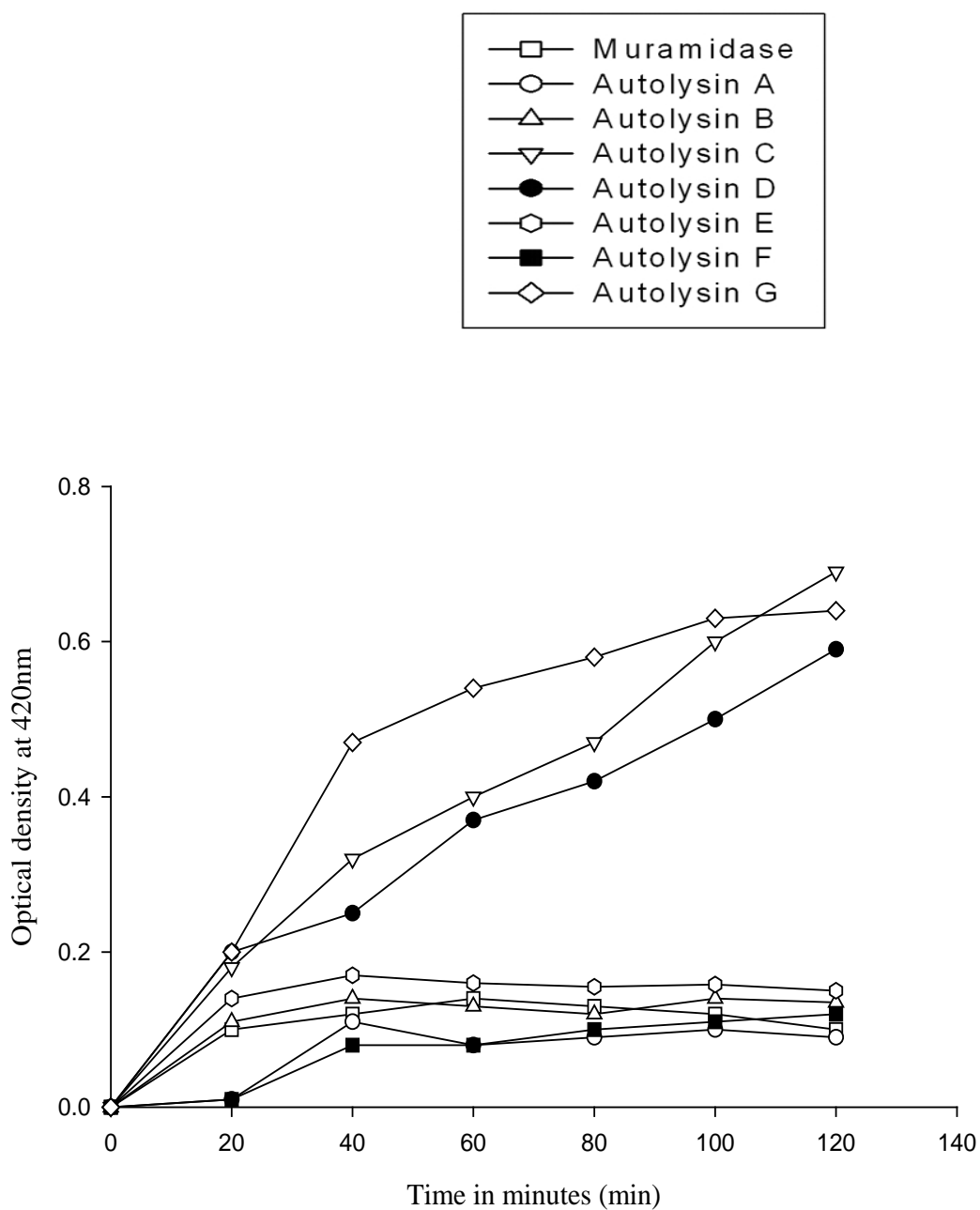


Figure 3.18 Graphical representation of the liberation of free amino groups from autolytic digests of Strain E 859 cell walls using 2,3-dinitrophenol (DNP) derivatization. The liberation of free reducing sugars was monitored as changes in the optical density at 585_{nm} over Time after digestion with the selected autolysins (A, B, C, D, E, F and G).

CHAPTER FOUR

CONCLUSION AND FUTURE RESEARCH

The research described in this thesis was designed to characterize selected autolysins in Enterococcal strains. In the presence of antibiotics, all twelve strains were resistant to Vancomycin, whereas only six strains were resistant to Penicillin G. A possible explanation for this phenomenon could be attributed to the failure of the antibiotic to trigger autolysis. One can conceive that the evolving bacteria could down-regulate autolysin activity as a mechanism to counteract the pressure exerted by the antibiotic. This resulted in the organisms being tolerant to antibiotic stress, thus escaping antibiotic induced cell lysis. The resistance to antibiotics, such as Vancomycin and Penicillin G, is an indication of a major problem in the treatment of Enterococcal related infections.

All twelve Enterococcal strains displayed autolytic activity throughout their growth cycle. This activity is vital in various biological functions such as cell separation, cell wall turnover, restructuring of cell walls, and bacterial autolysis (induced by antibiotics or adverse physiological conditions).

Generally, autolytic enzymes are characterized according to the chemical bond they degrade within the cell wall. From the autolytic profiles obtained in this study, seven autolysins were selected from seven Enterococcal strains for further characterization. The results from biochemical characterization revealed them to be similar to previously characterized muramidases, amidases and peptidases. Autolysins B and G displayed muramidase and peptidase activity, respectively. However, their sequence alignment searches were undefined. This is a possibility that these two autolysins have escaped detection previously and could be new putative autolysins.

Bacterial autolysins are potentially lethal enzymes capable of hydrolyzing the peptidoglycan component of the cell wall. They are thought to participate in the biosynthesis of the peptidoglycan by providing sites for the incorporation of new material. Hence, this class of enzymes plays a multifaceted role in the cell cycle. Therefore, a better understanding of the regulation of expression and identification of

new autolysins may aid in improved design of new classes of antimicrobial compounds to combat the ever-increasing number of antibiotic resistant bacteria.

In addition, little is known about the exact events that lead to the autolytic activity noted in this study. Further questions arise as to whether the autolysins identified, are active only during antibiotic stress. Hence, the enzymatic system would be another avenue to explore in developing a new class of antibiotics designed specifically to target this system. Generally, antibiotic resistance poses extreme problems in the treatment of bacterial induced diseases. Thus, further studies into the regulatory mechanisms that are involved in resistance to antibiotics would lead to improved methods for bacterial treatments.

Other future considerations would include investigating autolysis in varying buffer systems. This would be achieved by varying salt concentrations and pH ranges to identify the environment crucial for autolysis. Two-dimensional SDS-PAGE gel analysis can be used to reveal autolytic maps by virtue of the presence or absence of the proteins. Proteomic analysis can further be explored, to generate a complete two-dimensional map of the *Enterococcal* proteome on the basis of their autolysins. The regulation of the autolysins monitored in the presence of antibiotic stress can hold the key to the understanding of how these genes are expressed and subsequently regulated.

Phylogenetic characterization can also be done based on the sequences available for the autolysins. The molecular identities of similar molecular weight autolysins can be confirmed by intra-cellular and extra-cellular analysis of the amino acid sequences to elucidate mutual relations.

Even though the complete activities of bacterial cell wall metabolisms are not fully understood, it is obvious that it involves a dynamic system of specialized enzymes required for peptidoglycan activities. Hence, with a combination of a molecular and biochemical approach, the autolytic system can be investigated by cloning and expressing the autolytic genes, therefore contributing to future discoveries of the role of these enzymes in cell wall physiology.

Thus the application of this research has great potential in the development of antibiotics in relation to multiple drug resistance. Employing the knowledge attained from the characterization of these autolysins, the genomes of the bacterial strains can now be sequenced and the genes responsible for the switching on or off of these autolysins can be established. In this study, the renaturation SDS-PAGE method, N-terminal sequencing and biochemical assays proved to be convenient tools in establishing autolytic activity and analyses. On the contrary, the next step in research is to understand and determine the physiological role and total spectrum of activities of the identified autolysins. The fact that Autolysins B and G exhibited muramidase and peptidase activity, begs the need for further investigation to establish the possibility of novel autolysins.

CHAPTER FIVE

REFERENCES

1. **Aizenman, E., Engelberg-Kulka, H. and Glaser, G.** 1996. An *Escherichia coli* chromosomal 'addiction module' regulated by guanosine 3',5'-bispyrophosphate: a model for programmed bacterial cell death. Proc. Natl. Acad. Sci. USA **93**:6059-6063.
2. **Anon.** 2006, posting date. RCSB Protein Data Bank: Structure Explorer. [Online.]
3. **Aravind, L., Dixit, V. M. and Koonin, E. V.** 1999. The domains of death: evolution of the apoptosis machinery. Trends Biochem. Sci. **24**:47-53.
4. **Arthur, M., Reynolds, P. and Courvalin, P.** 1996. Glycopeptide resistance in enterococci. Trends Microbiol. **4**:401-407.
5. **Atlas, R. M.** 1995. Microorganisms in our world. Carlsbad, Mosby.
6. **Baele, M., Baele, P., Vanechoutte, M., Storms, V., Butaye, P., Devries, L. A., Verschraegen, G., Gillis, M and Haesebrouck F.** 2000. Application of tRNA Intergenic Spacer PCR for Identification of *Enterococcus* Species. J Clin Microbiol **38**:4201-4207.
7. **Baptists, M. F., Departieu, P., Courvalin, P. and Arthur, M.** 1996. Specificity of induction of glycopeptide resistance genes in *Enterococcus faecalis*. Antimicro. Agents Chemother. **40**:2291-2295.
8. **Beliveau, C., Potvin, C., Trudel, J., Asselin, A. and Bellemare, G.** 1991. Cloning, sequencing and expression in *Escherichia coli* of a *Streptococcus faecalis* autolysin. J. Bacteriol. **173**:5619-5623.

9. **Benaissa, M., Babin, P., Quellard, N., Pezennec, L., Cenatiempo, Y. and Fauchere, J. L.** 1996. Changes in *Helicobacter pylori* ultrastructure and antigens during conversion from bacillary to the coccoid form. *Infect. Immun.* **64**:2331-2335.
10. **Berry, A. M., Lock, R. A., Hansman, D and Paton, J. C.** 1989. Contribution of autolysin to virulence of *Streptococcus pneumoniae*. *Infect. Immun.* **57**:2324-2330.
11. **Berry, V., Jennings, K., and Woodnutt, G.** 1995. Bactericidal and morphological effects of amoxicillin on *Helicobacter pylori*. *Antimicrob. Agents. Chemother.* **39**:1859-1861.
12. **Betzner, A. S., and Keck, W.** 1989. Molecular cloning, over-expression and mapping of the *slt* gene encoding the soluble lytic transglycosidases of *Escherichia coli*. *Mol. Gen. Genet.* **219**:489-491.
13. **Beukes, M., Bierbaum, G. S. and Hastings, J. W.** 2000. Purification and partial characterization of a murein hydrolase, Millericin B, produced *Streptococcus milleri* NMSCC 061. *Appl. Environ. Microbiol.* **66**:23-28.
14. **BioRad.** 2002. Mini Trans-Blot Electrophoretic Transfer Cell: Instruction Manual. US.
15. **Bourne, R., Himmelreich, U., Sharma, A., Mountford, C and Sorrell, T.** 2001. Identification of *Enterococcus*, *Streptococcus*, and *Staphylococcus* by Multivariate Analysis of Proton Magnetic Resonance Spectroscopic Data from Plate Cultures. *J Clin Microbiol* **39**:2916-2923.

16. **Broome-Smith, J. K., Ioannidis, I, Endelman, A. and Spratt, B. G.** 1988. Nucleotide sequences of the penicillin-binding proteins 5 and 6 genes of *Escherichia coli*. *Nucleic Acid Res.* **16**:617.
17. **Brunskill, E. W., and Bayles, K. W.** 1996. Identification and molecular characterization of a putative regulatory locus that affects autolysis in *Staphylococcus aureus*. *J. Bacteriol.* **178**:611-618.
18. **Cetinkaya, Y., Falk, P. and Mayhall, C. G.** 2000. Vancomycin-resistant enterococci. *Clin. Microbiol. Rev.* **13**:686-707.
19. **Clark, A. J., and Dunpont, C.** 1992. O-Acetylated peptidoglycan: its occurrence, pathobiological significance and biosynthesis. *Can. J. Microbiol.* **38**:85-91.
20. **Clarridge, J. E., Osting, C., Jalali M., Osborn, J. and Waddington, M.** 1999. Genotypic and phenotypic characterization of "*Streptococcus milleri* group" isolates from a Veterans Administration hospital population. *J. Clin. Microbiol.* **37**:3681-3700.
21. **Devriese, L. A., Pot, B and Collins, M.D.** 1993. Phenotypic identification of the genus *Enterococcus* and differentiation of phylogenetically distinct enterococcal species and species group. *J Appl Bacteriol* **75**:399–408.
22. **Devriese, L. A., Pot, B., Kersters, K., Lauwers, S and Haesebrouck, F.** 1996. Acidification of methyl-(D)-glucopyranoside: a useful test to differentiate *Enterococcus casseliflavus* and *Enterococcus gallinarum* from *Enterococcus faecium* species group and from *Enterococcus faecalis*. *J Clin Microbiol* **34**:2607–2608.

23. **Dolinger, D. L., Daneo-Moore, L. and Shockman, G. D.** 1989. The second peptidoglycan hydrolase of *Streptococcus faecium* ATCC 9790 covalently binds penicillin. J. Bacteriol. **171**:4355-4361.
24. **Ehlert, K., Holtje, J. V. and Templin, M. F.** 1995. Cloning and expression of a murein hydrolase lipoprotein from *Escherichia coli*. Mol. Microbiol. **16**:761-768.
25. **Engel, H., Smink, J., van Wijngaarden, L. and Keck, W.** 1992. Murein-metabolising enzymes from *Escherichia coli*: on the existence of second lytic transglycosylases. J. Bacteriol. **175**:130-210.
26. **Engelberg-Kulka, H., Sat, B., Reches, M., Amitai, S and Hazan, R.** 2004. Bacterial Programmed Cell Death Systems as Targets for Antibiotics. Trends Microbiol. **12**:66-71.
27. **Fiedler, F., and Glaser, L.** 1973. Assembly of bacterial cell walls. Biochem. Biophys. Acta. **300**:467-485.
28. **Foley, M., Brass, J. M., Birmingham, J., Cook, W. R., Garland, P. B., Higgins, C. F. and Rothfield, L. I.** 1989. Compartmentalization of the periplasm at cell division sites in *Escherichia coli* as shown by fluorescence photo-bleaching experiments. Mol. Microbiol. **3**:1329-1336.
29. **Foster, S. J.** 1994. The role and regulation of cell wall structural dynamics during differentiation of endospore-forming bacteria. Appl. Bacteriol. **76**:25-39.
30. **Garcia, P., Gonzalez, M. P., Garcia, E., Lopez, R. and Garcia, J. L.** 1999. *LytB*, a novel pneumococcal murein hydrolase essential for cell separation. Mol. Microbiol. **31**:1275-1277.

31. **Garcia, P. G., P., Gonzalez, M. P., Garcia, E., Garcia, J. L and Lopez, R.** 1999. The molecular characterization of the first lysozyme of *Streptococcus pneumoniae* reveal evolutionarily mobile domains. *Mol. Microbial.* **33**:128-138.
32. **Gautam, S., and Sharma, A.** 2002. Involvement of caspase-3-like protein in rapid cell death of *Xanthomonas*. *Mol. Microbiol.* **44**:393-401.
33. **Ghuysen, J.-M., Tripper, D.J., and J.L. Stroimger.** 1966. Enzymes that degrade bacterial cell walls, p. 685-699. *In* I. E. F. Neufeld (ed.), *Methods in Enzymology*, vol. VII. Academic Press Inc.
34. **Giesbrecht, P., Kersten, T., Maidhof, H. and Wecke, J.** 1998. Staphylococcal cell wall: morphogenesis and fatal variations in the presence of penicillin. *Microbiol. Mol. Biol. Rev.* **62**:1371-1414.
35. **Gmeiner, J., and Kroll, H. P.** 1981. Membranes of the protoplast L-form of *Proteus mirabilis*. *FEBS. Lett.* **129**:142-144.
36. **Gray, T.** 2005. *Streptococcus anginosus* group: Clinical significance of an important group of pathogens. *Clin. Microbiol. Newsletter* **27**:155-159.
37. **Groicher, K. H., Firek, B. A., Fujimoto, D. F. and Bayles, K. W.** 2000. The *Staphylococcus aureus* *lrgAB* operon modulates murein hydrolase activity and penicillin tolerance. *J. Bacteriol.* **182**:1794-1801.
38. **Hakenbeck, R., and Messer, W.** 1977. Activity of murein hydrolases in synchronized cultures of *Escherichia coli*. *J. Bacteriol.* **129**:1239-1244.
39. **Hamilton, W. D.** 1964. The Genetic Evolution of Social Behavior. *J.Theor. Biol.* **7**:1-52.

40. **Hammond, S. M., and Lambert, P. A.** 1978. Antibiotics and Antimicrobial Action. Edward Arnold, London.
41. **Hardie, J. M. a. W., R.A.** 1994. Recent developments in streptococcal taxonomy: their relation to infections. Review of in Medical Microbiol **5**:151–162.
42. **Hartmann, R., Bock-Hennig, S. B. and Schwartz, U.** 1974. Murein hydrolases in the envelope of *Escherichia coli*. Properties in situ and solubilization from the envelope. Eur. J. Biochem. **41**:203-208.
43. **Harz, H., Burgdorf, K. and Holtje J. V.** 1990. Isolation and separation of the glycan strands from murein of *Escherichia coli*. By reversed-phase high performance liquid chromatography. Anal. Biochem. **190**:120-128.
44. **Heidrich, C., et al.** 2001. Involvement of N-acetylmuramyl-L-alanine amidases in cell separation and antibiotic-induced autolysis of *Escherichia coli*. Mol. Microbiol. **41**:167-178.
45. **Henderson, T. A., Dombrosky, P. M. and Young, K. D.** 1994. Artfactual processing of penicillin binding proteins 7 and 1B by the *OmpT* protease of *Escherichia coli*. J. Bacteriol. **103**:504-512.
46. **Henderson, T. A., Templin, M and Young K. D.** 1995. Identification and cloning of the gene encoding penicillin-binding protein 7 of *Escherichia coli*. J. Bacteriol. **177**:2074-2079.
47. **Hengartner, M. O.** 2000. The Biochemistry of Apoptosis. Nature **407**:770-776.

48. **Higgins, M. L., Pooley, H. M. and Shockman, G. D.** 1970. Site of initiation of cellular autolysis in *Streptococcus faecalis* as seen by electron microscopy. *J. Bacteriol.* **103**:504-512.
49. **Hochman, A.** 1997. Programmed Cell Death in Prokaryotes. *Crit. Rev. Microbiol.* **23**:207-214.
50. **Höltje, J.-V., and Tomasz, A.** 1975. Specific recognition of choline residues in the cell wall teichoic acid by the N-acetylmuramyl-L-alanine amidase of Pneumococcus. *J. Biol. Chem.* **250**:6072-6076.
51. **Holtje, J.-V., and Tuomanen, E. I.** 1991. The murein hydrolases of *Escherichia coli*: properties, functions and impact on the course of infections *in vivo*. *J. Gen. Microbiol.* **137**:441-454.
52. **Holtje, J. V., Mirelman, N. S. and Schwarz, U.** 1975. Novel types of murein transglycosylase in *Escherichia coli*. *J. Bacteriol.* **124**:1067-1076.
53. **Holtje, J. V.** 1995. From Growth to autolysis: the murein hydrolases in *Escherichia coli*. *Arch. Microbiol.* **164**:243-254.
54. **Jacobs, J. A., and Stobberingh, E.** 1996. In-vitro antimicrobial susceptibility of the "*Streptococcus anginosus*, *Streptococcus constellatus* and *Streptococcus intermedius*". *J. Antimicrob. Chemother.* **37**:371-375.
55. **Jerng, S.-H., Hsueh, P. -R., Teng, L. -J., Lee, L. -N., Yang, P. -C and Luh, K. -T.** 1997. Empyema Thoracis and Lung Abscess Caused by Viridans Streptococci. *American J. Respiratory and Critical Care Medicine* **156**:1508-1514.

56. **Jolliffe, L. K., Doyle, R. J. and Streips, U. N.** 1981. The energized membrane and cellular autolysis in *Bacillus subtilis*. *Cell* **25**:753-763.
57. **Joseph, R., and Shockman, G. D.** 1974. Autolytic formation of protoplast (autoplast) of *Streptococcus faecalis* 9790: Release of cell wall, autolysin and formation of stable autoplast. *Antimicro. Agents. Chemother.* **40**:789-801.
58. **Kariyama, R., and Shockman, G. D.** 1992. Extracellular and cellular distribution of muramidase-2 and muramidase-1 of *Escherichia hirae*. *J. Bacteriol.* **174**:3236-3241.
59. **Kawamura, T., and Shockman, G. D.** 1983. Evidence for the presence of a second peptidoglycan hydrolase in *Streptococcus faecium*. *FEMS. Microbiol. Lett.* **19**:65-69.
60. **Keck, W., van Leeuwen, A. M., Huber, M and Goodell, E. W.** 1990. Cloning and characterization of *mepA*, the structural gene of the penicillin-insensitive murein endopeptidase from *Escherichia coli*. *Mol. Microbiol.* **4**:209-219.
61. **Kitano, K., Tuomanen, E. and Tomasz, A.** 1986. Transglycosylase and endopeptidase participate in the degradation of murein during autolysis of *Escherichia coli*. *J. Bacteriol.* **167**:759-765.
62. **Koch, A. L.** 2001. Autolysis control hypothesis for tolerance to wall antibiotics. *Antimicro. Agents Chemother.* **45**:2671-2675.
63. **Koch, A. L.** 2000. *Bacterial growth and form.* Kluwer, Dordrecht, The Netherlands.
64. **Koch, A. L.** 2000. The bacterial way for safe enlargement and division. *Appl. Environ. Microbiol.* **66**:3657-3663.

65. **Koch, A. L.** 2002. Why are Rod-shaped bacteria rod shaped? Trends Microbiol. **10**:452-455.
66. **Kohner, P. C., Patel, R., Uhl, J. R., Garin, K. M., Hopkins, M. K., Wegener, L. T. and Cockerill, F. R.** 1997. Comparison of agar dilution, broth microdilution, E-test, disk diffusion, and automated vitek methods for testing susceptibilities of *Enterococcus* ssp. to vancomycin. J. Clin. Microbiol. **35**:3258-3262.
67. **Komatsuzawa, H., Sugai, M., Nakashima, S. and Suginaka, H.** 1995. Alteration of bacteriolytic enzyme profile of *Staphylococcus aureus* during growth. Microbiol. Immunol. **39**:629-633.
68. **Korat, B., Mottl, H and Keck, W.** 1991. Penicillin-binding protein 4 of *Escherichia coli*: molecular cloning of the *dacB* gene, controlled overexpression, and alterations in murein composition. Mol. Microbiol. Immunol. **5**:675-684.
69. **Kuroda, A., and Sekiguchi, J.** 1991. Molecular cloning and sequencing of a major *Bacillus subtilis* autolysin gene. J. Bacteriol. **173**:7304-7312.
70. **Kuroda, A., Asami, Y and Sekiguchi, J.** 1993. Molecular cloning of a sporulation-specific cell wall hydrolase gene of *Bacillus subtilis*. J. Bacteriol. **175**:6260-6268.
71. **Kuroda, A., Rashid, M. H. and Sekiguchi, J.** 1992. Molecular cloning and sequencing of the upstream region of the major *Bacillus subtilis* autolysin gene: a modifier protein exhibiting sequence homology to the major autolysin and the spoIID product. J. Gen. Microbiol. **139**:1067-1076.

72. **Kusters, J. G., Gerrits, M. M., van Strijp, J. A., and Vandenbroucke-Grauls, C. M.** 1997. Coccoid forms of *Helicobacter pylori* are the morphologic manifestation of cell death. *Infect. Immun.* **65**:3672-2679.
73. **Laemmli, U. K.** 1970. Cleavage of structural proteins during the assembly of head of bacteriophage T4. *Nature* **227**:680-685.
74. **Lazarevic, V., Margot, P., Soldo, B. and Karamata, D.** 1992. Sequencing and analysis of the *Bacillus subtilis* *lytRABC* divergon: a regulatory unit encompassing the structural genes of the N-acetylmuramoyl-L-alanine amidase and its modifier. *J. Gen. Microbiol.* **138**:1949-1961.
75. **Leclerc, H., Devriese, L.A and Mossel, D.A.A.** 1996. Taxonomical changes in intestinal (faecal) enterococci and streptococci: consequences on their use as indicators of faecal contamination in drinking water. *J Appl Bacteriol* **81**:459–466.
76. **Lewis, K.** 2000. Programmed death in bacteria. *Microbiol. Mol. Biol. Rev.* **64**:503-514.
77. **Lottspeich, F., Houthaeve, T. and Kellner, R.** 1994. The Edman Degradation, p. 117-130. *In* R. Kellner, Lottspeich, F. and Meyer, H. E. (ed.), *Microcharacterization of Proteins*. VCH, Weinheim.
78. **Lunn, J. V., Rahman, K. J. and Macey, A. C.** 2001. *Streptococcus milleri* infection. *J. Hand Surgery* **1**:56-57.
79. **Majcherczyk, P. A., Langen, H., Heumann, D., Fountoulakis, M., Glauser, M. P. and Moreillon, P.** 1999. Digestion of *Streptococcus pneumoniae* cell walls with its major peptidoglycan hydrolase releases branched stem peptides carrying proinflammatory activity. *J. Biol. Chem.* **274**:12537-12543.

80. **Margot, P., Mael, C. and Karamata, D.** 1994. The gene of the N-acetylglucosaminidase, a *Bacillus subtilis* cell wall hydrolase not involved in vegetative cell autolysis. *Mol. Microbiol.* **12**:535-545.
81. **Margot, P., Whalen, M., Gholamhoseinian, A., Piggot, P. and, and D. Karamata.** 1998. The *lytE* gene of *Bacillus subtilis* 168 encodes a cell wall hydrolase. *J. Bacteriol.* **180**:749-752.
82. **Markiewicz, Z., Broome-Smith, J., Schwartz, U. and . Spratt, B. -G.** 1982. Spherical *Escherichia coli* due to alleviated levels of D-alanine carboxypeptidase. *Nature* **297**:702-704.
83. **Metz, R., Henning, S. and Hammes, W. P.** 1986. LD-carboxypeptidase activity in *Escherichia coli*. II. Isolation, purification and characterization of the enzyme from *E. coli* K 12. *Arch. Microbiol.* **144**:181-186.
84. **Miguel, E. M., Hardisson, C. and Manzanal, M. B.** 1999. Hyphal death during colony development in *Streptomyces antibioticus*: morphological evidence for the existence of cell deletion in a multicellular prokaryote. *J. Cell. Biol.* **145**:515-525.
85. **Moreillon, P., Markiewicz, Z., Nachman, S and Tomasz, A.** 1990. Two bactericidal targets for penicillin in pneumococci: autolysis-dependent and autolysis-independent killing mechanisms. *Antimicro. Agents Chemother.* **34**:33-39.
86. **Naidoo, K.** 2005. Characterization of the Autolytic systems in selected *Streptococcal* species. University of Kwa-Zulu Natal, Pietermaritzburg.

87. **Ning, S. B., Guo, H.L., Wang, L., and Song, Y.C.** 2002. Salt stress induces programmed cell death in prokaryotic organism *Anabaena*. *J. Appl. Microbiol.* **93**:15-28.
88. **Normark, B. H., and Normark, S.** 2002. Antibiotic tolerance in pneumococci. *Clin. Microbiol. Infect.* **8**:613-622.
89. **Normark, B. H., Novak, R., Ortqvist, A., Kallenius, G., Tuomanen, E. and Normark, S.** 2001. Clinical isolates of *Streptococcus pneumoniae* that exhibit tolerance of vancomycin. *Clin. Infect. Diseases* **32**:552-558.
90. **Novak, R., Charpentier, E., Braun, J.S., and Tuomanen, E.** 2000. Signal transduction by a death signal peptide: uncovering the mechanism of bacterial killing by penicillin. *Mol. Cell.* **5**:49-57.
91. **Novak, R., Henriques, B., Charpentier, E., Normark, S., and Tuomanen, E.** 1999. Emergence of vancomycin tolerance in *Streptococcus pneumoniae*. *Nature* **399**:590–593.
92. **Ohnisi, R., Ishikawa, S. and Sekiguchi, J.** 1999. Peptidoglycan hydrolase *lytF* plays a role in cell separation with *lytE* during vegetative growth of *Bacillus subtilis*. *J. Bacteriol.* **181**:3178-3184.
93. **Parquet, C., Flouret, B., Leduc, M., Hirota, Y and van Heijenoort, J.** 1983. N-acetylmuramoyl-L-alanine amidase of *Escherichia coli* K12. Possible physiological functions. *Eur. J. Biochem.* **133**:371-377.
94. **Pedersen, K., Christensen, S.K., and Gerdes, K.** 2002. Rapid induction and reversal of a bacteriostatic condition by controlled expression of toxins and antitoxins. *Mol. Microbiol.* **45**:501-510.

95. **Piscitelli, S. C., Shwed, J., Schreckenberger, P. and DANziger, L. H.** 1992. *Streptococcus milleri* group: renewed interest in an elusive pathogen. Eur. J. Clin. Microbiol. Infect. Diseases **11**:491-498.
96. **Pooley, H. M., and Shockman, G. D.** 1970. Relationship between the location of autolysin, cell wall synthesis, and the development of resistance to cellular autolysis in *Streptococcus faecalis* after inhibition of protein synthesis. J. Bacteriol. **103**:457-466.
97. **Prescott, L. M., Harley, J. P. and Klein, D. A.** 1999. Microbiology, 4th ed. WCB, McGraw-Hill, Boston.
98. **Rashid, M. H., Mori, M. and Sekiguchi, J.** 1995. Glucosaminidase of *Bacillus subtilis*: cloning, regulation, primary structure and biochemical characterization. Microbiol. **141**:2391-2404.
99. **Rogers, H. J., Perkins, H. R. and Ward, J. B.** 1980. The Bacterial Autolysins, p. 437-445, Microbial Cell Walls and Membranes. Chapman and Hall, London.
100. **Rogers, H. J., Perkins, H. R. and Ward, J. B.** 1980. The Cell Wall in Growth and Division, p. 509-519, Microbial Cell Walls and Membranes. Chapman and Hall.
101. **Romeis, T., Vollmer, W. and Holtje, J. V.** 1993. Characterization of three different lytic transglycosylases in *Escherichia coli*. FEMS Microbiol. Lett. **111**:141-146.
102. **Ronda, C., Garcia, J. L., Garcia, E., Sanchez-Puelles, J. M. and Lopez, R.** 1987. Biological role of the pneumococcal amidase: cloning of the *lytA* gene in *Streptococcus pneumoniae*. Eur. J. Biochem. **164**:621-624.

103. **Ruolff, K. L.** 1995. *Streptococcus*, p. 299-307. In P. R. Murray, Baron, E. J., Tenover, F. C. and Tenover, F. C. and Tenover, F. C. and Tenover, F. C. and Tenover, F. C. and Tenover, F. C. and Tenover, F. C. and Tenover, F. C. and Tenover, F. C. and Tenover, F. C. (ed.), Manual of Clinical Microbiology, 6th ed. American Society for Microbiology, Washington, DC.
104. **Sambrook, J., Fritsch, E. J. and Maniatis, T.** 1989. Molecular Cloning, A Laboratory Manual, 2nd ed. Cold Spring Harbor Laboratory Press.
105. **Sat, B., Reches, M., and Engelberg-Kulka, H.** 2003. The *Escherichia coli* *mazEF* suicide module mediates thymineless death. J. Bacteriol. **185**:1803-1807.
106. **Schleifer, K. H. a. K.-B., R.** 1984. Transfer of *Streptococcus faecalis* and *Streptococcus faecium* to the genus *Enterococcus* nom. rev. as *Enterococcus faecalis* comb. nov. and *Enterococcus faecium* com. nov. Int. J. Sys. Bacteriol. **34**:31-34.
107. **Shibata, Y., Kawada, M. Nakano, Y., Toyoshima, K. and Yamashita, Y.** 2005. Identification and Characterization of an autolysin-encoding gene of *Streptococcus mutans*. Infect. Immun. **73**:3512-3520.
108. **Shinzato, T., and Saito, A.** 1995. The *Streptococcus milleri* group as a cause of pulmonary infections. Clin. Infect. Diseases **21**:238-243.
109. **Shockman, G. D., and Holtje, J.-V.** 1994. Microbial peptidoglycan (murein) hydrolases, p. 131-166. In J.-M. a. H. Ghysen, R. (ed.), Bacterial cell wall, vol. 27. Elsevier Science B. V., Amsterdam, The Netherlands.
110. **Smith, P. K., Krohn, R. I., Hermanson, G. T., Mallia, A. K., Gartner, F. H., Provenzano, M. D., Fujimoto, E. K., Goeke, N. M., Olson, B. J. and Klenk, D. G.** 1985. Measurement of Protein using bicinchoninic acid. Anal. Biochem. **150**:76-85.

111. **Smith, T.** 2003, posting date. The Emergence of Vancomycin Resistant *Staphylococcus aureus* (VRSA): The Peptidoglycan Layer. [Online.]
112. **Smith, T. J., and Foster, S. J.** 1995. Characterization of the involvement of two compensatory autolysins in mother cell lysis during sporulation of *Bacillus subtilis* 168. *J. Bacteriol.* **177**: 3855-3862.
113. **Strating, H., and Clarke, A. J.** 2001. Differentiation of Bacterial Autolysins by Zymogram Analysis. *Anal. Biochem.* **291**:149-154.
114. **Sugai, M. F., T., Akiyama, T., Ohara, M., Komatsuzawa, H., Inoue, S. and Singinaka, H.** 1997. Purification and molecular characterization of glycyglycine endopaptidase produced by *Staphylococcus capitis* EPK1. *J. Bacteriol.* **179**:1193-1202.
115. **Thunnissen, A. M. W. H., Dijkstra, A. J., Kalk, K. H., Rozeboom, H. J, Engel, H., Keck, W. and Dijkstra, B. W.** 1994. Doughnut-Shaped Structure of a Bacterial Muramidase Revealed by X-Ray Crystallography. *Nature* **367**:750-754.
116. **Tomohisa, H., Kimura, S. and Mori, N.** 2005. *Auris. Nasus. Larynx.* **32**:55-58.
117. **Tortora, G., Funke, B. R and Case, C.** 2004. *Microbiology: An Introduction*, 8th ed. Pearson Education, Inc, San Francisco.
118. **Tuomanen, E., and Schwartz, J.** 1987. Penicillin-binding protein 7 and its relationship to lysis of nongrowing *Escherichia coli*. *J. Bacteriol.* **169**:4912-4915.
119. **Ursinus, A., and Holtje, V.** 1992. Purification of a membrane-bound lytic transglycosylases from *Escherichia coli*. *J. Bacteriol.* **176**:338-343.

120. **Valence, F. a. L., S.** 1995. Zymogram and preliminary characterization of *Lactobacillus helveticus* autolysins. Appl. Environ. Microbiol. **61**:3391-3399.
121. **van der Linden, M. P., de Haan, L., Hoyer, M. A. and Keck, W.** 1992. Possible role of *Escherichia coli* penicillin-binding protein 6 in stabilization of stationary-phase peptidoglycan. J. Bacteriol. **174**:7572-7578.
122. **van Heijenoort, J., Praque, C., Flouret, B. and van Heijenoort, Y.** 1975. Envelope-bound N-acetylmuramyl-L-alanine amidase of *Escherichia coli*. Eur. J. Biochem. **58**:611-619.
123. **Vollmer, W., and Höltje, J. V.** 2001. Morphogenesis of *Escherichia coli*. Curr. Opin. Microbiol. **4**:625-633.
124. **Waltho, J. P., and Williams, D. H.** 1991. The natural design of vancomycin family antibiotics to bind their target peptides. Presented at the Ciba. Found. Symp. **158**:73-86.
125. **Wanahita, A., Goldsmith, E. A., Musher, D. M., Clarridge, J. E., Rubio, J., Krishnan, B and Trial, J.** 2002. Interaction between Human Polymorphonuclear Leukocytes and *Streptococcus milleri* Group Bacteria. J. Infect. Diseases **185**:85-90.
126. **Weinstein, M. P.** 2001. Comparative evaluation of penicillin, ampicillin, and imipenem MICs and susceptible breakpoints for vancomycin-susceptible and vancomycin-resistant *Enterococcus faecalis* and *Enterococcus faecium*. J. Clin. Microbiol. **39**:2729-2731.

127. **Whiley, R., Fraser, H., Hardie, M., et al.** 1990. Phenotypic differentiation of *Streptococcus intermedius*, *Streptococcus constellatus*, and *Streptococcus anginosus*. Strains within the "*Streptococcus milleri* group". J. Clin. Microbiol. **28**:1497-1501.
128. **Whiley, R. A., and Beighton, D.** 1991. Emended descriptions and recognition of *Streptococcus constellatus*, *Streptococcus intermedius*, and *Streptococcus anginosus* as distinct species. Int. J. Syst. Bacteriol. **41**:1-5.
129. **Whiley, R. A., Beighton, D., Winstanely, T. G., Fraser, H. Y. and Hardie, J. M.** 1992. *Streptococcus intermedius*, *Streptococcus constellatus*, and *Streptococcus anginosus* (the *Streptococcus milleri* group): association with different body sites and clinical infections. J. Clin. Microbiol. **30**:243-244.
130. **Wireman, J. W., and Dworkin, M.** 1977. Developmentally induced autolysis during fruiting body formation *Myxococcus xanthus*. J. Bacteriol. **129**:798-802.
131. **Yamamoto, H., Kurosawa, S. and Sekiguchi, J.** 2003. Localization of the vegetative cell wall hydrolases *LytC*, *LytE* and *LytF* on the *Bacillus subtilis* cell surface and stability of these enzymes to cell wall-bound or extracellular proteases. J. Bacteriol. **185**:6666-6677.
132. **Yamamoto, M., Fukushima, T., Ohshiro, S., Go, Y., Tsugu, H., Kono, K. and Tomonaga, M.** 1999. Brain Abscess Caused by *Streptococcus intermedius*: Two Case Reports. Surg. Neurol. **51**:219-22.
133. **Yem, D. W., and Wu, H. C.** 1976. Purification and properties of β -N-acetylglucosaminidase from *Escherichia coli*. J. Bacteriol. **125**:324-331.

134. **Yoshinori, G., Tsugu, H., Kono, K., Tomonaga, M.** 1999. Head and neck infections caused by *Streptococcus milleri* group: An analysis of 17 cases. Surg. Neurol. **51**:219 -222.